Intestinal Monoacylglycerol Metabolism: Regulation and Function

by

Su-Hyoun Chon

A Dissertation submitted to the

Graduate School-New Brunswick

Rutgers, The State University of New Jersey

in partial fulfillment of the requirements

for the degree of

Doctor of Philosophy

Graduate Program in Nutritional Sciences

Written under the direction of

Judith Storch

and approved by

_____

_____

_____

_____

New Brunswick, New Jersey

[October, 2008]

ABSTRACT OF THE DISSERTATION

Intestinal Monoacylglycerol Metabolism; Regulation and Function

by **Su-Hyoun Chon**

Dissertation Director:
Judith Storch

Sn-2-MG is a major product of dietary lipid digestion, yet its intestinal metabolism has not been investigated beyond its anabolic processing. Recently, a potential for *sn*-2-MG catabolism in the enterocyte has been proposed. Thus, we examined the regulation of the two known MG metabolizing enzymes, monoacylglycerol acyltransferase (MGAT) and monoacylglycerol lipase (MGL), in mouse small intestine and liver during development and under nutritional modifications. Furthermore, intestinal MGL function was explored by generating transgenic mice (iMGL mice) overexpressing MGL specifically in small intestinal enterocytes.

Dynamic changes in MG metabolism were observed during mouse ontogeny. Hepatic MGL and MGAT expression showed a reciprocal regulation under apparent transcriptional control whereas intestinal MG metabolism did not exhibit any inverse regulation: MGAT2 protein expression and activity were markedly induced during lactation, and then declined. MGL activity increased rapidly at birth and was maintained thereafter. Moreover, discordances in mRNA, protein, and activity levels of intestinal MGAT and MGL were observed, suggesting complex regulatory mechanisms involved in their expression. In addition, intestinal MGL was significantly up-regulated by a high fat diet, indicating its potential role in lipid assimilation.

During high fat feeding, iMGL mice exhibited an obese phenotype secondary to hyperphagia and hypometabolic rate compared to wild type littermates. Dietary lipid absorption and intracellular TG reesterification in iMGL mice intestine were intact. Interestingly, the level of cellular 2-arachidonoyl glycerol (2-AG), one of the endocannabinoids (EC), and cannabinoid

receptor 1 (CB1) expression were decreased in iMGL mice intestine. Antagonism of EC signaling is known to reduce appetite and adiposity, and MGL terminates EC signaling by hydrolyzing 2-AG. Here we have a paradox in that intestinal MGL induction caused a phenotype associated with EC system activation rather than termination. While the molecular mechanisms underlying this paradox remain to be elucidated, these studies are the first to indicate that intestinal MG levels significantly affect whole body energy balance via altering appetite and metabolic rate. Thus, we propose a new function for intestinal MG, in which MGL activity is associated with regulatory mechanisms for energy homeostasis, possibly through appetite signaling systems.

Acknowledgement

I was so lucky to have such precious people to help me during my Ph.D. dissertation research. I would like to thank my wonderful advisor, Dr. Judith Storch for her consistent support and guidance. Specially, her invaluable scientific insight as well as a heart warming mentoring helped me through this uneasy journey. Also, I would like to thank my dissertation committee, Drs. Loredana Quadro, Dawn Brasaemle, and Chuck Martin, for their critical review of my research as well as their sincere encouragement throughout my graduate life. In addition, I really appreciate all the members in Dr. Storch's lab for their great support. Finally, I would like to give a special thank you for my family, my dear husband and cutie son, Sunggu and Daniel.

Table of Contents

Lists of Tables

Lists of Figures

Lists of Abbreviations

ACAT	Acyl CoA : cholesterol acyltransferase
ACS	Acyl-Co A synthase
AEA	Arachidonoyl ethanolamide
2-AG	*Sn*-2-arachidonoyl glycerol
AgRP	Agouti-related protein
ATGL	Adipose tissue triacylglycerol lipase (desnutrin)
AP	Apical
ARE	AU rich element
BBM	Brush border membrane
BL	Basolateral
BSAL	Bile salt activated lipase
CCK	Cholecytokinin
CB	Cannabinoid receptor
CE	Cholesterol ester
CEL	Carboxyl ester lipase
CNS	Central nervous system
CRH	Corticotrophin-releasing hormone
DG	Diacylglycerol
DGL	Diacylglycerol lipase
DGAT	Diacylglycerol acyltransferase
DPP	Dipeptidyl peptidase
EC	Endocannabioid
ENS	Enteric nervous system
ER	Endoplasmic reticulum
FA	Fatty acid
FAAH	Fatty acid amide hydrolase
FABP	Fatty acid binding protein
FABPpm	Plasma membrane fatty acid-binding protein
FATP	Fatty acid transport protein
G3P	Glycerol-3-phosphate
GHSR	Growth hormone secretagogue receptor (ghrelin receptor)
GLP-1	Glucagon-like peptide-1
GPAT	Glycerol-3-phosphate acyltransferase
GI	Gastrointestinal
GPCR	G protein-coupled receptor
HSL	Hormone sensitive lipase
IFABP	Intestinal fatty acid binding protein
LCFA	Long chain fatty acids
LCMS	Liquid chromatography mass spectrometry
LFABP	Liver fatty acid binding protein
MCH	Melanin-concentrating hormone
MG	Monoacylglycerol
MGL	Monoacylglycerol lipase
MGAT	Monoacylglycerol acyltransferase

NPY	Neuropeptide Y
OEA	Oleoylethanolamide
OXM	Oxyntomodulin
PC	Phosphatidylcholine
PL	Phospholipid
PLRP	Pancreatic lipase related protein(s)
PP	Pancreatic polypeptide
PPAR-α	Peroxisome proliferateor-activated receptor-α
PTL	Pancreatic lipase
PYY	Peptide YY
RQ	Respiratory quotient
TG	Triacylglcyerol
TLC	Thin layer chromatography
TM	Transmembrane
UTR	Untranslated region
UWL	Unstirred water layer
VLDL	Very low density lipoprotein

Chapter 1.

Introduction and Review of the Literature

1. Introduction

The running title of a recent elegant review on the gut, published in *Science* magazine in March, 2005, is "The inner tube of life." The article begins by pointing out that the "average adult human is, in essence, a 10-meter-long tube." Truly, everyone carries this inner-lining tube in their body, where most of the digestion and absorption of nutrients take place.

Digestion and absorption of dietary lipids are highly efficient processes, since more than 90% of ingested lipids are hydrolyzed and absorbed into body, even with high fat diets. Due to their hydrophobic nature, the digestion and absorption of lipids are complicated processes. The overall assimilation of dietary lipids includes several steps: mechanical emulsification, enzymatic digestion, solubilization with bile salt, uptake into the enterocyte, reesterification, and finally, secretion into the circulation. Beginning with the anatomy of the small intestine, this chapter will review the current knowledge of digestion and absorption of dietary lipids, particularly triacylglycerol (TG), since > 90% of ingested lipid is composed of TG.

Sn-2-MG is one of the major hydrolysis products of dietary TG, along with fatty acids, by pancreatic enzyme digestion in the small intestine. Once inside the enterocyte, moreover, *sn*-2-MG initiates TG reesterification via the MGAT pathway. Despite its significant role in lipid absorption, *sn*-2-MG metabolism in enterocytes has not been well studied, and MG is generally thought of simply as a metabolic intermediate in TG assimilation. However the catabolism of *sn*-2-MG has been recently documented, implicating a more complex metabolic profile in the small intestine. Thus, the present studies will focus on the regulation and function of intestinal *sn*-2-MG metabolism.

Recently another aspect of gut function has been highlighted, namely the sensing and signaling of nutritional status to the brain. The discovery of numerous gut signaling molecules has established the gastrointestinal tract as an important organ system in controlling appetitive behavior. Since our studies of intestinal MG utilization suggest a link to food intake, a brief summary of gut signaling functions relevant to appetite will be reviewed in this chapter as well.

2. Anatomy of the small intestine; organization and characterization of the small intestinal epithelium

The architecture of the small intestine is highly polarized, with an elaborate organization of numerous cell types each with diverse functions. The small intestine is composed of four distinct strata: mucosa, submucosa, muscularis propria, and serosa, as shown in Figure 1-1-A. The mucosa is further subcategorized as a single layer of epithelium, lamina propria, and muscularis mucosa (Fig. 1-1-A). In the epithelium are found several types of highly differentiated cells: absorptive epithelial cells, goblet cells, enteroendocrine cells, and Paneth cells are distributed heterogeneously from the crypt to villus regions according to their function (Fig. 1-1-B). Absorptive epithelial cells comprise 99 % of the mucosal cell population (1) , and a single enterocyte again demonstrates a polarized structure, with numerous microvilli in the apical membrane facing the intestinal lumen, and the basolateral membrane facing the circulation (Fig. 1-1-C).

Amplification of the apical surface area by folding of the mucosa and projection of villi and microvilli is one of the unique features of the small intestine. This specialized structure increases surface area up to 600 fold, relative to the surface area of a cylinder of the same diameter, to facilitate efficient digestion and absorption of food (2). The organization of the small intestine will be now reviewed in terms of a) polarity of the enterocyte (apical to basal organization) b) crypt to villus and proximal to distal axes of the epithelium and c) structure beyond the mucosa, i.e. muscle and nervous systems.

2.1 Apical to basal organization of the absorptive enterocyte

The enterocytes of the small intestine are highly polarized, tall columnar cells, as depicted in Fig. 1-1-C. Following digestion in the lumen, nutrients are absorbed across the apical surface (AP) of the enterocyte, processed intracellularly and finally secreted via the basolateral side (BL) for transport of nutrients to distant organs. Due to the vital role of the AP surface in nutrient absorption, the AP membrane has a unique and specialized structure which is distinct from that of

the BL membrane. The apical pole is characterized by numerous microvilli, estimated at 1000-4000 per cell (3), amplifying the surface area for efficient absorption. The core of the microvilli contain actin filaments which extend to the cytoplasm, where they are arranged parallel to the surface of cell as a terminal web structure (Fig. 1-1-C) (4). Typical cellular components such as endoplasmic reticulum (ER), Golgi, lysosomes, mitochondria, peroxisomes, microtubules and other related organelles are found throughout the cytoplasm. The nucleus is usually found in the basal region of the enterocyte (3). The microvillus membrane is rich in intramembrane proteins such as proteases and disaccharidases (5-7), and membrane-bound glycoproteins form a glycocalyx surface that coats the AP surface. The carbohydrate side chains of glycoproteins trap water to create an unstirred water layer (UWL), overlying the microvilli (2). The function of the glycocalyx is known to be protection of membrane proteins from pancreatic enzyme digestion (8); a sensory function for the glycocalyx was proposed as well (9).

The lateral membranes of neighboring enterocytes are attached to each other with various junctions, establishing an important barrier function for the intestinal epithelium. Tight junctions (zonular occludens) are found immediately beneath the microvilli, sealing the intercellular compartment from the luminal environment (2). The intermediate junction (zonula adherens) is located just below the tight junction, and desmosomes (macular adherens) are found in the more basal regions of the lateral membrane. Epithelial permeability is regulated in part by tight junctions, allowing paracellular flow of fluid and solute (10). The basolateral (BL) membrane encloses the surface of the enterocyte facing the intercellular space and the basal lamina. The morphologic, biochemical, and functional features of the BL membrane are markedly different from those of the AP membrane. For example, the protein to lipid ratio in the BL membrane is approximately three times lower, and the cholesterol to phospholipid ratio is also 20% lower (5). Saturation of fatty acyl chains attached to PL is lower in BL membrane lipids (11), consistent with the greater fluidity of the BL membrane.

Figure. 1-1

A
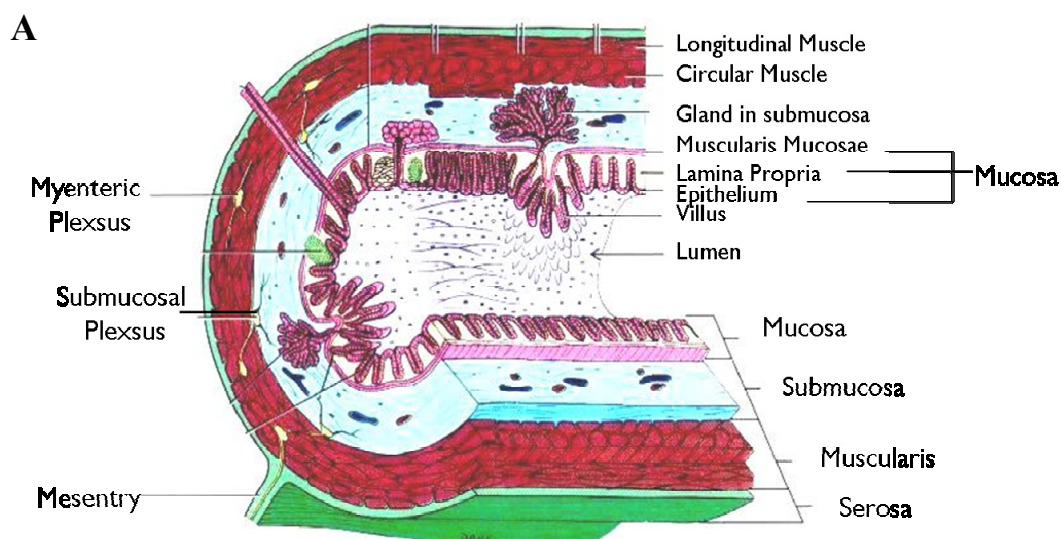
Figure 1-1-A. Anatomy of the small intestine (Sectional view)

B
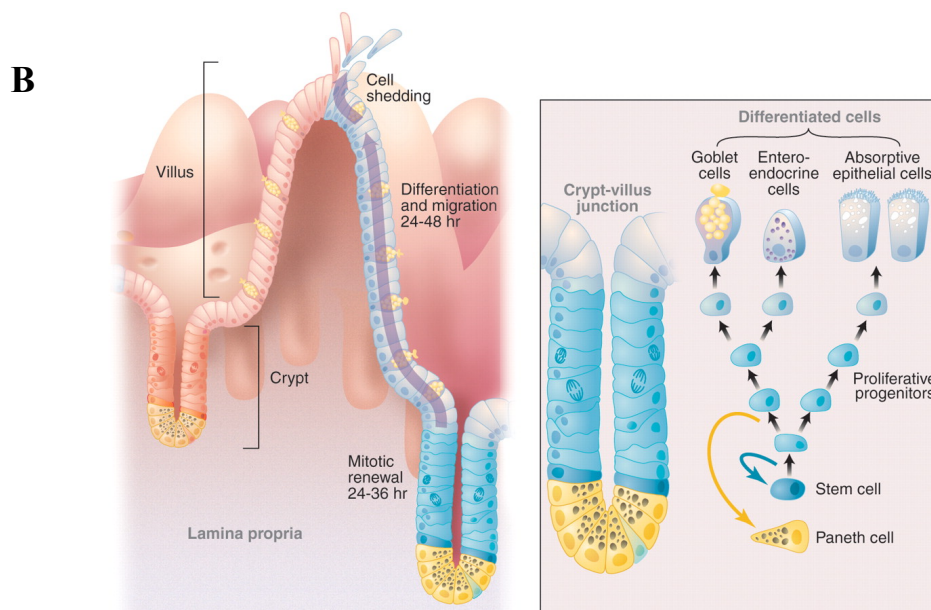
Figure 1-1-B. Anatomy of the small intestine (Crypt to villus organization)
Adapted from Radtke, F. and Clevers, H. (1)

Figure. 1-1

C
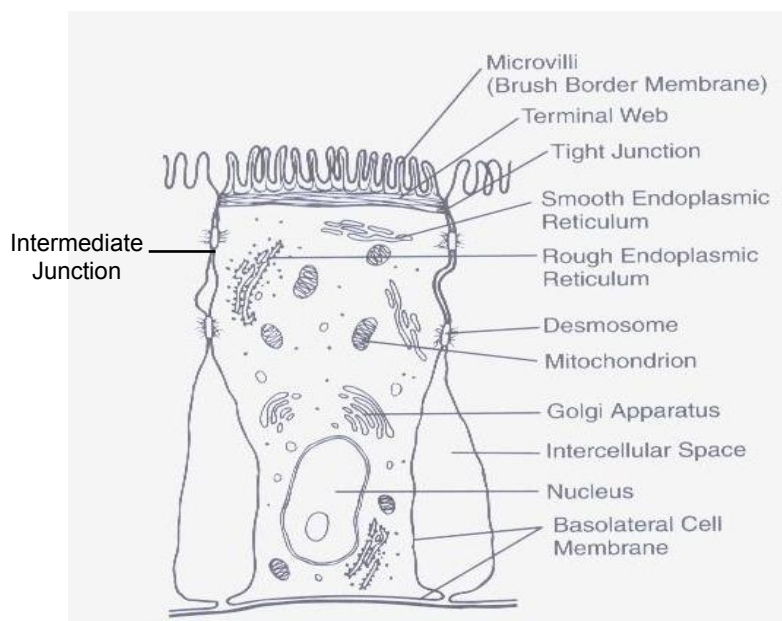
Figure 1-1-C. Apical to basal organization of the intestinal epithelium
Adapted from Tso, P. and Crissinger, K. (2)

D
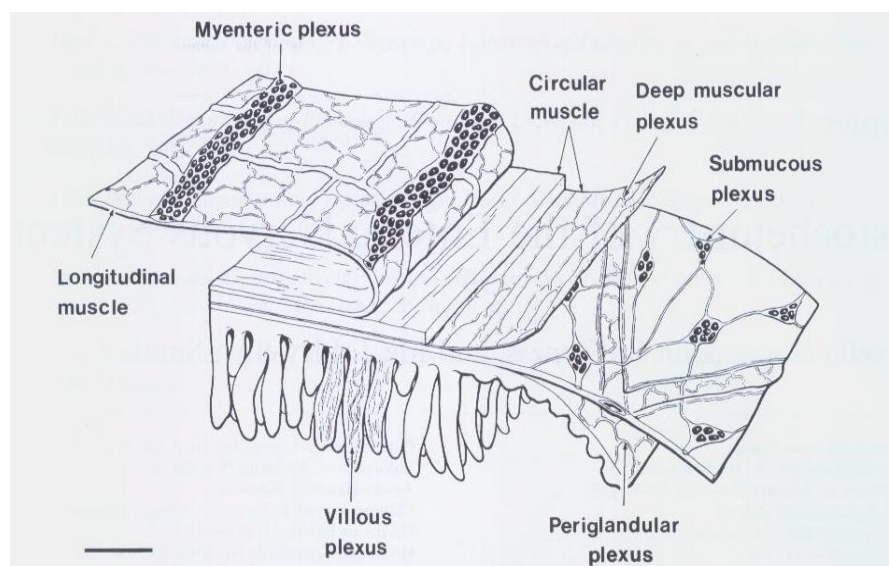
Figure 1-1-D. Muscle and nerve systems in the GI tract
Adapted from Costa, M. and B.Llewellyn-smith, I.J. (12)

In addition to morphological and biochemical differences, lipid metabolic polarity is also present in intestinal epithelial cells (13-16). Long chain fatty acids and *sn*-2-MG absorbed from the lumen are predominantly metabolized to TG, whereas basolaterally derived fatty acids and MG are incorporated into PL synthesis and/or oxidized (13-17). These observations implicate the presence of distinct metabolic channeling, creating this metabolic polarity in the enterocyte.

2.2 Crypt to villus organization

Longitudinally, the intestinal epithelium is organized along a crypt to villus axis (Fig.1-1-B). The main function of the villus region is nutrient absorption, and in the crypt region, epithelial cell renewal and exocrine and endocrine secretions into both the lamina propria and lumen occur (5). The self renewal capacity in the crypt is remarkable; 70 billion cells are typically replaced per day in an adult small intestine (1). Stem cells in the crypt differentiate continuously to distinct cell types which migrate toward the villus tips and are ultimately shed, following apoptosis, in a few days (Fig. 1-1-B).

Differentiation occurs into two main lineages, an absorptive lineage and a secretory lineage. The former generates enterocytes which are abundantly distributed throughout villus, and are essential for nutrient absorption. The latter differentiates into goblet cells secreting mucin, enteroendocine cells secreting hormones such as secretin, and finally Paneth cells residing at the bottom of crypt and secreting antimicrobial agents (Fig. 1-1-B) (1). These secretory cells represent less than 1% of the intestinal epithelium, but they play important functions distinct from enterocytes. As enterocytes mature and migrate up to the villus tip, the cells acquire more cytoplasmic organelles with spatial organization; endoplasmic reticulum (ER) becomes abundant, occupying much of the cytoplasm, and the Golgi complex is also well developed (3). Microvilli becomes taller and a much thicker glycocalyx is formed (3, 5). Enterocytes mature within 2-3 days during their migration toward the villus tip (1).

In addition to these morphological changes, functional maturity is also obtained, for example, enzyme activities for TG synthesis are increased during enterocyte differentiation (18, 19). It was reported that MGAT activity in rat intestine is significantly increased along the longitudinal axis, with 60 fold higher activity in villus than crypt cells (18). In contrast, PL synthetic enzyme activities are similar throughout the crypt to villus axis (20).

2.3 Proximal to distal organization

From the pyloric sphincter to the ileocecal valve, the small intestine is a long "inner lining" tube which connects the stomach and the cecum (1). The human duodenum is a foot long proximal region which receives the chyme from the stomach, as well as pancreatic and gallbladder secretions (2). The 8 foot long jejunum is the middle part of small intestine, where most of the nutrient absorption takes place (2). The 11 foot long ileum is the distal region, where bile salts are reabsorbed for enterohepatic recycling, and where gut hormones such as peptide YY (PYY) are released to signal satiety (2, 21).

Many genes related to lipid trafficking and metabolism demonstrate proximal to distal gradients of expression, being higher in the proximal and lower in the distal region, as dietary fat absorption predominantly occurs in the proximal and medial regions of the small intestine. For example, CD36/FAT, a transmembrane protein involved in FA uptake (22), two fatty acid binding proteins (FABP) present in the small intestine (IFABP and LFABP) (23) and monoacylglycerol acyltransferase 2 (MGAT2) (24) and diacylglycerol acyltransferase 1 (DGAT1) (25), key enzymes for intestinal TG synthesis, are all known to be highly expressed in the more proximal intestine, with diminished expression toward the distal region.

2.4 Small intestinal structure beyond the epithelium; muscle layers and nervous systems

The most apical portion of the small intestine is a single layer of epithelial cells, as described above. Beneath the epithelium are multiple muscle strata innervated with a complex

nervous system (12). These neuromuscular layers play important roles in gut motility, secretion and signaling (12, 26). GI muscle layers are composed of two types; one is longitudinal muscle coating the outside of the small intestine, and the other is a circular muscle forming the inner layer of the GI muscular structure (Fig. 1-1-A and 1-1-D) (12). The enteric nervous system (ENS) is a complex neuronal network innervating the intestinal muscle layers and directly controlling various GI functions. Surprisingly, the number of neurons in the ENS is similar to the number present in the spinal cord (26). The intrinsic nervous system of the ENS is composed of two layers; one is the myenteric plexus (Auerbach's plexus), embedded between the longitudinal and circular muscle layers; the other is the submucosal plexus (Meissner's plexus), located between the circular muscle and the submucosa (Fig.1-1-D) (12, 26). The latter has ganglia from which nerve fibers penetrate to the muscularis mucosae, a mucosal muscle layer, and make a connection to the villus plexus (Fig.1-1-A and D). Depending on the class of neurons, diverse patterns of longitudinal (myenteric plexus to mucosal fibers) or lateral (proximal to distal axis) projections have been reported (12). Communication from mucosal nerve fibers to the CNS is accomplished via this complex interconnection within the intrinsic as well as with the extrinsic (sympathetic and parasympathetic) nervous systems. Various GI functions such as gastric secretion, motility, blood supply, and secretion of gut hormones are enabled by this elaborate neuronal networking.

3. Lipid digestion

More than 90% of dietary lipids are composed of TG, which are mainly acylated with long chain fatty acids (LCFA). The remaining dietary lipid consists of phospholipids (PL), cholesterol ester (CE), free cholesterol, and lipid soluble vitamins (A, D, E, and K). TG digestion begins in the stomach by gastric lipase, hydrolyzing up to 30% of dietary TG (27). The partially digested lipids are mixed with pancreatic and biliary secretions in the duodenum, promoting further digestion (28). Complete TG digestion is carried out by pancreatic enzymes including pancreatic lipase (PTL),

producing fatty acids and *sn*-2-MG. Dietary cholesterol, mainly present as free cholesterol (28), is emulsified directly into bile salt micelles. Cholesterol ester, which contributes 10-15% of dietary cholesterol, is broken down to free cholesterol and fatty acids by another pancreas-derived enzyme, carboxy ester lipase (CEL), also known as cholesterol esterase and bile salt activated lipase (BSAL) (29). Phospatidylcholine (PC), the most abundant dietary PL, is hydrolyzed to fatty acid and lyso-PC by another pancreatic enzyme, phospholipase A2, which is first activated by trypsin in the intestinal lumen. These hydrolysis products are emulsified together with bile salts and form a micelle, which crosses the UWL and reaches the surface of the intestinal epithelium where monomeric absorption takes place. Lipases relevant to TG digestion in the GI tract are described below.

3.1 Gastric lipase

Lipolysis of dietary TG begins in the stomach by the action of gastric lipase. It is secreted by chief cells of the stomach mucosa, and is also called acid lipase since its optimal pH is 4, although it works at pH 6 - 6.5 as well (28). Thus most of the TG hydrolysis by gastric lipase occurs in the stomach, but residual activity is still present in the upper part of the duodenum (30). Trypsin secreted by the pancreas into the proximal intestine inactivates gastric lipase activity, thus gastric lipase is not significantly involved in intestinal lumen lipolysis (27). Gastric lipase preferentially cleaves TG containing medium chain fatty acids rather than LCFA, thus playing an important role in digestion of milk fat, which is rich in short and medium chain fatty acids (28). Gastric lipase hydrolyzes the *sn*-1/*sn*-3 position of TG predominantly (28), however in vivo, the products of gastric lipase action are fatty acid and 1,2-diacylglycerol (31). Further hydrolysis is continued in the small intestinal lumen by pancreatic enzymes.

3.2 Pancreatic lipase

Most of dietary TG digestion is believed to be carried by pancreatic lipase (PTL) in the proximal intestine. PTL is a 49 kDa protein synthesized by the exocrine pancreas and secreted into the duodenum. PTL preferentially hydrolyzes TG over CE and PL (32, 33). Two other proteins possessing homology with PTL have also been identified, pancreatic lipase related proteins (PLRP) 1 and 2. PLRP2 has TG lipolytic activity, but PLRP1 does not (34). The former is thought to be important in luminal TG digestion during the neonatal period (35), whereas the function of PLRP1 remains to be elucidated.

PTL works poorly on bile salt-lipid mixtures since it is unable to access the TG droplet coated with bile salt, and it has been shown that bile salts inhibit PTL activity (28, 32). This paradox led to the discovery of colipase, an 11 kDa small pancreatic protein activated via proteolytic cleavage by trypsin in the intestinal lumen. This cofactor is required for bringing PTL onto the TG droplet/ aqueous interface. In vivo evidence for its significance was demonstrated by colipase deficient mice, which exhibited steatorrhea under a high fat challenge (36). By its binding with colipase, PTL efficiently accesses lipid emulsions and carries out its lipolytic function. PTL preferentially acts on the *sn*-1/*sn*-3 position of TG, releasing two fatty acids and *sn*-2-MG as the final digestive products in the intestinal lumen.

3.3 Carboxyl ester lipase (CEL)

Carboxyl ester lipase (CEL), also known as bile salt stimulated lipase (BSL) or cholesterol esterase, catalyzes hydrolysis of many types of dietary lipids. Its broad substrate specificity includes CE, TG, DG, MG, PL, ceramide, and retinyl ester (29, 37). Activation by bile salt is required for its hydrolysis of lipophilic molecules, but more water soluble substrates such as carboxyl esters with short chain fatty acids are able to be hydrolyzed by CEL without bile salt (29).

CEL is highly expressed in pancreas as well as mammary gland, and lower expression was reported in liver, macrophages, and endothelial cells. Milk has an abundant amount of CEL derived from mammary gland, which plays an important role in milk fat digestion during the

suckling stage when PTL secretion has not yet started. In CEL knock out (KO) mice, pups nursed by CEL-KO dams have large amounts of TG, DG, and MG in their colon contents, resulting in injuries to the intestinal epithelium. This implies a significant role for CEL in milk fat digestion (38, 39).

Despite this clear role in lipid digestion during lactation, the significance of CEL for hydrolysis of ingested lipids in the adult is still uncertain. In the adult, it has been generally thought that TG digestion is primarily carried out by PTL, and that CEL is functioning in the digestion of cholesterol ester. However in vivo studies using knock out models suggest that lipid digestion and absorption is not such a distinct and clear cut process as one and the other, but that CEL and PTL affect each other's activities (40-42). For example, total TG digestion and absorption was minimally affected by either individual KO of CEL or PTL (40, 41), but was considerably exacerbated in the double KO (42), suggesting the importance of complementary functions for both enzymes, and even perhaps additional unknown lipases. In terms of cholesterol absorption, it was not altered in the CEL KO, but a marked reduction was observed in the PTL KO, and further reduction was found in double KO mice. Since PTL does not have CEL activity, decreased cholesterol absorption in the PTL KO was speculated to result from a delay in lipid absorption to the ileum, where cholesterol is poorly absorbed (41). Interestingly, absorption in the double KO mice was reduced by only 30-50%, suggesting that lipid digestion was still being carried out by other lipases. Thus, mutual compensatory functions for lipid digestion and the possibility of as-yet unidentified lipases involved in luminal lipid digestion were clearly demonstrated in these knock out mouse studies, strongly supporting the fundamental importance of lipid digestion and absorption in the small intestine.

In addition to functioning in luminal digestion, the uptake of CEL into the intracellular compartment of the enterocyte, and even further, its secretion via the BL membrane into the circulation, have been reported (29, 43, 44). Its uptake mechanism was proposed to be via endocytosis mediated by chaperone protein Grp 94 (43). The amount of CEL present in the small

intestine showed a proximal to distal gradient, abundant in the proximal region and decreased thereafter (29). It is anchored to the AP surface of the brush border membrane (BBM) via its heparin binding domain (45). Transport to the Golgi complex, to the BL membrane and secretion of intact CEL protein were reported, suggesting its diverse function in addition to luminal digestion (44). Unlike PTL, CEL is able to hydrolyze *sn*-2-MG, though *sn*-1-MG hydrolysis is preferred (46, 47). The importance of the MG lipolytic action of CEL in the enterocyte will be discussed further in chapter 2.

3.4 Lipases in the intestinal epithelium

The presence of lipolytic activity in the intestinal epithelium was reported as long as 50 years ago (48, 49). Abram *et. al.* suggested that there is a distinct TG pool present in the cytosolic compartment which is undergoing hydrolysis, but is separate from a TG pool destined for chylomicron synthesis (50). Enzymes catalyzing this process were suggested to be internalized CEL as well as PTL and hormone sensitive lipase (HSL). Mahan *et. al.* reported mRNA expression of PTL in rat small intestine with higher expression in the proximal region and up-regulation by dietary fat (51). In addition, intestinal HSL expression was shown by Grober *et. al,* with abundant expression found mostly in differentiated enterocytes of the villi, but not in undifferentiated crypt cells (52). Metabolism of this putative separate cytosolic TG pool has not been explored thoroughly. Physiological roles for mucosal TG hydrolysis and its connection with the well known anabolic processes that forms chylomicron TG, if any, need to be elucidated in order to understand completely intracellular lipid metabolism in the intestine.

4. Uptake of lipid digestion products by the enterocyte; Fatty acid and MG absorption.

The brush border membrane (BBM) in intestinal epithelial cells is surrounded by an unstirred water layer (UWL) which is formed by the thick glycocalyx present at the BBM luminal

surface(8, 28). Since the major hydrolysis products from luminal TG digestion, fatty acid and sn-2-MG, are lipophilic molecules, this UWL is a barrier for their uptake into enterocytes (28, 53). Bile salts, biological detergents secreted into the intestinal lumen, play a critical role in lipid delivery to the BBM. Once hydrophobic digestive products are mixed with bile salts, they form a micellar structure which can cross the UWL readily to reach the surface of the BBM (28, 53). It has long been controversial as to how fatty acids are taken up by enterocytes, and the same is true for sn-2-MG, although much less is known about MG than FA. Two mechanisms have been proposed. One is a passive diffusion mechanism (54, 55), and the other is a carrier mediated process (56, 57). Fatty acid and sn-2-MG uptake processes are discussed below.

4.1 Passive diffusion

Once digested lipids are introduced into the AP surface, they are proposed to diffuse into the enterocyte due to the concentration gradient between the AP surface and the intracellular compartment of epithelial cells. The rapid reesterification process existing intracellularly creates a concentration gradient, allowing the diffusion process to continue (28). Supporting evidence was provided by Strauss et. al. who reported that FA uptake from a micellar solution by intestinal sacs occurred even at 0ºC, indicating the uptake process was not energy dependent (54). In addition, Dietschy et. al. showed a linearity of FA uptake as a function of total FA concentration, and that uptake was not competitive (55). Nevertheless it should be pointed out that studies by Dietschy et. al. were mostly done using short chain fatty acids for uptake kinetics.

4.2 Carrier-mediated uptake

A carrier-mediated uptake mechanism was suggested by kinetics demonstrating that long chain fatty acid (LCFA) uptake was a saturable function of the monomer concentration (56, 58). Stremmel et. al. showed that the uptake of radiolabeled oleate by rat intestinal cells exhibited saturation with a Km in the nM range of monomer concentrations (56). In addition, competitive FA

uptake was recently reported by Chen *et. al* (22), showing that the Vmax for labeled FA uptake in isolated rat enterocytes was markedly decreased following intraduodenal administration of oleic acid. Studies using BBM prepared from jejunum and ileum, a model excluding intracellular metabolic processes, also exhibited saturable kinetics (56), as have primary enterocytes and two model cell lines, Caco-2 and intestinal epithelial cell 6 (IEC-6). Following heat and trypsin treatment of epithelial BBM and Caco-2 cells, a reduced uptake of lipid digestion products was reported, supporting a protein mediated uptake mechanism (56, 58, 59).

In contrast to intensive studies of FA uptake by enterocytes, the uptake mechanism for *sn*-2-MG, the other luminal hydrolysis product of TG, has not been well investigated. Recently, it was shown that at low monomer concentrations, saturable functions were observed for both FA and MG uptake (Fig.1-2-A). In addition, trypsin incubation reduced *sn*-2-MG uptake, suggesting MG uptake is also facilitated by protein. Furthermore, LCFA and *sn*-2-MG compete with each other for uptake by Caco-2 cells (Fig. 1-2-B and C), implying the possibility of sharing the same transporter for uptake, i.e. a common mechanism of *sn*-2-MG and FA uptake by Caco-2 cells (58, 60). However diffusional uptake was also apparent at higher monomer concentration (Fig. 1-2-A), suggesting that the enterocyte exhibits dual uptake mechanisms for both FA and MG, in agreement with previous work by Chow and Hollander for FA uptake (61).

Several plasma membrane proteins have been proposed as putative LCFA or *sn*-2-MG transporters in the enterocyte; FABPpm, FATP4, and CD36/FAT. Plasma membrane fatty acid binding protein (FABPpm) is a 40 kDa protein isolated from the plasma membrane of rat liver and jejunal BBM (56, 59, 62). Treatment of rat and rabbit jejunal BBM with FABPpm antibody reduced FA and MG uptake, supporting its function (59, 63). Nevertheless, a precise role for this protein remains controversial since FABPpm is identical to mitochondrial aspartate aminotransferase which functions intracellularly in the malate-aspartate shuttle (64, 65). The next candidate is CD36/FAT, an integral membrane glycoprotein with two transmembrane domains (66). CD36 is highly expressed in rodent small intestine apical plasma membrane with proximal to

Figure. 1-2
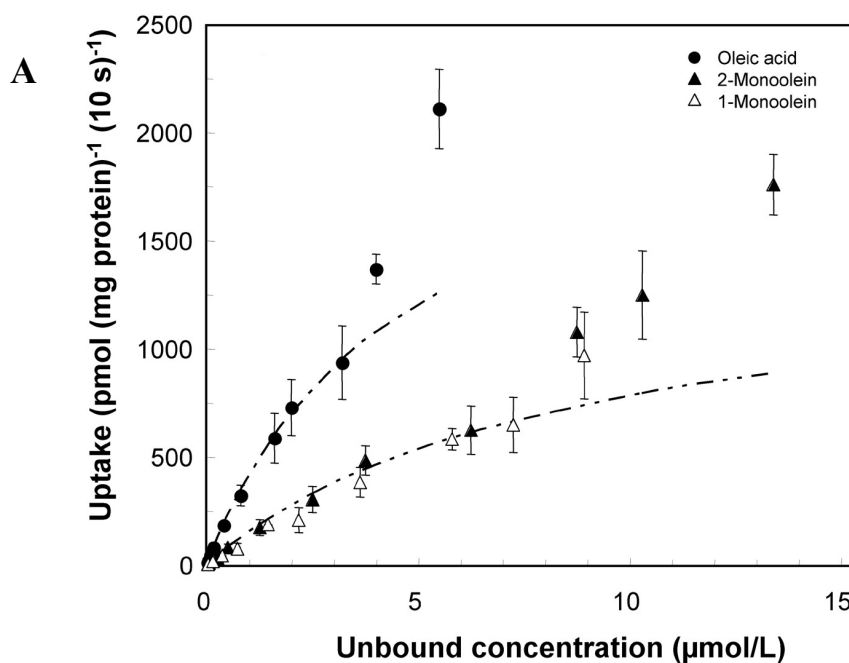
Figure 1-2-A. LCFA and *sn*-2-MG uptake by Caco-2 cells display dual uptake mechanisms. Initial rates of apical taurocholate (TC) -mixed lipid uptake into Caco-2 cells. Caco-2 cells were incubated with TC-mixed radiolabeled lipid (oleic acid, 2-monoolein, or 1-monoolein) for 10 s, and the intracellular radioactivity was measured. Dashed lines show the Michaelis-Menten fits for oleic acid and 2-monoolein. The uptake data for concentrations ≲3.2 μmol/L of unbound oleate and ≲6.5 μmol/L of unbound 2-MG were fit to the Michaelis-Menten equation. Results are means ± SD, *n* = 5. Adapted from Murota, K., and Storch, J. (60)

Figure. 1-2
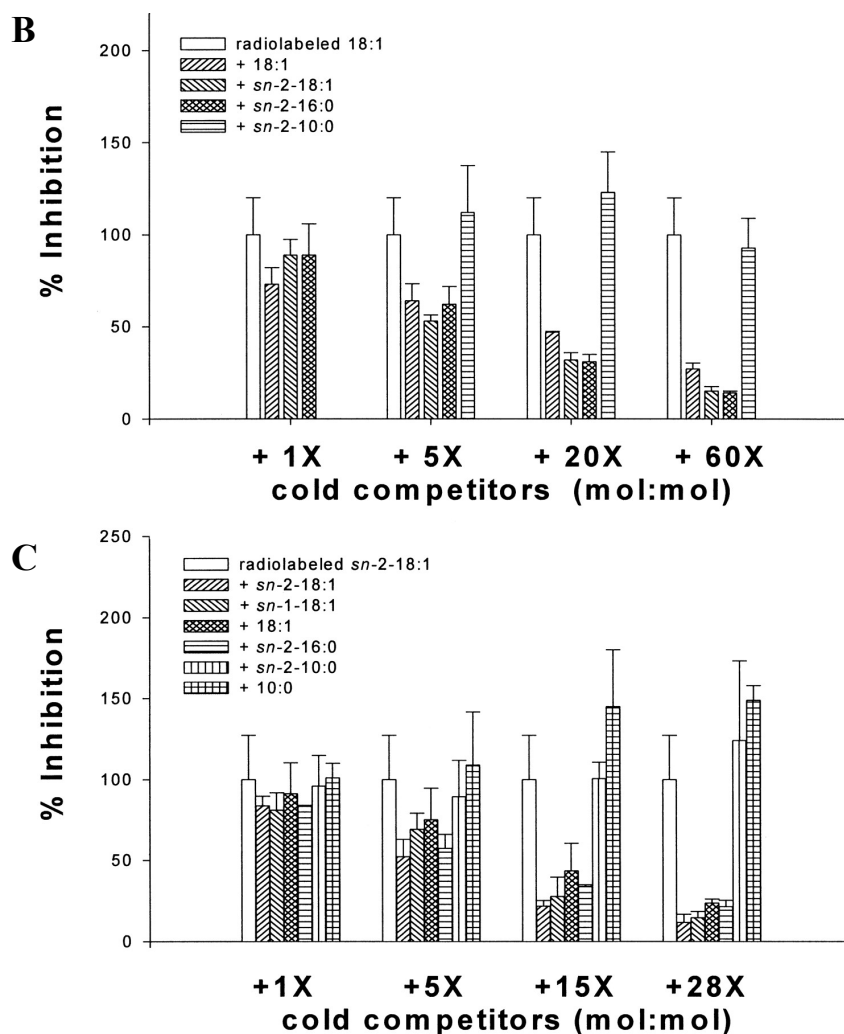
Figure 1-2-B. C. LCFA and *sn*-2-MG uptake by Caco-2 cells (Competitive uptake)

Uptake media were prepared by adding excess unlabeled lipids (below their critical micellar concentration (CMC) to radiolabeled BSA-bound lipids. (B) radioactive 18:1 uptake: competition by unlabeled free fatty acids (FFA) and monoacylglycerols (MG). *sn*-2-16:0, *sn*-2-Monopalmitin; *sn*-2-10:0, *sn*-2-monocaprin; 1× cold competitors = 0.02 μM unbound lipid concentration. (C) radioactive *sn*-2-18:1 uptake: competition by unlabeled FFA and MG. 10:0, Capric acid; 1× cold competitors = 0.03 μM unbound lipid concentration. Results are means ± SD (*n* = 3) from a representative of 3 separate experiments. Adapted from Ho, S.Y., and Storch, J. (58)

distal and villus to crypt gradients, and its expression is up-regulated by high fat feeding (67). A functional study was carried by Nassir *et. al.*(68), using the CD36- null mouse model. Initial rates of FA uptake in CD36 null mice were impaired in proximal but not in distal enterocytes. Furthermore a significant defect in chylomicron secretion in null mice enterocytes was demonstrated (68, 69). These results suggest an essential role for this protein in lipid absorption, via uptake from the AP surface in the proximal intestine as well as, perhaps, directing lipid digestion products to a certain intracellular compartment for the reesterification and secretion process. Finally, FATP4 (fatty acid transport 4), one of the members of the FATP family, is considered as a potential membrane associated FA transporter. Among the isoforms, only FATP4 is expressed in small intestine and it has been localized to the AP surface (57). Its expression in Caco-2 cells was also demonstrated (58). Reduced expression by antisense oligonucleotide treatment resulted in a 50% decrease in FA uptake in primary enterocytes (57). Colocalization with CD36 and acyl-Co A synthase (ACS) activity of FATP4 have been proposed as well (57), further suggesting a potential role for this protein in intestinal FA absorption. However, a recent report questioned the localization of FATP4, suggesting it was not present at the AP surface but rather was found only intracellularly (70).

Although protein-mediated *sn*-2-MG uptake in the enterocyte has not been extensively studied, these candidates might be involved in *sn*-2-MG absorption as well, since a common mechanism for FA and *sn*-2-MG was proposed (58). For example, Stremmel et. al. demonstrated that treatment of jejunal mucosal cells with antibody against FABPpm reduced monopalmitin as well as FA uptake, suggesting FABPpm as a common carrier for FA and MG (59). More direct studies are necessary to understand the precise roles for these trasmembrane proteins as intestinal MG transporters. Collectively, *sn*-2-MG uptake by intestinal epithelial cells appears to be mediated by a dual mechanism, depending on its monomer concentration, as shown for LCFA uptake. Protein mediated uptakes at low monomer concentration of *sn*-2-MG might be facilitated by the same membrane transporters involved in LCFA absorption.

5. Intracellular MG metabolism

5.1 Intracellular MG transport

Intestinal epithelium abundantly expresses two types of cellular fatty acid binding proteins; intestinal fatty acid binding protein (IFABP) and liver fatty acid binding protein (LFABP), which are believed to facilitate intracellular trafficking of fatty acids and other hydrophobic intermediates. Both proteins are highly expressed in proximal and villus rather than distal and crypt regions (71) and LFABP is significantly induced by high fat feeding (72), indirectly suggesting their role in intestinal lipid absorption. Despite the similarities of the two proteins, differences are indicated by their ligand binding properties and ligand transfer mechanisms. One of the major differences between the two FABPs is in their ligand binding specificity. Unlike IFABP, LFABP is able to bind with various molecules such as lysophospholipids, MG, fatty acyl CoA, and eicosanoids (57). MG binding capacity of LFABP was previously demonstrated in our laboratory (73) and our current investigations of LFABP null mice show altered intestinal MG metabolism (Lagakos, W., and Storch, J., unpublished observations), supporting the idea that LFABP may function as an MG transporter in the enterocyte. Distinct functions were further suggested by the absence of compensatory induction in mice carrying each gene deletion (74, 75). Precise roles for both proteins in intracellular lipid trafficking need to be elucidated. To date, there is no other candidate proposed as an intracellular MG binding protein, except LFABP, however more supporting evidence for LFABP as an MG carrier needs to be provided and it will be of interest to identify potential new MG transporters.

5.2 Anabolic process toward TG esterification

Following absorption, *sn*-2-MG and fatty acids are rapidly reincorporated into TG in the endoplasmic reticulum (ER) via the so-called monoacylglycerol (MG) pathway which is catalyzed by two enzyme activities, monoacylglycerol acyltransferase (MGAT) and diacylglycerol acyltransferase (DGAT). The re-esterified TG is assembled into chylomicron particles with

apolipoproteins including B-48, A-1, A-2, and A-4, which are then secreted into the lymphatic circulation (Fig. 1-3-A) (28).

In addition to the MG pathway for TG synthesis, the intestine contains another pathway for TG synthesis, the glycerol-3-phosphate (G3P) pathway, which is the dominant TG synthetic pathway in other tissues such as adipose tissue and liver (Fig. 1-3-B) (28). Depending on the fatty acid and sn-2-MG supply in the enterocyte, the relative contribution of these pathways can vary. After ingestion of a lipid rich meal, 80% of TG resynthesis is thought to be catalyzed by the MG pathway (76, 77).

Recently, genes encoding for enzymes in the MG pathway as well as the G-3-P pathway have been cloned and their properties and functions investigated. In the case of MGAT, several isoforms have been identified. In the mouse, mMGAT1 is highly expressed in kidney, stomach and adipose tissue but not in small intestine, where the highest MGAT activity is found (78). mMGAT2 protein has 52.5% identity with mMGAT1 and it is exclusively expressed in small intestine (79, 80). In humans, three MGAT genes have been identified and two distinct forms, hMGAT2 and 3, are expressed in the gastrointestinal tract, suggesting a critical role for MGAT in dietary fat absorption (79, 81). Subcellular localization of all MGAT enzymes is known to be in the ER based on immunocytochemical analysis (82).

Two DGAT genes, DGAT 1 and 2, have been identified. Both are expressed in the enterocyte (83, 84). DGAT1 is part of the acyl CoA : cholesterol acyltransferase (ACAT) 1 and 2 family, possessing putative multiple transmembrane domains (83). DGAT2 does not share sequence homology with DGAT1, but is rather part of an independent family that includes other acyltransferases such as MGAT1, 2, and 3 (84). Different biochemical and physiological properties of the two DGAT gene products have been demonstrated, suggesting distinct roles. For example, DGAT1 has multiple acyltransferase activities, synthesizing wax ester, retinyl ester, and DG as well as TG (85), whereas DGAT2 does not catalyze substrates other than DG. DGAT1 null mice

Figure. 1-3
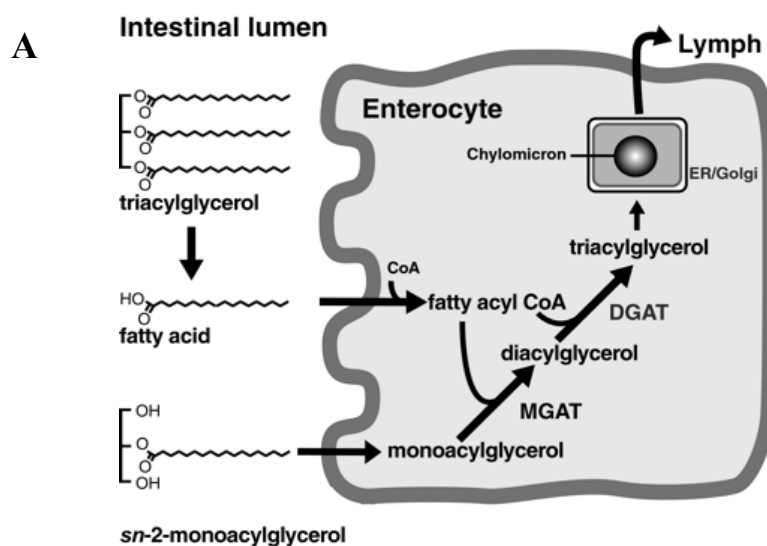
Figure 1-3-A. Intestinal MG metabolism (TG resynthesis by MGAT pathway)
Adapted from Yen, C.-L., and Farese, Jr., R.V. (79)
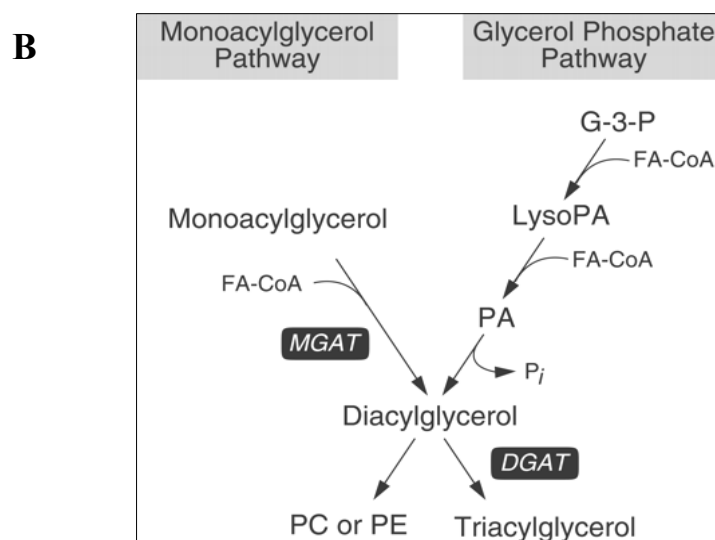
Figure 1- 3-B. Two TG reesterification pathways in small intestine
Adapted from Yen, C.-L., and Farese, Jr. , R.V. (78)

exhibit a modest reduction in liver and adipose tissue TG content when animals are fed a high fat diet, resulting in an obesity- resistant phenotype (86). In contrast, DGAT2 deletion affects the mouse more critically; mice die within a few hours after birth due to lipopenia (87). Despite the abundant expression of both DGAT genes in the small intestine, precise roles for each isoforms are currently not well understood. Results from global deletions of each gene show that DGAT1 deficiency does not quantitatively affect intestinal TG reesterification and chylomicron synthesis, even with a high fat diet. Only a reduced rate of dietary lipid absorption was found (25), suggesting that multiple mechanism are present for intestinal TG resynthsis. However, the role of DGAT2 in intestinal lipid metabolism was unable to be addressed using the DGAT2 null due to the lethality (87). Intestinal specific deletion of DGAT2 will provide more valuable insight into its function in intestinal lipid metabolism.

In the cellular compartment, the catalytic sites of each isoform of MGAT and DGAT might be different, with one facing toward the cytosol and the other toward the ER lumen. In 1997, before the two DGAT genes were identified, two distinct DGAT activities on both sides of the ER membrane were reported by Zammit and coworkers in rat liver microsome, one an overt DGAT catalyzing cytosolic TG synthesis and the other a latent DGAT associated with TG synthesis for VLDL secretion (88, 89). Although it remains to be examined whether these activities are derived from the separate DGAT genes identified, the recent topological analysis of DGAT2 by Stone et. al. suggests that DGAT2 catalytic residues face toward the cytosolic compartment (90). Though the orientation of the DGAT1 catalytic sites has not yet been addressed, it is possible that separate subcellular catalytic sites of DGAT1 and DGAT2 are present. The different localizations of DGAT 1 and 2 have been also suggested by immunocytochemistry following recombinant expression of the two DGAT genes as well as the three MGAT genes in Cos-7 cells (82). In contrast to the strict colocalization of DGAT2 and all MGAT isoforms with an ER marker, more widespread distribution of DGAT1 expression was observed in transfected Cos-7 cells (82). All MGAT isoforms were found to be ER localized according to Cao *et.al.*'s observation (82). However,

topological studies of MGAT 2 and 3, both present in human intestine, need to be done to address the orientation of the catalytic sites, as has been done for DGAT2. The precise localization and especially the exact function of each isoform of DGAT and MGAT in intestinal TG synthesis remains to be elucidated in detail.

Multiple substrate specificities of MGAT and DGAT enzymes have been suggested by several investigators, further supporting functional differences. Cao *et.al.* reported DGAT activities in all three MGAT gene products in the order MGAT3> MGAT1> MGAT2, in addition to their MGAT activities (82). Yen *et. al.* also demonstrated that DGAT1 posseses MGAT as well as DGAT activities (85). The presence of redundant acylating enzymes, as well as the possibility that at least some of the enzymes are capable of serial acylation, likely reflects the physiological importance of TG reesterification in the small intestine.

5.3 Catabolic processing: MG hydrolysis and intestinal MGL expression

In general, intestinal MG metabolism has been thought to involve only the anabolic fate of TG re-esterification via the MGAT pathway. However the presence of a MG hydrolytic activity in small intestine was reported a few decades ago (91) and partial purification of MG lipase from rat intestinal mucosa was attempted (92). It was also noticed that the majority of MGL activity was found in the microsomal fraction of the intestinal mucosa, suggesting its localization (91). Nevertheless, there was no further investigation in terms of functional analysis and regulation of this enzyme in the enterocyte. In 1997, Holm and her collegues cloned the MG lipase (MGL) gene by screening a mouse adipocyte cDNA library, and identified the residues of a catalytic triad (93). A detailed genomic organization of mouse MGL was performed, which demonstrated that the gene is localized on chromosome 6, and the coding region is found on seven exons (94). The MGL mRNA transcript was found in various tissues such as liver, testis, kidney, adipose tissue, and skeletal muscle (93), but its expression in the small intestine was not reported. MG hydrolysis in the enterocyte has again been confirmed recently (16). After incubation of ^{3}H-*sn*-2-MG labeled on the

fatty acyl moiety, at either the apical or basal lateral surface of Caco-2 cells, a substantial amount of radioactivity was recovered in the unesterified fatty acid fraction (Table 1-1) (16). *sn*-2-MG metabolism studies using rats and mice showed a similar result, implicating the existence of *sn*-2-MG hydrolysis within the enterocyte (17). MGL mRNA expression was detected in Caco-2 cells and rodent small intestine (Fig.1-4), supporting the idea of catabolic processing of *sn*-2-MG in the intestine, in addition to the well known anabolic processing (16).

Enzyme reactions mediated by MGL and MGAT are shown in Fig. 1-5. The regulation and function of the intestinal MGL were explored to understand its physiological significance in lipid metabolism, as described in chapters 2 and 3.

6. Possible functions of MGL

The function of MGL in intestinal epithelium is currently unknown. MGL seems to have various functions according to its tissue localization. In adipose tissue, the physiological function of MGL in lipid metabolism is thought to be the complete hydrolysis of TG after the action of hormone sensitive lipase and desnutrin (also known as ATGL), which produce *sn*-2-MG and fatty acids (95, 96). Many TG lipases such as lipoprotein lipase, hormone sensitive lipase and pancreatic lipase are preferentially able to hydrolyze fatty acids esterified at the *sn*-1(3)-position but not the *sn*-2-positon. MGL has no activity against TG or DG but can cleave *sn*-2-MG as efficiently as it does *sn*-1(3) MG, allowing for the complete breakdown of an intermediate in the process of TG hydrolysis, to release free FA and free glycerol (Fig. 1-5).

It has been shown that the adult rodent liver expresses a considerable amount of MGL (93). Hepatic MGL has been purified from rat and chicken liver microsomal fractions and separated as a distinct enzyme from other esterases present in liver microsomes (97, 98). Most studies of hepatic MGL have focused on its purification and biochemical characterization, without further physiological characterization of this enzyme. Thus, the precise function of hepatic MGL remains to be defined.

Table. 1-1

	Percentage of total incorporation								
Lipid Class	2h			6h			24h		
	TC(AP)	BSA(BL)	BSA(AP)	TC(AP)	BSA(BL)	BSA(AP)	TC(AP)	BSA(BL)	BSA(AP)
CE	4 ± 1	0.4 ± 0.1	0.1± 0.3	1.0± 0.3	2.0 ± 1.1	1.0 ± 0.5	1.0± 0.3	1.0± 0.5	2.0± 1.1
TG	37 ± 3	20 ± 6	32 ± 6	57 ± 8	34 ± 4	46 ± 2	73 ± 8	58 ± 15	49 ± 8
FA	21 ± 3	19 ± 7	21 ± 5	23 ± 3	19 ± 3	17 ± 2	8 ± 2	14 ± 7	15 ± 7
DG	10 ± 7	9 ± 1	10 ± 3	4 ± 2	10 ± 5	5 ± 1	11 ± 6	4 ± 2	3 ± 1
MG	10 ± 2	12 ± 5	11 ± 2	5 ± 1	6 ± 1	6 ± 1	3 ± 1	2 ± 1	6 ± 3
PL	18 ± 4	40 ± 4	26 ± 6	10 ± 3	29 ± 3	25 ± 1	4 ± 3	21 ± 3	25 ± 3

Table 1-1. *Sn*-2-MG metabolism in Caco-2-cells.

Caco-2 cells grown on Tranwells filters for 14 to 18 days after confluence were incubated either with 30 uM ^{3}H-*sn*-2-monoolein complexed to 100 uM BSA (either at the AP or at the BL surfaces) or with 2 mM mixed with 10 mM taurocholate (at the AP surface) for various times. The cellular metabolites of ^{3}H- *sn*- 2 monoolein were determined by TLC analysis. [a]Mean % of total radioactive lipids incorporated into metabolite $\pm$ S.E., n=9. Adapted from Ho, S.Y., and Storch, J. (16)

Figure. 1-4
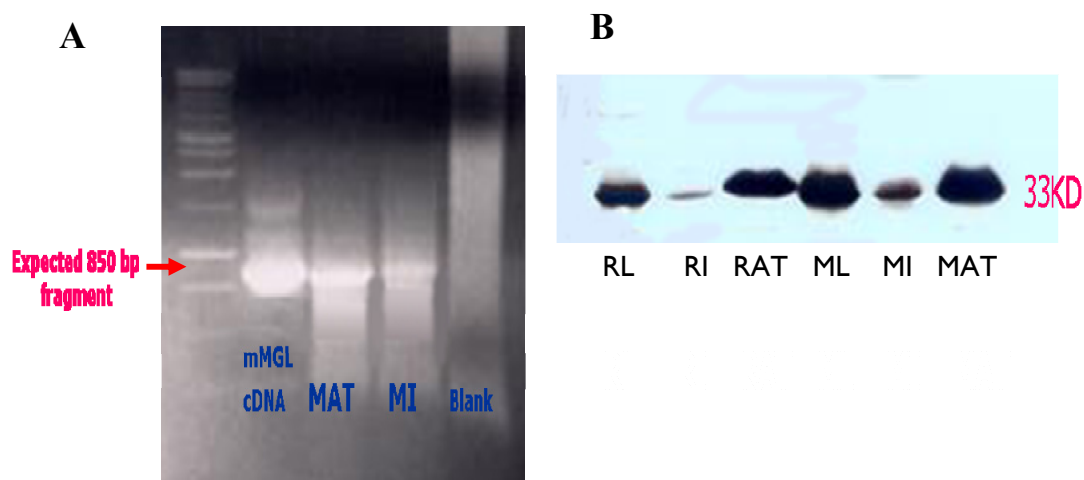
Figure 1-4. MGL expression in rodent small intestine. (A) MGL mRNA detection by RT-PCR. Mouse adipose tissue RNA was used as a positive control Expected 850 bp fragment was found in mouse intestine, showing its expression. (B) MGL protein expression by Western analysis. 50ug of tissue protein loaded for each sample and probed with anti-m MGL antibody. Expected 33Kd MGL protein was dectected in rodent intestine. Liver and adipose tissue were used as a positive control. RL; rat liver, RI; rat intestine, RAT; rat adipose tissue, ML; mouse liver, MI; mouse intestine, MAT; mouse adipose tissue.

Recently another physiological function of MGL has been proposed in the brain, where it has been suggested to be a primary regulator of *sn*-2-arachidonoyl glycerol (2-AG) signaling action (99). 2-AG is a monoacylglycerol believed to work as a signaling molecule by binding to cannabinoid (CB) receptors, thereby modulating neuronal activity in the central nervous system (100). MGL overexpression via adenovirus transfection in neuronal cells resulted in the attenuation of stimulus-dependent 2-AG accumulation, indicating that MGL is participating in endocannabioid (EC) inactivation by reducing CB receptor ligand (99). The biological function of the EC system seems not to be restricted to the central nervous system (CNS), but also to be involved in cardiovascular, intestinal and reproductive systems (100). One of the main functions of the EC system is in regulating energy balance, mediated by controlling food intake as well as metabolic rate (101) . Activation of the EC system works as a hunger signal, increasing food intake. In contrast, blockage of EC signaling, for example, treatment with rimonabant, a selective CB1 receptor antagonist, results in reduced appetite and weight loss (101). Though it is unknown whether *intestinal* MGL is participating in EC signaling, modulation of signaling pathways should be considered as a potential function. Functional aspects of intestinal MGL and additional discussion of the EC system are presented in chapter 3.

7. The GI tract and energy balance: gut satiety signals and appetite stimulating signals

In addition to its function in digestion and absorption, the GI tract has another important function in maintaining energy balance, by sensing and communicating nutritional status to the brain and other peripheral tissues. In 1973, cholecytokinin (CCK) was reported as the first gut hormone, and was shown to be associated with appetite regulation (102). This prompted more investigation of GI signaling functions in energy balance. In recent decades, knowledge of GI endocrine functions has expanded rapidly, along with the discovery of many gut satiety regulating hormones.

Figure. 1-5
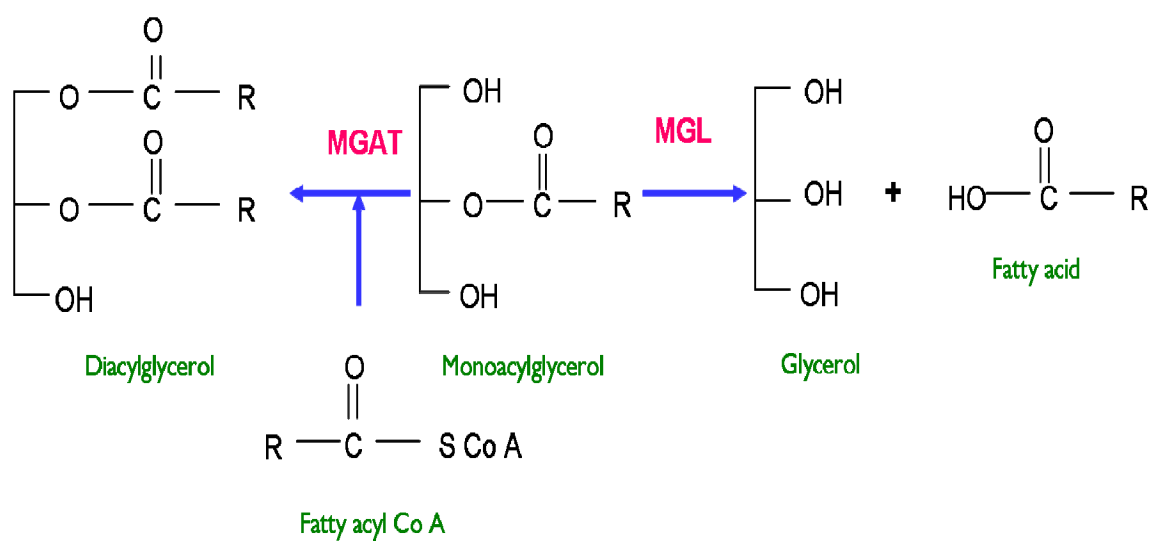
Figure 1-5. Enzymatic reactions for MGAT and MGL

The GI tract signals satiety or hunger to the brain via neural and endocrine mechanisms (Fig. 1-6). The enteric nervous system participates in the gut-brain axis for satiety signals via vagal afferents. By this neuronal circuit, information related to stomach distention and hormonal milieu in the bowel is transported to the nucleus tractors solitarius in the hindbrain to control feeding, gastric emptying, and metabolic rate (21). In addition to this neural pathway, gut hormones send hunger or satiety signals to the brain as well. The hypothalamus, in particular, integrates these gut signals with long term signals such as insulin and leptin, and regulates energy homeostasis by controlling food intake and metabolic rate. The major orexigenic and anorexic gut hormones are summarized below.

7.1 Orexigenic hormones

7.1.1 Ghrelin

Ghrelin is an appetite stimulating, 28- amino acid acylated hormone, primarily synthesized in the stomach. The acylation of ghrelin on serine at 3 with an octanoyl group is critical for binding to the ghrelin receptor, also known as the growth hormone secretagogue receptor (GHSR), and for exerting its orexigenic effects (103). GHSR is present in the gut, as well as in the vagus nerve, brain, and pituitary gland (104, 105). Plasma ghrelin levels rise during starvation or before a meal, and decline within an hour of food intake (21). The orexigenic effect of ghrelin is known to be mediated by activation of neuropeptide Y (NPY) and agouti-related protein (AgRP)-expressing neurons in the arcuate nucleus of the hypothalamus, as well as by activation through the vagal neuronal circuit (106) (Fig. 1-6). The precise mechanism of ghrelin secretion is not clearly understood, though food intake seems one of the regulators. Fat digestion and LCFA were suggested as suppressors of ghrelin release (107). The physiological impact of ghrelin on long

Figure. 1-6
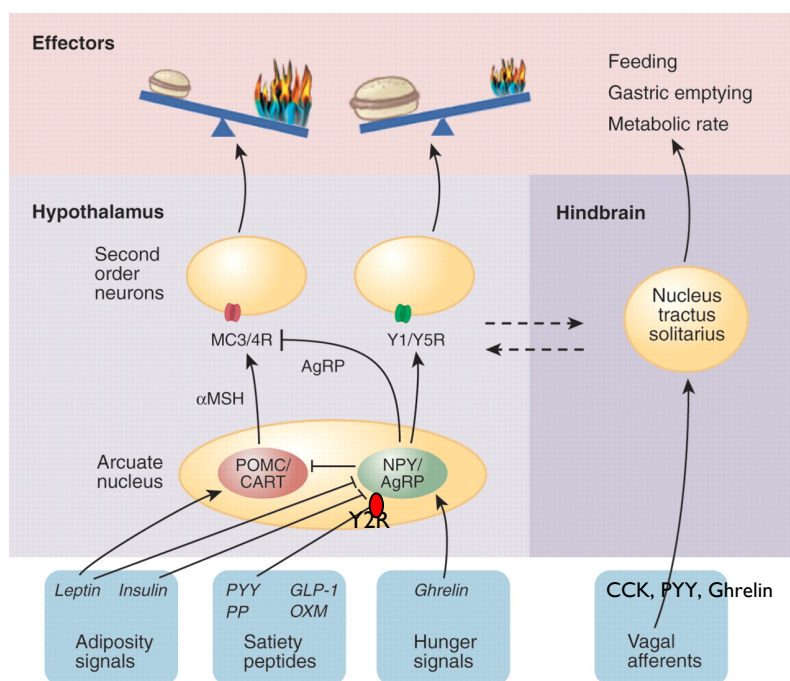
Figure 1-6. Gut Satiety signals. Simplified representation of potential action of gut peptides on the hypothalamus. Primary neurons in the arcuate nucleus contain multiple peptide neuromodulators. Appetite-inhibiting neurons (red) contain pro-opiomelanocortin (POMC) peptides such as melanocyte-stimulating hormone (MSH), which acts on melanocortin receptors (MC3 and MC4) and cocaine- and amphetamine-stimulated transcript peptide (CART), whose receptor is unknown. Appetite-stimulating neurons in the arcuate nucleus (green) contain neuropeptide Y (NPY), which acts on Y receptors (Y1 and Y5), and agouti-related peptide (AgRP), which is an antagonist of MC3/4 receptor activity. The anorexic effect of PYY is known to be mediated by binding to Y2 receptors in the hypothalamus to inhibit NPY neural activation. Integration of peripheral signals within the brain involves interplay between the hypothalamus and hindbrain structures including the NTS, which receives vagal afferent inputs. Inputs from the cortex, amygdala, and brainstem nuclei are integrated as well, with resultant effects on meal size and frequency, gut handling of ingested food, and energy expenditure. Modified from Badman, M.K., and Flier, J.S. (21)

term energy balance is controversial. Surprisingly, deletion of ghrelin or its receptor did not affect either food intake or body weight, and obese human have low circulating ghrelin levels (21). In contrast, chronic ghrelin administration via the intracerebroventricular route promoted food intake and adiposity in rats (108). Moreover, the typical postprandial drop in plasma ghrelin is absent in obese subjects, suggesting its role in the development of obesity (109, 110). More recently, Zorrilla *et.al.* demonstrated an interesting new approach to treatment of obesity, by ghrelin vaccination using a rodent model (111). Following a vaccination of adult rats with ghrelin immunoconjugates significantly reduced food intake, relative adiposity, and body weight gain (111). However, the potential for anti-ghrelin treatment for obesity awaits more clinical studies.

7.2 Satiety hormones

7.2.1 Cholecytokinin (CCK)

CCK is a satiety hormone synthesized and secreted into the circulation by mucosal endocrine cells in the proximal intestine upon food ingestion. It is composed of varying numbers of amino acids according to post-translational modification of the CCK gene product (112). CCK58, CCK33, and CCK8 are considered to be biologically active forms (112). It prompts gallbladder and pancreatic secretion into the proximal gut, and reduces gastric emptying, creating optimal conditions for digestion and absorption in the small intestine (113). By binding its receptor in the vagus nerve, CCK reduces meal size and inhibits gastric emptying (21). CCK infusion suppressed food intake via earlier meal termination in humans (114), whereas antagonist treatment caused higher food intake (115).

7.2.2 Peptide YY (PYY)

PYY is a 36 amino acid satiety peptide hormone, forming a family with NPY and pancreatic polypeptide (PP). It is released postprandially by the distal small intestine and colon, acting as an "ileal break" to slow down gastric emptying (21). The N-terminal truncated PYY_{3-36} is

the predominant form present in the body and is biologically more potent than full length PYY (106). Its anorexic effect is known to be mediated by binding to Y2 receptors in the hypothalamus to inhibit NPY neural activation (21), as well as by working through the vagal nervous system (116). Though the PYY null mouse does not show straightforward phenotypes (106), chronic and peripheral infusion of PYY_{3-36} in rodents and humans suppressed appetite and body weight (117-119), suggesting the possibility for obesity therapeutics.

7.2.3 Glucagon-like peptide-1 (GLP-1)

In the gut, the preproglucagon gene produces two satiety peptides via a posttranslational mechanism; one is GLP-1 and the other is oxyntomodulin (OXM). GLP-1 is secreted into the plasma following food ingestion, and it seems that the bulk of ingested food itself induces its production, rather than specific nutrients (120). GLP-1 receptors are widely expressed in various tissues such as pancreatic islets, brain, heart, kidney, and the GI tract (21, 121). Diverse functions of GLP-1 in energy and glucose metabolism have been reported. Blockage of GLP-1 receptors by exendin, a specific GLP-1 antagonist, caused hyperphagia and the development of obesity (21, 106). Secreted GLP-1 is readily inactivated by dipeptidyl peptidase 4 (DPP4). Therefore, stabilizing GLP-1 is a key for maintaining its anorexic effect. Peripheral infusion of Exendin-4, a long acting DPP4-resistant GLP-1 agonist, significantly reduced food intake and body weight in the rat (122). In addition to acting as an appetite suppressor, GLP-1 also inhibits gastric acid secretion and stimulates postprandial insulin release. Pancreatic beta cell neogenesis by GLP-1 has been also proposed (123). Clinical trials of exenatide, a long acting GLP-1 receptor agonist, showed a potential for regulating body weight and glucose homeostasis in type 2 diabetes and it has been recently approved by the FDA as a medication for type 2 diabetes (124, 125).

7.2.4 Oxyntomodulin (OXM)

In addition to GLP-1, OXM is the other gut peptide produced from the preproglucagon gene, and it too has an anorexic effect. OXM is known to bind to the GLP-1 receptor and inhibits appetite efficiently as GLP-1 does, although its relative binding affinity is weaker than GLP-1 (106). Chronic central or peripheral injection of OXM resulted in reduced food intake and weight gain in rats and humans (126, 127). OXM was suggested not only to control appetite, but also to increase energy expenditure, as pair-fed rats treated with OXM lost more weight than controls (128). Parlevliet *et.al.* showed that OXM also has a beneficial effect on glucose metabolism, by elevating glucose-induced insulin secretion (129). Unique features of OXM relative to GLP-1 have not yet been reported, except that OXM stimulates a different area of the brain than GLP-1(21).

7.2.5 Obestatin

Obestatin is an anorexic peptide hormone, primarily synthesized by stomach and small intestine. It is encoded by the same gene producing ghrelin, an orexigenic gut peptide, exerting an opposite effect on appetite (130). The intraperitoneal and intracerebroventricular injection of obestatin in mice suppressed appetite, gastric emptying, and jejunal muscle contraction (131). Obestatin binds to the orphan G protein-couple receptor, GPR39, which is a distinct from the ghrelin receptor, thus two peptides from same gene exert opposite physiological effects through their distinct receptors (131). GPR39 is expressed in various regions of the brain, as well as in small intestine, stomach, pancreas, thyroid, and colon (132).

7.3 Other gut appetite regulating signals

7.3.1 Oleoylethanolamide (OEA)

OEA is a naturally occurring lipid mediator, synthesized from phospholipids in various tissues such as liver, brain, adipose tissue, and small intestine, which functions as a satiety signal and regulator for energy metabolism. Though its structure is similar to anandamide (Fig. 1-7), one of the endogenous cannabinoids, it is unable to bind to cannabinoid receptors, but rather binds to

peroxisome proliferateor-activated receptor-α (PPAR-α), exerting anorexic effects in the small intestine (133). Intestinal OEA levels significantly rise after food ingestion, and its administration clearly resulted in reduced food intake and body weight in wild type mice, but not in PPAR-α KO mice, demonstrating its function as a satiety signal via PPAR-α activation (133). In addition to appetite regulation, OEA stimulates lipolysis in adipose tissue and increases FA oxidation in muscle and liver, also mediated by PPAR-α (134). An effect of OEA in intestinal lipid metabolism was also suggested by Yang *et.al.*, who demonstrated that OEA induced CD36/FAT expression in both small intestine as well as adipose tissues, and increased FA uptake in enterocytes (135).

7.3.2 Endocannabinoids (EC)

The psychotropic and appetite stimulating properties of the natural compound, Δ9-tetrahydrocannabinol (Δ9-THC) derived from Cannabis sativa, also known as marijuana, have been known for centuries without knowing its mechanisms of action (101). The first receptor cannabinoid receptor 1 (CB1) for this compound was only identified in the early 1990s (136), followed by discovery of its isoform, the CB2 receptor (137). CB receptors are members of the G protein-coupled membrane receptor family. CB1 is highly expressed in brain and also other peripheral tissues including liver, adipose tissue, and small intestine, and CB2 is abundantly present in immune cells (101, 137, 138). Along with the discovery of CB receptors, two main endogenous ligands for CB receptors were also identified; one is N-arachidonoyl ethanolamide (anandamide, AEA) (139), and the other is 2-arachidonoyl glycerol (2-AG) (Fig. 1-7) (140, 141). Our knowledge of the EC system, including mechanisms for biosynthesis and degradation of endocannabinoids (Fig. 1-8-A) and its various physiological actions (Fig. 1-8-B), has been markedly accelerated in the recent decade, and one of the key therapeutic applications of EC system modulation is in obesity treatment, via appetitive and metabolic regulation (101, 142).

The orexigenic effect of brain endocannabinoids has been well established by many studies (Fig. 1-8-B)(143-146). For example, administration of cannabinoids into the hypothalamus triggers

Figure. 1-7

2-arachidonoyl glycerol (2-AG)

Arachidonocylethanolamide (AEA), Anadamide

Oleoylethanolamide (OEA)
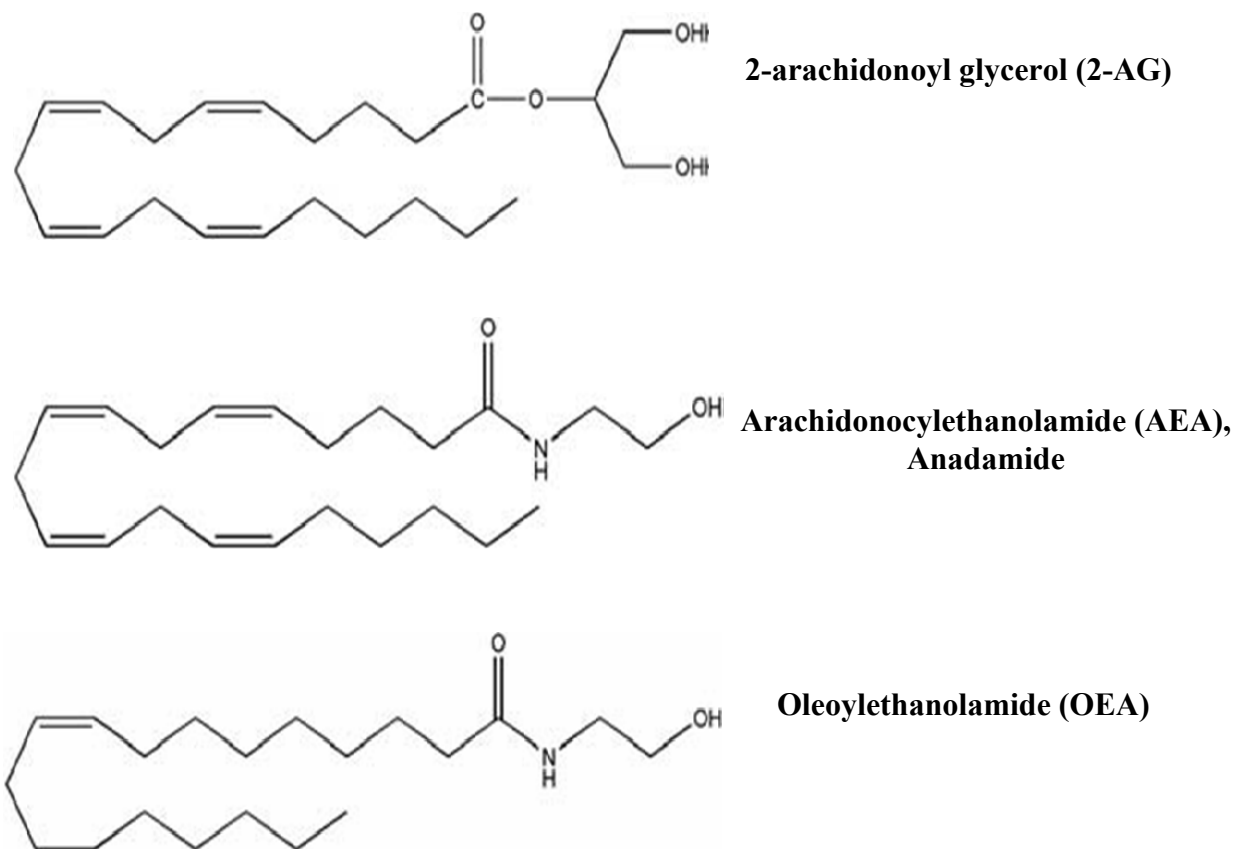
Figure 1-7. Structure of endocannabinoids (2-AG and AEA) and OEA

hyperphagia (143, 144). Food deprivation increased 2-AG levels in the hypothalamus, inducing appetite, and returned to normal levels upon feeding (145, 146). Further, it has been reported that the EC system regulates the expression or activities of other hypothalamic appetitive mediators, including corticotrophin-releasing hormone (CRH), exerting orexigenic signals, and melanin-concentrating hormone (MCH), triggering anorexic effects (147, 148). EC signaling is regulated by biosynthesis and degradation of CB receptor ligands (Fig. 1-8-A). As mentioned earlier, brain MGL is the key enzyme for 2-AG degradation via hydrolysis (99, 149), and fatty acid amide hydrolase (FAAH) is responsible for AEA degradation (150).

As noted above, EC signaling is not only restricted to brain, but also exerts various physiological effects on many peripheral tissues (Fig. 1-8-B) (101, 142, 151, 152). In liver and adipose tissue, activation of the EC system triggers lipogenesis (101, 153, 154). CB1 expression was detected in the enteric plexus of the gastrointestinal tract (155, 156), and the two major endocannbinoids, 2-AG and AEA, are present in the small intestine (140, 157). Functions for the gut EC system have emphasized gastroprotection against inflammation and control of intestinal motility (158, 159), but there is emerging evidence that the EC system in the gut also mediates eating behaviors (152, 157, 160). A significant increase in anandamide (AEA) levels in the small intestine was reported during starvation (152), and it has been shown that fasting increased and feeding decreased CB1 expression in the vagus nerve termini innervating the gastrointestinal tract (160). In contrast to AEA action, the significance of intestinal 2-AG in EC signaling and appetite regulation has not been well investigated. It is also unknown whether intestinal MGL functions as an EC signaling regulator, as shown in the central nervous system. These aspects will be discussed in further depth in chapter 3.

Figure. 1-8

A
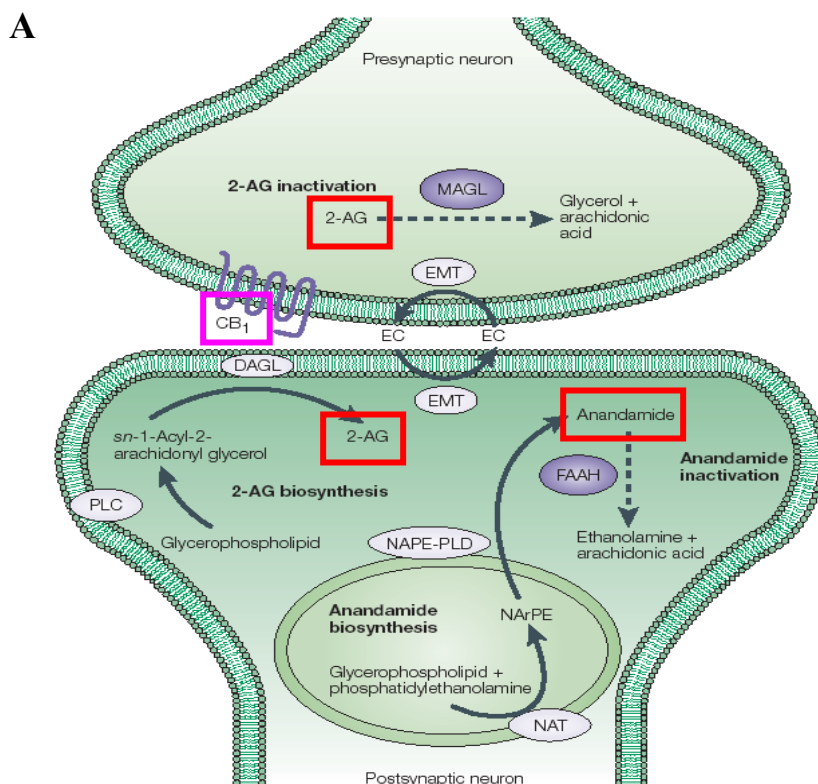
Figure 1-8-A. Biosynthesis and degradation pathways of endocannabinoids. The enzymes for degradation of 2-arachidonoylglycerol (2-AG) and anandamide (AEA) inactivate EC signaling cascade as depicted, MAGL and FAAH, respectively. 2-AG biosynthesis is carried out by phospholipases C (PLC) and the *sn*-1-selective diacylglycerol lipases (DAGLs). N-acyltransferase (NAT) and N-acylphosphatidyl-ethanolamine-specific phospholipase D (NAPE-PLD) are responsible for AEA biosynthesis. Finally, an as-yet uncharacterised endocannabinoid membrane transporter (EMT) seems to facilitate both endocannabinoid release and re-uptake. Endocannabinoids are boxed in red and the CB1 receptor is in pink. Adapted from Di Marzo *et. al.* (100)

Figure. 1-8

B

Δ⁹-Tetrahydrocannabinol
Anandamide (AEA)
2-Arachidonoylglycerol
(2-AG)

CB1

Brain	Adipose Tissue	Muscle	Liver	GI Tract

Appetite Regulation (Orexigenic signal)

Increase Lipogenesis

Decrease Glucose Uptake

Increase Lipogenesis

Appetite Regulation (Orexigenic signal), Decrease gut motility
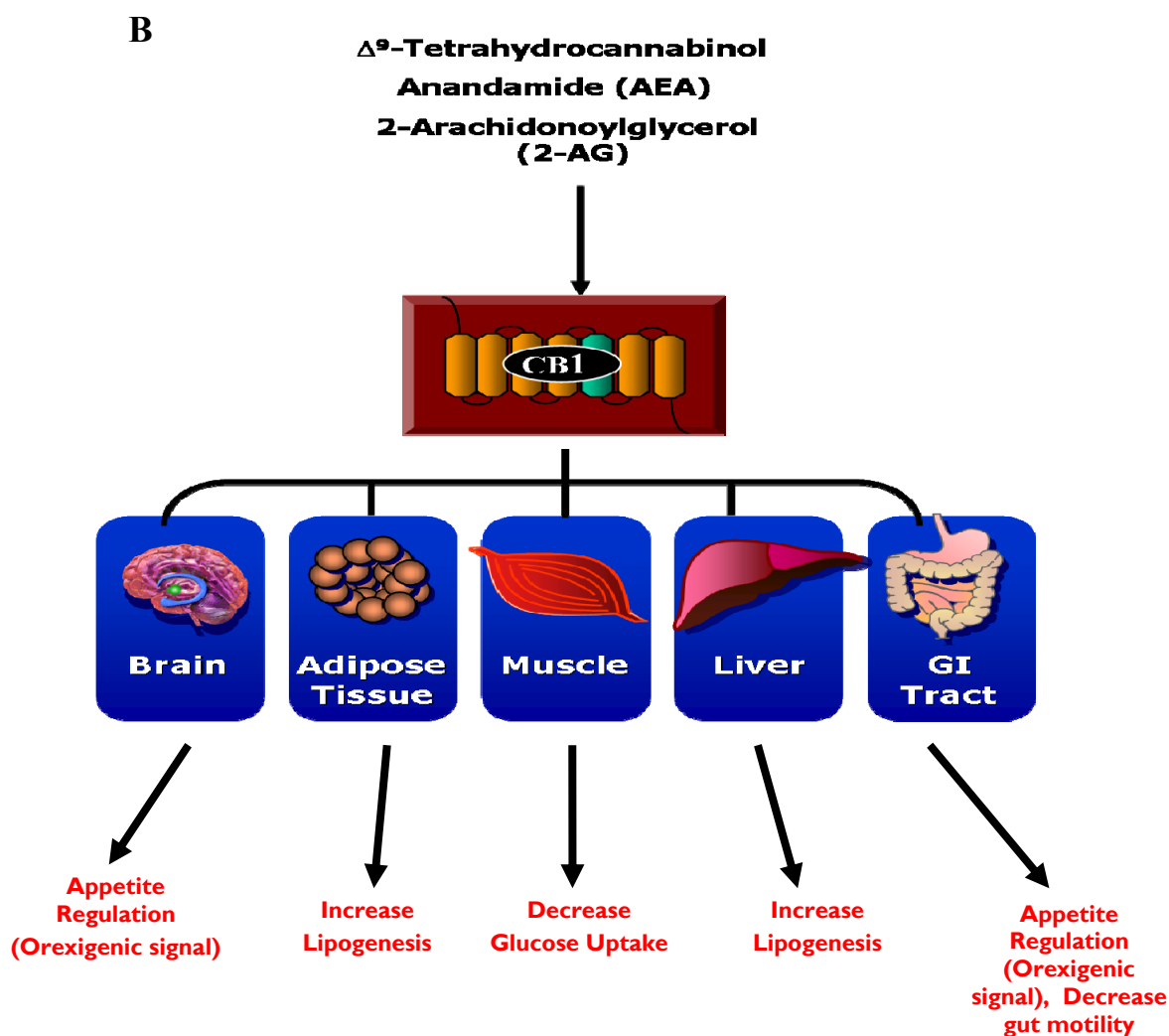
Figure 1-8-B. Physiological functions of EC systems. EC systems play an important role in energy balance via appetite and metabolic regulation. CB1 receptors are present centrally in the brain, and peripherally in adipose tissue, liver, skeletal muscle and the gastrointestinal tract. In the brain, activation of the EC system triggers hyperphagia and decreases metabolic rate. Peripherally, the EC system stimulates lipogenesis in adipose tissue and the liver, and a reduced glucose uptake in skeletal muscle was observed upon the activation of EC system. All of these central and peripheral effects suggest that the hyperactivity in theEC system could lead into an increased risk of obesity and metabolic syndrome. Modified from Lipids online slide library in Baylor College of Medicine. http://www.lipidsonline.org

8. Specific aims of the studies

Intestinal MG metabolism has been well characterized as part of the dietary lipid assimilation process, as discussed earlier in this chapter. In addition, a potential for catabolic processing of MG in the enterocyte has also been proposed, based on its hydrolysis in Caco-2 cells and rodent intestine, as well as the presence of monoacylglycerol lipase (MGL) gene expression. Although the intestinal enterocyte metabolizes large quantities of MG following dietary fat ingestion, the regulation of MG metabolism and the function of this MG hydrolytic activity have not been explored. Therefore, the objective of this research is to understand the regulation and function of the two MG metabolizing enzymes in the small intestine, MGL and MGAT2 and, further, to elucidate the impact of intestinal MG metabolism on whole body energy homeostasis. The specific aims were:

1. To explore the regulation of intestinal MG metabolizing enzymes during development and by nutritional status: Regulation of the two known murine MG metabolizing enzymes, MGL and MGAT2, was investigated by examining their mRNA expression, protein expression, and activities in C57BL/6 mouse small intestine, as well as liver and adipose tissues, during development and under nutritional modifications.

2. To understand the function of intestinal MGL in the small intestine and in whole body energy homeostasis: The functional analysis of intestinal MGL was explored using targeted overexpression of MGL in mouse small intestine. Tissue specific expression of MGL was derived from the IFABP promoter, which directs expression to the small intestine villus cells, exclusively. Potential roles for intestinal MGL were assessed by phenotypic analyses of the transgenic mice relative to non-transgenic littermates.

Chapter 2.

Regulation of Intestinal Monoacylglycerol (MG) Metabolism:

Developmental and Nutritional Regulation of Monoacylglycerol Lipase

(MGL) and Monoacylglycerol Acyltransferase (MGAT)

1. Abstract

Intestinal monoacylglycerol (MG) metabolism is well known to involve its anabolic reesterification to triacylglcyerol (TG). We recently provided evidence for enterocyte MG hydrolysis, and demonstrated expression of the monoacylglcyerol lipase (MGL) gene in human intestinal Caco-2 cells and rodent small intestinal mucosa. Despite the large quantities of MG derived from dietary TG, the regulation of MG metabolism in the intestine has not been previously explored. In the present studies, we examined the mRNA expression, protein expression, and activities of the two known MG metabolizing enzymes, MGL and MGAT2, in C57BL/6 mouse small intestine, as well as liver and adipose tissues, during development and under nutritional modifications. Results demonstrate that MG metabolism undergoes tissue-specific changes during development. Marked induction of small intestinal MGAT2 protein expression and activity were found during suckling. Moreover, while substantial levels of MGL protein and activity were detected in adult intestine, its regulation during ontogeny was complex, suggesting post-transcriptional regulation of expression. In addition, during the suckling period MG hydrolytic activity is likely to derive from carboxyl ester lipase (CEL) rather than MGL. In contrast to intestinal MGL, liver MGL mRNA, protein and activity all increased 5-10 fold during development, suggesting that transcriptional regulation is the primary mechanism for hepatic MGL expression. Three weeks of high fat feeding (40% kcal) significantly induced MGL expression and activity in small intestine relative to low fat feeding (10% kcal), but little change was observed upon starvation, suggesting a role for MGL in dietary lipid assimilation following a high fat intake.

1. Introduction

   Sn-2-monoacylglycerol (MG) is one of the major digestive products of dietary triacylglycerol (TG). Along with fatty acid, it is formed by the action of pancreatic triacylglycerol lipase (PTL) in the intestinal lumen, since PTL preferentially cleaves the *sn*-1 and 3 positions of TG (28). Both hydrolysis products are absorbed as monomers across the apical membrane of the intestinal epithelial cell (28, 58). The mechanism of *sn*-2-MG uptake into the enterocyte has been demonstrated to be a saturable function of the monomer concentration of *sn*-2-MG at both apical and basal lateral surfaces of the cell, suggesting carrier mediated uptake (58, 60). At higher concentrations, a diffusional uptake pathway is also apparent (58, 60). After absorption, *sn*-2-MG is rapidly reincorporated into TG in the endoplasmic reticulum (ER) via the so-called monoacylglycerol acyltransferase (MGAT) pathway, which is catalyzed by two enzymes, MGAT2 and diacylglycerol acyltransferase (DGAT). Two DGAT isoforms (DGAT1 and 2) have been identified, and both are expressed in small intestine (83, 84). In addition to the MG pathway, the intestine can also synthesize TG via the glycerol-3-phosphate (G3P) pathway, which is the dominant TG synthetic pathway in other tissues such as adipose and liver (28). In the intestine, however, more than 75% of postprandial TG resynthesis is catalyzed by the MGAT pathway (76, 77). Reesterified TG and apolipoproteins are assembled into chylomicron particles which are then secreted into the lymphatic circulation.

   Intestinal MG metabolism has generally been thought to involve only an anabolic pathway, the reesterification to TG via the MGAT pathway. Nevertheless, the presence of a MG hydrolytic activity in small intestine was noted several decades ago (91) and the partial purification of MG lipase (MGL; EC 3.1.1.23) activity from rat intestinal mucosa was reported (92). Recently, additional insight into intestinal MG metabolism was obtained. After incubation of Caco-2 cells with [^{3}H] *sn*-2-MG at either the apical or basal lateral surface, a substantial amount of radioactivity was recovered in the unesterified fatty acid fraction (16). In addition, human MG lipase mRNA expression was detected in Caco-2 cells, and the murine MG lipase gene (93) was also shown to be

expressed in rodent small intestine (16). These results suggested that catabolic processing of *sn*-2-MG may occur in intestinal mucosa, in addition to the well known anabolic processing. The regulation and function of this MG hydrolytic activity in the enterocyte are at present entirely unknown.

On a daily basis, the human small intestine metabolizes an estimated average of 100g of dietary fat which is composed of more than 90% TG (28). Therefore, the mechanism by which the enterocyte metabolizes *sn*-2-MG, which is one of the major products of luminal TG hydrolysis and a backbone for TG reesterification, is of great importance for dietary lipid assimilation. Despite this physiological significance, surprisingly little is known about the regulation of intestinal MG metabolism. In the liver, MG metabolism has been shown to be developmentally regulated, with hepatic MGAT activity dramatically higher in the suckling period than in adult rat liver (161). At present, nothing is known about the developmental expression of hepatic MGL, nor about the developmental expression of either MGL or MGAT2 in the intestine. Therefore, in the present studies, we examined the expression and activity of the two MG metabolizing enzymes, MGAT and MGL, in intestine as well as liver during ontogeny.

Cao et. al. reported that a high fat diet induced MGAT2 expression and activity in small intestine, indicating a functional role for this enzyme in dietary fat absorption (24). It is known that the expression of other genes involved in intestinal lipid metabolism are also altered upon a change in nutritional status. For example, the induction of small intestinal liver fatty acid binding protein (LFABP) expression by high fat feeding has been reported (72, 162), as has the expression of microsomal triacylglycerol transfer protein (MTP), an essential protein for chyromicron assembly (72). Furthermore, it is well known that a standard fasting and refeeding regime markedly alters hepatic lipid metabolism (163, 164), but the influence on intestinal lipid metabolism is less clear. Thus, the effects of nutritional status on intestinal MG metabolism, in comparison with other tissues, were also investigated in the present studies.

The results show that MG metabolism is dramatically altered in a tissue-specific manner in both intestine and liver during development and following a high fat diet. Intestinal MGL expression and activity are increased by high fat feeding whereas little or no changes are found in the fasted state, suggesting a potential role for MGL in dietary lipid assimilation.

2. Experimental procedures

Materials- [^{14}C] *sn*-2-Monoolein (Oleoyl-1-[^{14}C], 55 mCi/ mmol) was purchased from American Radiolabeled Chemicals, Inc. (St. Louis, MO). [^{14}C] Oleoyl CoA (Oleoyl-1-[^{14}C], 57 mCi/ mmol) was purchased from Perkin Elmer Life Science (Boston MA). Unlabeled *sn*-2-monoolein was obtained from Doosan Serdary Research Laboratories (Toronto, Canada). The 3% borate impregnated thin layer chromatography (TLC) plates were purchased from Analtech (Newark, DE). Silica gel G TLC plates were obtained from Sigma (St. Louis, MO). Mouse MGL cDNA was a generous gift from Dr. Cecilia Holm (Lund Univ., Sweden), and mouse MGAT1 and 2 cDNAs were generously provided by Dr. Robert Farese (UCSF, CA). Antibodies against mouse MGL and MGAT2 sequences were generous gifts from Dr. Daniele Piomelli (UC Irvine, CA) and Dr. Yuguang Shi (Lilly Research Laboratory, IN), respectively. The anit-CEL antibodies were generously provided by Dr. David Hui (Univ. Cincinnati). β-actin antibody was purchased from Sigma (St. Louis, MO), and mouse cychlophilin A antibody and cDNA were obtained from Ambion (Austin, TX).

Animals, diets, and tissue collection- For each developmental regulation study, wild type mice (C57BL/6, n = 3 at each age) from ages 6 days before birth to 3 months old were reared in the animal facility at Rutgers University. Prenatal mice were obtained from pregnant dams. The day when the vaginal plug was seen was considered as gestational day 0, with embryonic days counted thereafter. Litter size was consistent at 7-10. Animals were maintained on a 12 hr light and dark cycle and fed regular chow diet (Purina Mouse Chow 5015, Purina Co., St. Louis, MO) ad libitum after weaning. For the high fat feeding studies, 3 month old male mice (C57BL/6) were divided into two groups (n = 8 per group). Purified rodent diet (10% fat by calories, from soybean oil) was given to the control group and the high fat group was fed a 40% kcal fat diet containing the additional 30% kcal from coconut oil, rich in short chain saturated fatty acids (D12325 and D12327,

respectively, Research Diets, New Brunswick, NJ) for 3 weeks ad libitum. In a second high fat

feeding protocol, female mice were divided into three groups (n = 8) and fed with either a 10% kcal

fat diet, or high fat diets rich in saturated fat from lard (45%, or 60% kcal) for 3 months. (D12450B,

D12451 and D12492, respectively, Research Diets, New Brunswick, NJ). For the starvation and

refeeding trial, 3 month old male mice were divided into 4 groups (n = 7 per group) as follows: fed

(Purina Mouse Chow 5015, Purina Co., St. Louis, MO), starvation for 12 hr, starvation for 24 hr,

and refeeding with a high sucrose diet (D11725, Research Diet, New Brunswick, NJ) after a 24 hr

starvation (165, 166). Animals were sacrificed using CO_2 and the entire small intestine from

pylorus to cecum was immediately excised. For the nutritional regulation studies, the intestine was

rinsed twice with saline and then the mucosa was harvested by scraping. For developmental

studies, whole intestine was collected followed by rinsing. Samples were immediately frozen on

dry ice and kept at -70ºC. Liver and adipose tissue (peri-renal and epididymal fat) were also

collected, snap frozen on dry ice, and stored at -70ºC.

Northern blot analysis of MGL and MGAT1 and 2 mRNA expression- Tissues were

homogenized in Solution D (4 M Guanidinium thiocyanate, 25 mM Na Citrate, 0.1 M

2-mercaptoethanol) using several strokes of a Polytron. Total RNA was further purified by phenol

extraction. For detecting MGAT2 transcript in liver, poly A^+ RNA was prepared using a QIAGEN

mRNA extraction kit. 20-40 μg of total RNA or 2 μg of poly A^+ RNA were loaded onto 1% agarose

gels, separated by electrophoresis, and transferred onto nylon membranes (Perkin Elmer Life

Science, Boston, MA). Full length coding regions of MGL, MGAT1 and MGAT2 cDNA were

labeled with [^{32}P] (Perkin Elmer Life Science, Boston, MA) using the Random Prime labeling

system (GE Healthcare, Piscataway, NJ). Membranes were pre-hybridized for 1 hr and hybridized

for 2-3 hr at 68 ºC using Quik-hybridization solution (Strategene, La Jolla, CA). Blots were washed

twice at room temperature with 2×SSC, 0.1% SDS for 15 min. An additional high temperature (65

°C) wash with 0.1× SSC, 0.1% SDS for 30 min was completed before exposing the blots to a

PhosphorImager screen. Quantification was done using the Molecular Dynamics STORM scanner and ImageQuaNT software (Molecular Dynamics, Sunnyvale, CA). Blots were stripped and reprobed with 18S rRNA cDNA or mouse cychlolphilin A cDNA for internal loading controls.

Quantitative RT-PCR for intestinal MGL mRNA expression - Relative MGL mRNA expression in small intestine was analyzed by quantitative RT-PCR (SYBR Green method). Total RNA was extracted as described above and further purified using the RNeasy clean up kit (Qiagen, Valencia, CA) along with DNase 1 treatment to minimize genomic DNA contamination. Reverse transcription was performed using 1 μg of total RNA, random primer, RNase inhibitor and AMV reverse transcriptase (Promega Madison, WI) in a total volume of 25 μl. Primer sequences for MGL and β-actin (endogenous control) were retrieved from Primer Bank (Harvard Medical School QPCR primer database), as follows: MGL: forward 5'-CAG AGA GGC CAA CCT ACT TTT C-3', reverse 5'-ATG CGC CCC AAG GTC ATA TTT-3'; β-actin: forward 5'-GGC TGT ATT CCC CTC CAT CG-3', reverse 5'-CCA GTT GGT AAC AAT GCC ATGT-3'. Efficiencies of PCR amplification for both primers were tested during preliminary experiments and similar PCR efficiencies were confirmed. Real time PCR reactions were performed in triplicate using an Applied Biosystems 7300 instrument. Each reaction contained 80 ng of cDNA, 250 nM of each primer, and 12.5 μl of SYBR Green Master Mix (Applied Biosystems, Foster City, CA) in a total volume of 25 μl. Relative quantification of MGL expression was calculated using the comparative Ct method normalized to β-actin.

Western Blot analysis of protein expression - Tissues were homogenized in 5-10 volumes of homogenization buffer on ice for 30 sec. using a Wheaton tissue homogenizer (Wheaton Science, Millville, NJ), and crude tissue homogenates were centrifuged at 600×g for 10 min at 4 ºC to remove unbroken cell debris. Homogenization buffer contained 50 mM Tri-HCl and 0.32 M sucrose (pH 8) with 0.5% (v/v) protease inhibitors (Sigma. Cat. # 8340). For MGAT2 detection, a

total membrane fraction was obtained by further ultracentrifugation (100,000×g, 1hr at 4 ºC).

Protein concentration was determined by the Bradford assay (167). 30-50 µg of total cell protein or

5-10 µg of membrane protein were loaded onto 12% polyacrylamide gels and separated by

SDS-PAGE. The proteins were transferred onto PVDF membranes using a semi-dry transfer

system (Bio-Rad, Hercules, CA) for 1 hr at 20 V. All membranes were incubated in a 5% nonfat dry

milk blocking solution overnight at 4ºC and then probed with primary antibody for 1 hr. Dilution of

the anti-mMGL antibody was 1:5,000-10,000, and for anti-mMGAT2 dilution was 1:1,000.

Dilution of the anti-CEL antibody was 1:1,000. After washing three times, blots were incubated

with anti-rabbit IgG-horseradish peroxidase conjugate at 1:10,000 dilution for 1 hr and then

developed by chemiluminescence (ECL reagent, GE Healthcare, Piscataway, NJ). Blots were

stripped and reprobed with mouse β-actin (Sigma, St. Louis, MO) or cyclophilin A antibody

(Ambion, Austin, TX) as indicated to check the integrity of the sample and as loading controls.

Quantification of protein bands was conducted using Image J software (NIH).

In vitro MGL assay - The MGL assay was established in the laboratory based on previous reports

(92, 99), and measures the release of fatty acid from *sn*-2-MG. The purity of $[^{14}C]$ *sn*-2-monoolein

(labeled on the fatty acyl chain, 55 mCi/ mmol, American Radiolabeled Chemicals, St. Louis, MO)

was checked using 3% borate-impregnated TLC plates and a solvent system of $CHCl_3$/ acetone/

methanol/ acetic acid (90:5:2:0.5, v/v). The $[^{14}C]$ *sn*-2-monoolein was > 90% pure. $[^{14}C]$

radiolabeled *sn*-2-monoolein was mixed with unlabeled *sn*-2-monoolein (Doosan Serdary

Research, Toronto, Canada) to obtain the desired concentrations. The mixture of $[^{14}C]$ radiolabeled

and unlabeled *sn*-2-monoolein was dried under N_2 gas, and 0.125 M Tri-HCl buffer containing

1.25% BSA was added. Substrate emulsions were prepared by brief sonication (1 min) on ice. 0.4

µl of substrate emulsion containing *sn*-2-monoolein was allocated in each reaction tube. Samples

containing 100-200 µg of protein were introduced as an enzyme source. Reaction conditions for

each tissue were optimized during preliminary experiments to ensure linearity with time and

protein concentration. 2.5 mM *sn*-2-monoolein was used for liver and adipose tissue MGL assays, and 25 μM was used for intestine samples. The reaction was initiated by adding tissue homogenate. Liver and adipose tissue samples were incubated for 5 min and intestinal samples for 10 min at 23ºC. Lipids were extracted using chloroform: methanol (2:1, v/v) and the organic phase was subjected to TLC analysis. In order to monitor isomerization of substrate, 3% borate-impregnated TLC plates (Analtech, Newark, DE) were used for separation of lipids. Spontaneous isomerization to the *sn*-1 isomer (20-30%) was always accounted for when determining the enzyme activity. All reaction times and temperatures were optimized in order to minimize spontaneous isomerization during the assay. Quantification of the specific activity of [^{14}C] labeled end products separated by TLC was done using the Molecular Dynamics STORM scanner and ImageQuaNT software (Molecular Dynamics, Sunnyvale, CA). On each plate, known amounts of specific radioactivity of [^{14}C] oleate (Perkin Elmer Life Science, Boston, MA) were spotted and used for formulating standard curves to calculate enzyme activities for each sample.

In vitro MGAT assay - The MGAT assay followed a well established protocol based on the method of Coleman and colleagues, with slight modification (161). Activity was measured as the incorporation of [^{14}C]-oleoyl CoA into diacylglycerol (DG). 25 μM of oleoyl CoA and 250 μM of *sn*-2-monoolein (Doosan Serdary Research, Toronto, Canada) were used as substrates. [^{14}C]-Oleoyl CoA was purchased from Perkin Elmer Life Science Inc. (57 mCi/ mmol, Boston, MA) and cold oleoyl CoA was purchased from Sigma (St. Louis, MO). The assay buffer contained 100 mM Tris-HCl, 4 mM MgCl$_2$, 1 mg/ml BSA and 100 μM each of phosphatidylcholine and phoshpatidylserine. 5 or 10 μg of membrane fraction protein, prepared by ultracentrifugation at 100,000 x g for 1 hr at 4ºC, were used as enzyme source. The enzyme assay was initiated by adding [^{14}C]-oleoyl Co A and incubation was for 5 min at 25ºC. Lipids were extracted using chloroform: methanol (2:1, v/v) and the organic phase was subjected to TLC analysis using standard silica gel plates (Sigma, St. Louis, MO) and a solvent system of hexane/ethyl ether/ acetic acid, 70:30:1, v/v.

The plates were exposed to a PhosphorImager screen to visualize incorporation of $[^{14}C]$-oleoyl CoA into neutral lipids. Specific activities found in the DG fraction plus half of the TG fractions were considered as MGAT activity (78, 161). Quantification of each lipid fraction was analyzed using ImageQuaNT software (Molecular Dynamics, Sunnyvale, CA).

3. Results

Developmental regulation of intestinal MGL and MGAT2 - Changes in mRNA and protein expression of the two MG metabolizing enzymes, as well as both enzyme activities were determined over the course of intestinal ontogeny. The results showed a relatively abundant expression of MGL mRNA at early developmental stages, declining thereafter to a lower but detectable level (Fig. 2-1-A). The expression pattern for MGL protein over the same time period was not consistent with the changes in its mRNA expression. MGL protein was detected in prenatal and adult intestine but not in the suckling period (Fig.2-1-B). MGL activity was measured as the release of radiolabeled fatty acid from [^{14}C] *sn*-2-monoolein, and it was found that activity increased throughout intestinal development, plateauing at a relatively high level after day 6 (Fig. 2-1-C). Thus, MGL activity shows discrepancies with the expression of both mRNA and protein levels (Fig. 2-1-D), particularly during the suckling period.

We hypothesized that carboxyl ester lipase (CEL; also known as bile salt-stimulated lipase), another enzyme with known *sn-2*-monoacylglycerol hydrolytic activity, might be present in suckling intestine. The results in Figure 2-1-E show that CEL protein was detected in neonatal intestine at approximately equivalent levels to those in adult intestine.

For intestinal MGAT2, mRNA levels were very low at day -6 but then rose and remained relatively constant from day -3 to day +90 (Fig. 2-2-A). Protein and activity levels were also very low at day -6 and increased thereafter; both appeared to be up-regulated during the early suckling period, and declined thereafter (Fig. 2-2-B, C).

Developmental regulation of hepatic MGL and MGAT2 - In marked contrast to intestinal MGL, similar patterns were observed for liver MGL mRNA, protein, and activity levels. All were increased 5-10 fold during development (Fig. 2-3-D), suggesting that transcriptional regulation is the primary mechanism of hepatic MGL expression (Fig. 2-3-A, B, and C).

Figure 2-1

A

B

C

D

E

CEL

Cychlophilin A

1   2   3   4   5   6

1. Pancreas
2. Day 60 Intestine
3. Day 30 Intestine
4. Day 20 Intestine
5. Day 16 Intestine
6. Dav 6 Intestine

Figure 2-1. Developmental regulation of intestinal MGL. (A) Relative mRNA expression was estimated by Northern blot analysis. 40 µg of total RNA was loaded in each lane and probed with mMGL or 18S ribosomal RNA sequence as a loading control. (B) Relative MGL protein expression was estimated by Western blotting. 50 µg of homogenate protein was loaded in each lane. Membranes were stripped and reprobed with mouse cychlophilin A antibody for an internal control. (C) MGL activity was measured by release of the $[^{14}C]$ oleoyl moiety from $[^{14}C]$ *sn*-2-monoolein during a 10 min incubation with 100 µg of intestinal homogenate at 23ºC. (D) Comparison of the relative MGL mRNA (——), protein (·······), and activity levels (-----). Relative expression at each time point was calculated based on the highest value being 100. Day 0 designates day of birth. One representative series is shown out of three independent series, with n = 3 separate samples for each time point. (E) Detection of CEL in mouse small intestine by immuno-blotting. 50 µg of tissue homogenate protein was loaded in each lane. Pancreas was used for a positive control.

Figure 2-2

Figure 2-2. Developmental regulation of intestinal MGAT2. (A) Relative mRNA expression was estimated by Northern blot analysis. 20 µg of total RNA was loaded in each lane and probed with m MGAT2 or 18S ribosomal RNA sequence as a loading control. (B) Relative MGAT2 protein expression was estimated by Western blotting. The total membrane fraction was prepared as described in Experimental Procedures. 10 µg of membrane protein were loaded in each lane and probed with mMGAT2 antibody. (C) MGAT activity was determined as described in Experimental Procedures. (D) Comparison of the relative MGAT2 mRNA (——), protein (·······), and activity levels (-----). Relative expression at each time point was calculated based on the highest value being 100. Day 0 designates day of birth. One representative series is shown out of three independent series, with n = 3 separate samples for each time point.
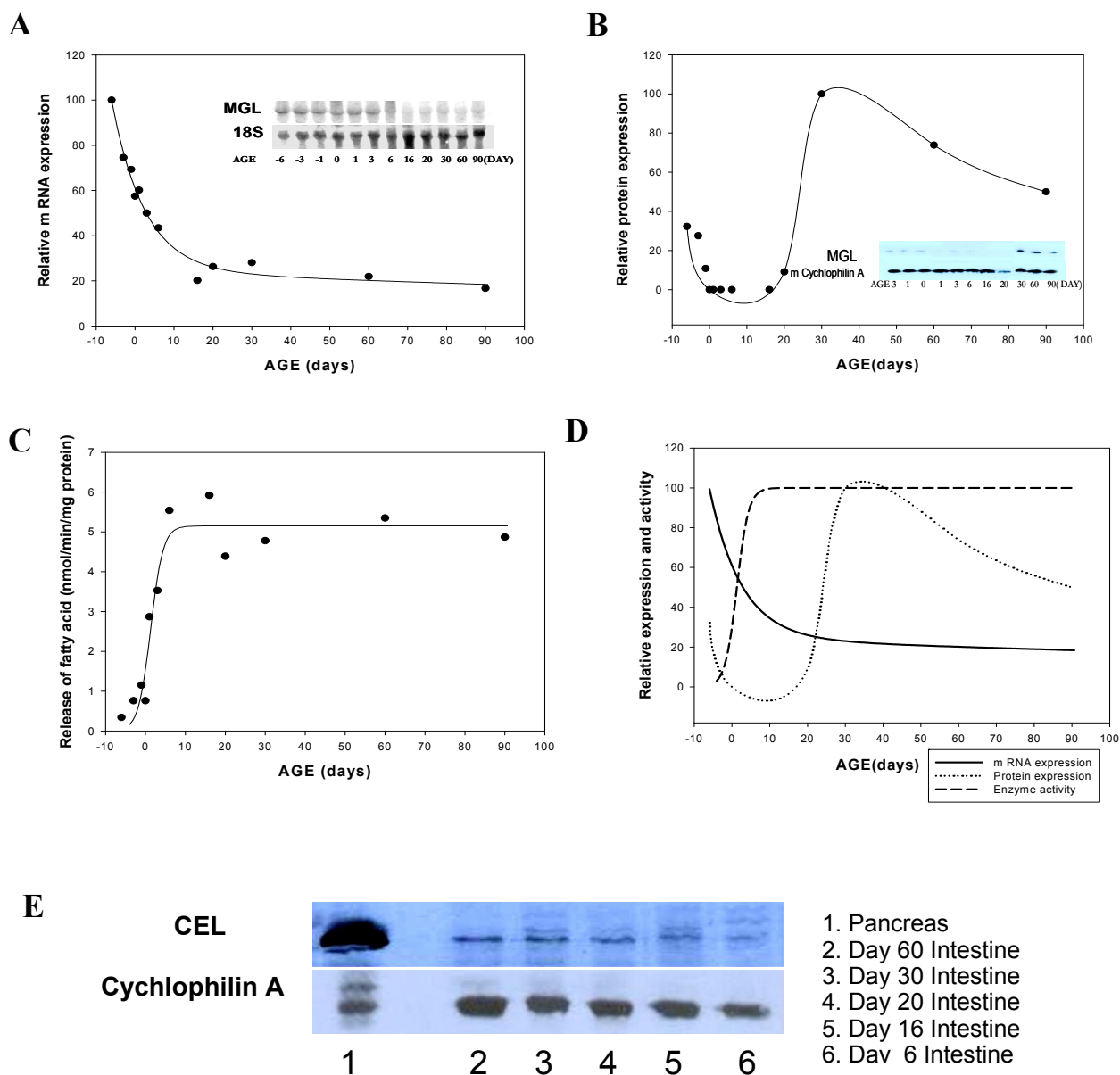
Figure 2-3

A

B

C

D

Figure 2-3. Developmental regulation of hepatic MGL. (A) Relative mRNA expression was estimated by Northern blot analysis. (B) Relative MGL protein expression was estimated by Western blotting. 30 μg of protein is loaded in each lane and probed with MGL antibody. (C) Hepatic MGL activity. (D) Comparison of the relative MGL mRNA (——), protein (······), and activity levels (-----). Relative expression at each time point was calculated based on the highest value being 100. Day 0 designates day of birth. One representative series is shown out of three independent series, with n = 3 separate samples for each time point.

It has been reported that the MGAT1 transcript was detected in adult mouse liver by Northern analysis (78), however we were unable to detect MGAT1 in the present studies. The reason for the discrepancy is unknown. As described below, the MGAT1 transcript was detected in adipose tissue, in agreement with Yen et al. (78). The MGAT2 transcript was readily detected in 2 µg of liver mRNA, consistent with the report of Cao et. al. (80). Thus, the present results for mRNA regulation in liver represent changes in the MGAT2 transcript during ontogeny. In contrast to the developmental pattern found for hepatic MGL, hepatic MGAT2 mRNA was detected during the pre and post-natal stages but declined after day 6 (Fig. 2-4-A). MGAT activity levels were generally consistent with this pattern of mRNA expression (Fig. 2-4-B), suggesting that, as for hepatic MGL, transcription is the predominant mechanism of MGAT regulation in the liver during development. Overall, an inverse regulation of MGAT and MGL during ontogeny was found in liver (Figs. 2-3 and 2-4), however such reciprocal regulation of the two MG metabolizing enzymes was not found in small intestine (Figs. 2-1 and 2-2).

Since liver TG content has been reported to decline to low adult levels during development in the rat (168, 169), we wanted to determine whether a similar decline is found in mouse liver. The results in Fig. 2-4-D show that TG levels in adult mouse liver are 5-fold lower than those found in day 0 liver.

Nutritional control of intestinal MGL and MGAT2 - In order to examine the effect of an increased substrate supply on intestinal MGL, 3 month old C57BL/6 male mice were fed either a high fat (40% kcal) or standard fat diet (10% kcal) for 3 weeks. Body weight was significantly elevated in the high fat fed group, along with a marked increase in total fat pad weight, nearly 4 fold greater than control (Fig. 2-5-A, B). Interestingly, we found that intestinal MGL protein expression increased 2-3 fold, and significant elevations in MG hydrolysis in small intestine were observed following high fat feeding (Fig. 2-5-C). Relative mRNA levels of MGL were determined by quantitative RT-PCR, and also showed a consistent induction although it did not reach statistical

Figure 2-4

A

B

C

D

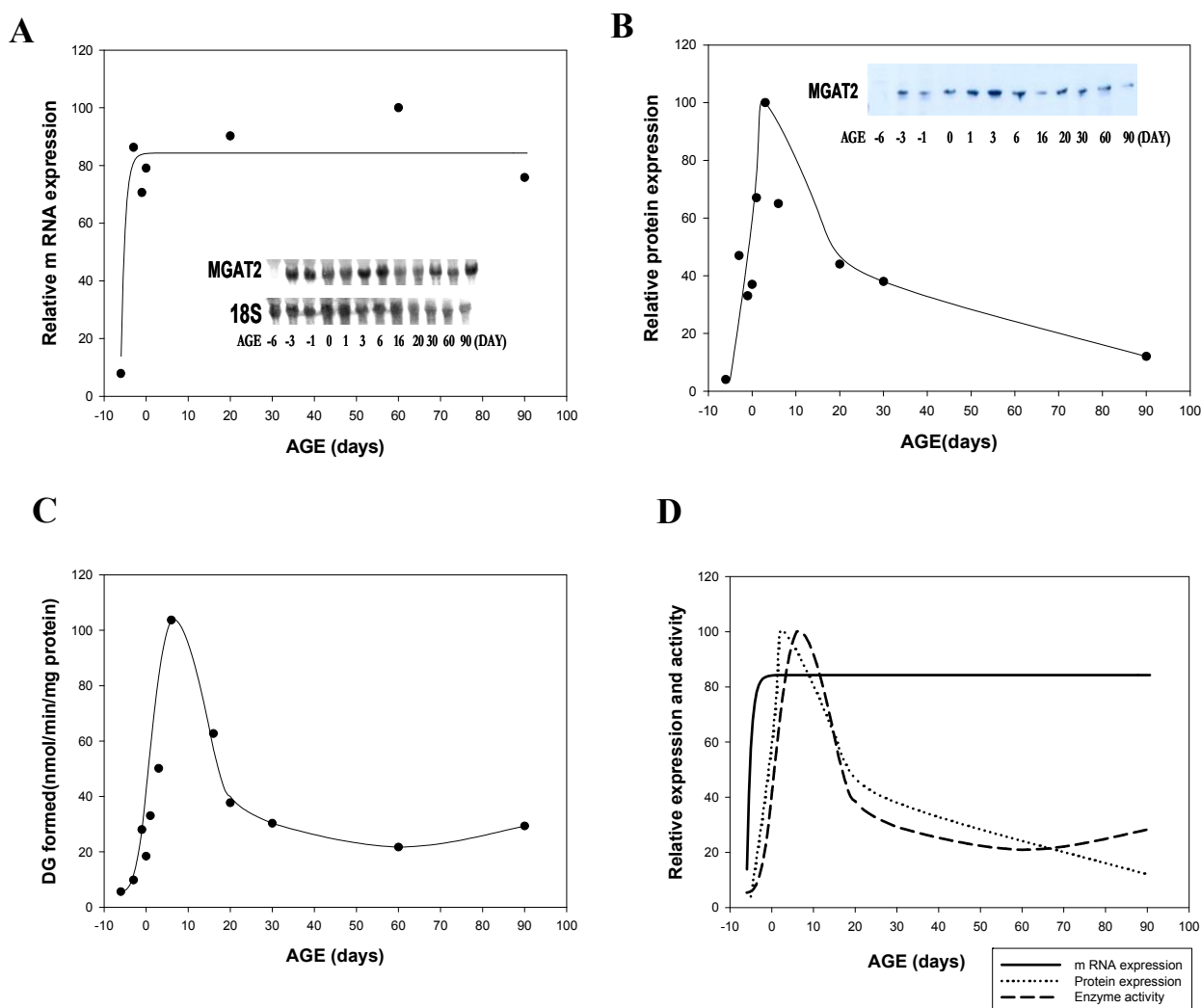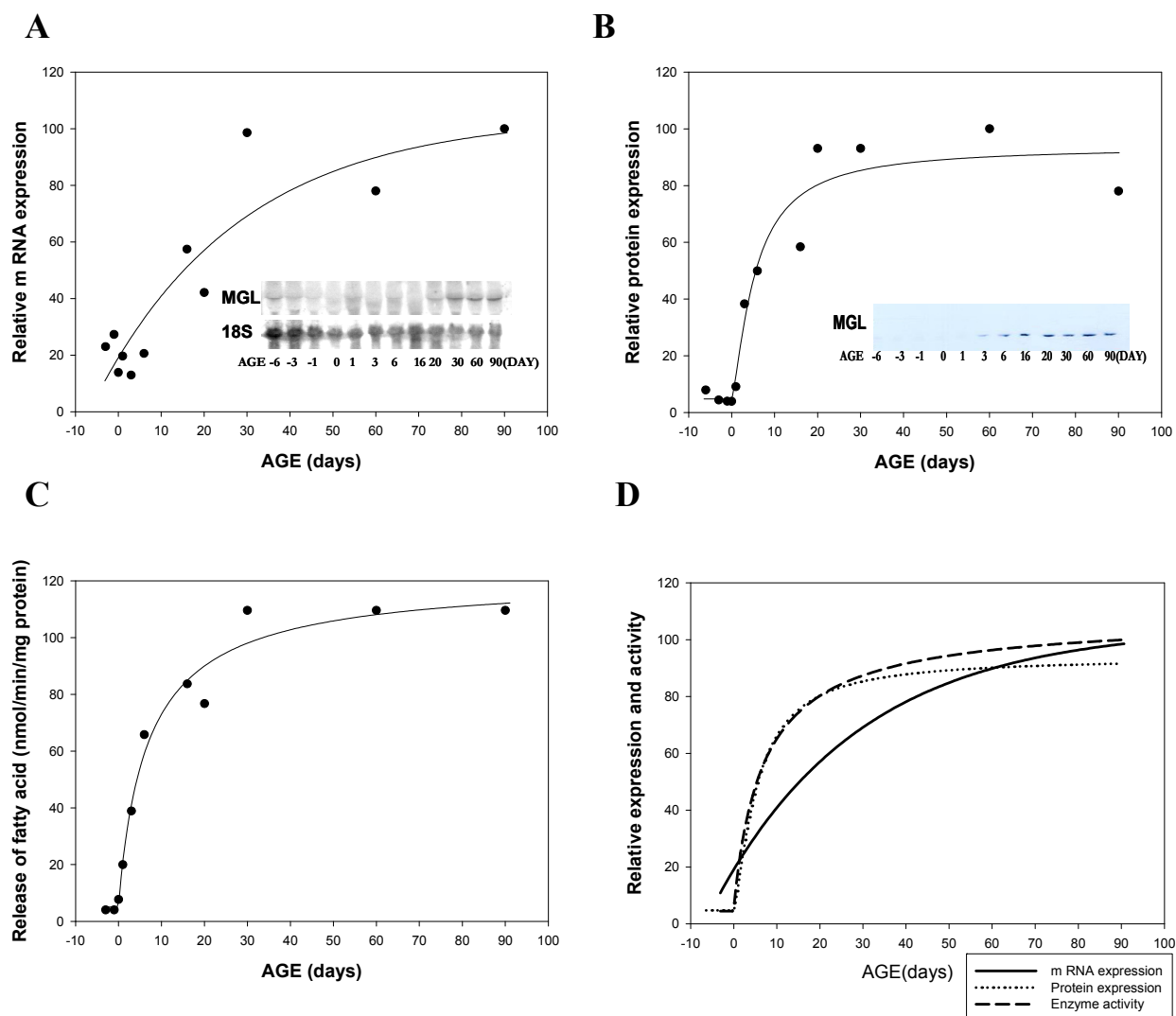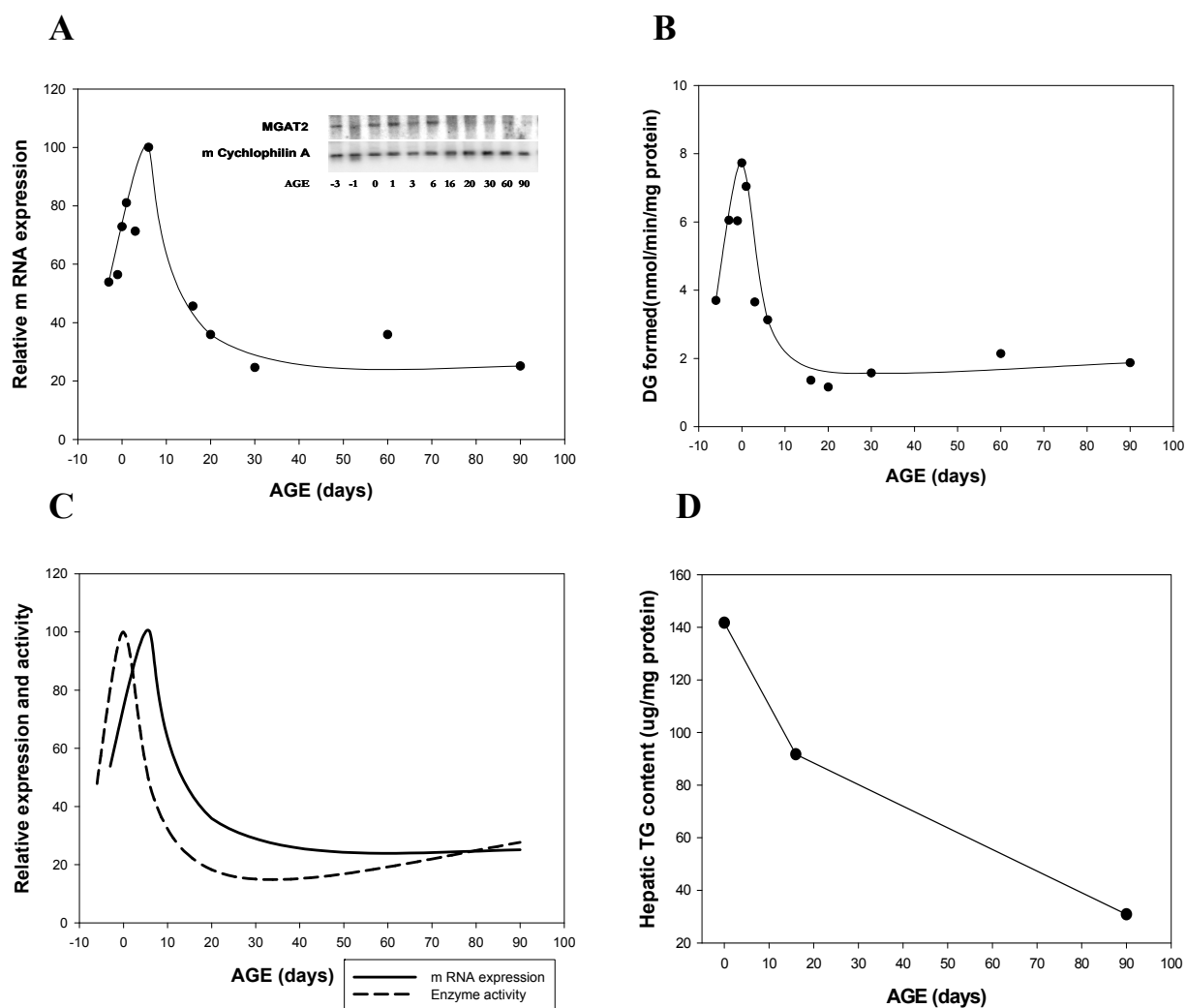**Figure 2-4. Developmental regulation of hepatic MGAT2.** (A) Relative mRNA expression was estimated by Northern blot analysis. Poly A^+ RNA was purified for MGAT2 transcript detection and 2 µg of poly A^+ RNA was loaded in each lane and probed with mMGAT2 or mouse cychlophilin A sequence for loading control. (B) Hepatic MGAT activity. (C) Comparison of the relative MGAT mRNA (——) and activity levels (-----). (D) Hepatic TG content during mouse development. Estimation was obtained by densitometry following lipid extraction and TLC separation using authentic standards to quantify TG. Relative expression at each time point was calculated based on the highest value being 100. Day 0 designates day of birth. One representative series is shown out of three independent series, with n = 3 separate samples for each time point.

Figure 2-5
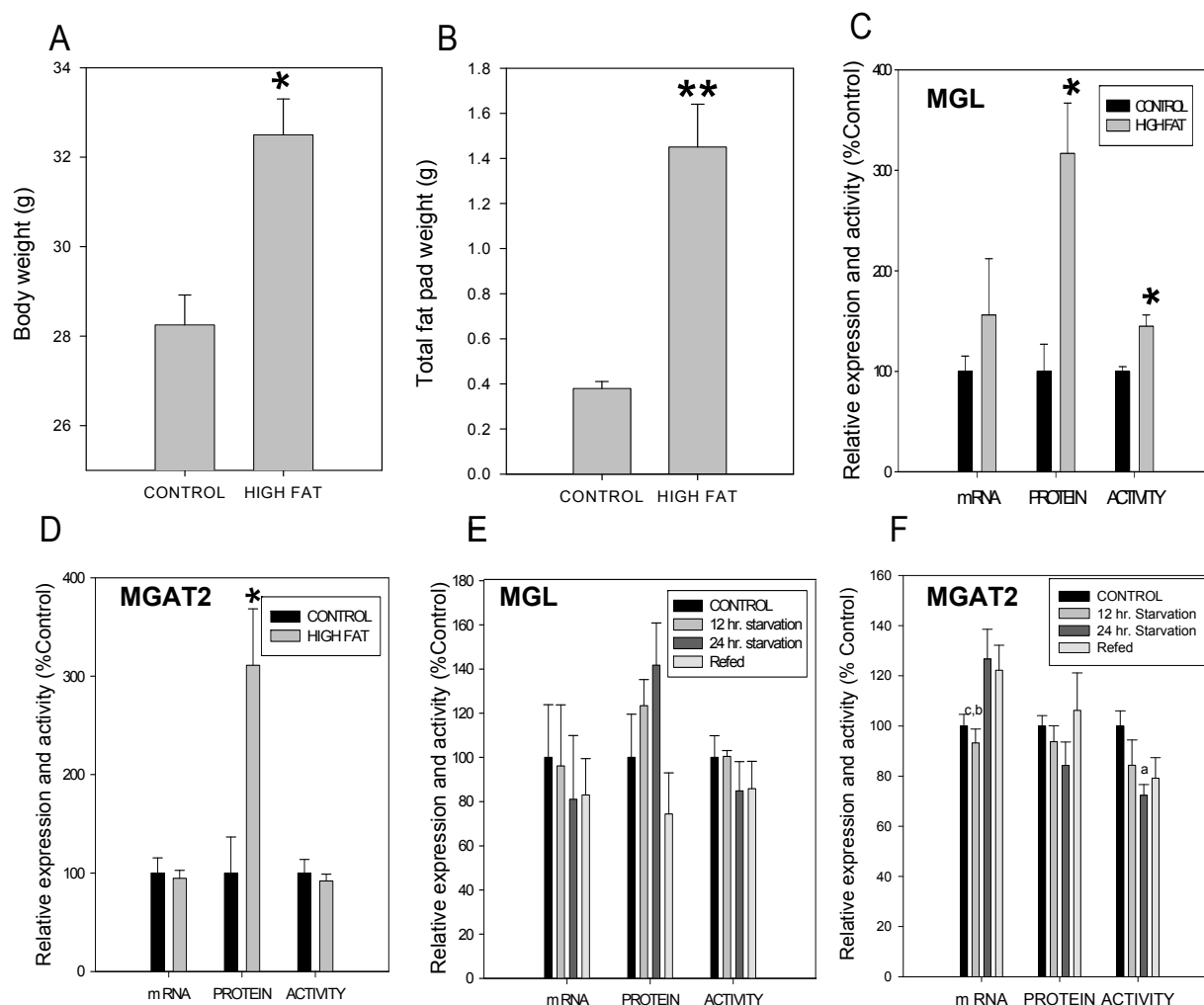
Figure 2-5. Nutritional regulation of intestinal MGL and MGAT2. (A) Body weight after 3 weeks of high fat feeding (10% vs 40% kcal), n = 8 per group. (B) Weight of total fat pads after 3 weeks of high fat feeding. (C) Intestinal MGL expression and activity following 3 weeks of high fat feeding. Relative mRNA expression was determined by Q-PCR. MGL activity for the control was 3.4 nmol/min/mg protein. (D) Intestinal MGAT2 expression and activity following 3 weeks of high fat feeding. Absolute MGAT activity for the control was 77.3 nmol/min/mg protein. (E) MGL expression and activity in small intestine following starvation and refeeding. Relative mRNA expression was determined by Q-PCR. MGL activity for the control was 8.05 nmol/min/mg protein. (F) MGAT2 expression and activity in small intestine following starvation and refeeding. MGAT activity for the control was 36.5 nmol/min/mg protein. Values are presented relative to the expression and activity of the control group set to 100%. Data represent mean ± S.E. from n = 8 or n = 4-7 samples per group for the high fat feeding study or the starvation and refeeding study, respectively. * $p < 0.05$, ** $p < 0.01$ relative to control. **a**, $p < 0.05$ versus control, **b**, $p < 0.05$ versus 24 hr starvation, **c**, $p < 0.05$ versus refed group.

significance. A similar result was observed in a relatively long term, 3 month high fat feeding study (10%, 45%, or 60% kcal), though the response was somewhat blunted compared to results from the short term feeding study (results not shown). In contrast to this induction by a high fat challenge, starvation up to 24 hr did not significantly alter MGL expression and activity (Fig. 2-5-E). These results show that upon increased lipid flux to the enterocyte, MG catabolism was stimulated, but fasting did not affect intestinal MGL expression or activity.

MGAT2 protein expression in small intestine was increased 3 fold following a 3 week high fat diet without altering its mRNA or activity (Fig. 2-5-D). The starvation-refeeding regimen revealed little or no change in either MGL or MGAT levels (Fig. 2-5-E, F).

Nutritional control of hepatic MGL and MGAT - The 3 week high fat diet stimulated liver MGL activity, along with a 2-fold elevation in the amount of MGL protein (Fig. 2-6-A). In contrast, starvation up to 24 hr, or refeeding, did not affect MGL activity despite a significant induction of mRNA expression during fasting (Fig. 2-6-C).

Hepatic MGAT activity was not changed after the high fat diet (Fig. 2-6-B), but refeeding with a high carbohydrate diet following starvation resulted in a modest but significant decrease (~35%) in MGAT activity compared to any other group (Fig. 2-6-D).

Nutritional control of adipose tissue MGL and MGAT1 - In general, MG metabolism in adipose tissue was not substantially changed by high fat feeding, in spite of the large increase in adipose mass (Fig. 2-5-B, and 2-7-A, B). The MGAT1 transcript was significantly down regulated by high fat feeding, however MGAT activity was not changed (Fig. 2-7-B). MGL protein and activity did not change as well, and an increase in MGL mRNA levels (Fig. 2-7-A) did not reach statistical significance. Starvation and refeeding also did not alter MG metabolic enzyme levels (Fig. 2-7-C, D).

Figure 2-6
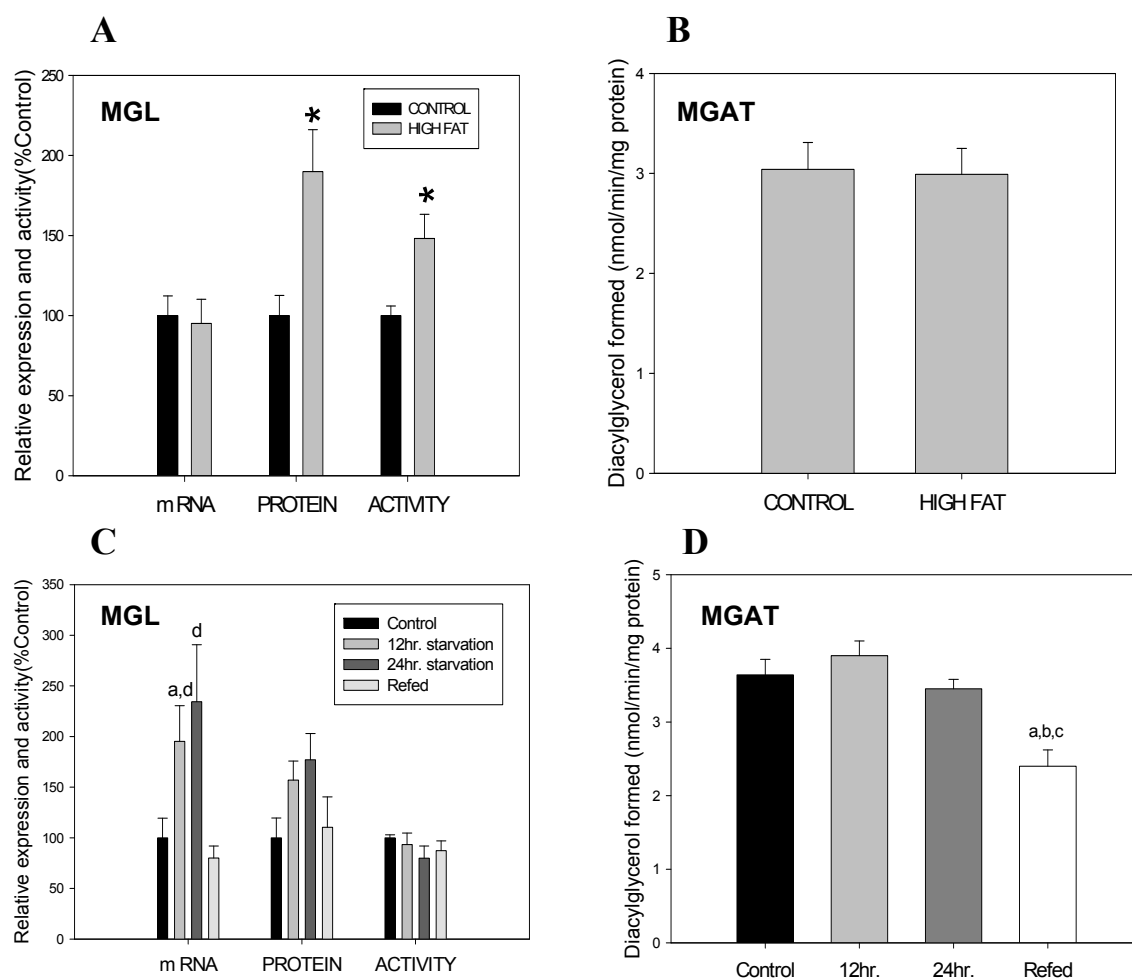
Figure 2-6. Nutritional regulation of hepatic MGL and MGAT. (A) Hepatic MGL expression and activity following 3 weeks of high fat feeding. MGL activity for the control was 148.5 nmol/min/mg protein. (B) Hepatic MGAT activity in Control (10% Kcal) versus high fat (40% Kcal) fed mice. (C) Hepatic MGL expression and activity following starvation and refeeding. MGL activity for the control was 186.3 nmol/min/mg protein. (D) Hepatic MGAT activity following starvation and refeeding with high carbohydrate diet. Values are presented relative to the expression and activity of the control group set to 100%. Data represent mean ± S.E. from n = 8 or n = 4-7 samples per group for the high fat feeding or the starvation and refeeding study, respectively. * $p < 0.05$ relative to control, **a**, $p < 0.05$ versus control, **b**, $p < 0.05$ versus 12 hr starvation, **c**, $p < 0.05$ versus 24 hr starvation, **d**, $p < 0.05$ versus refed group.

Figure 2-7
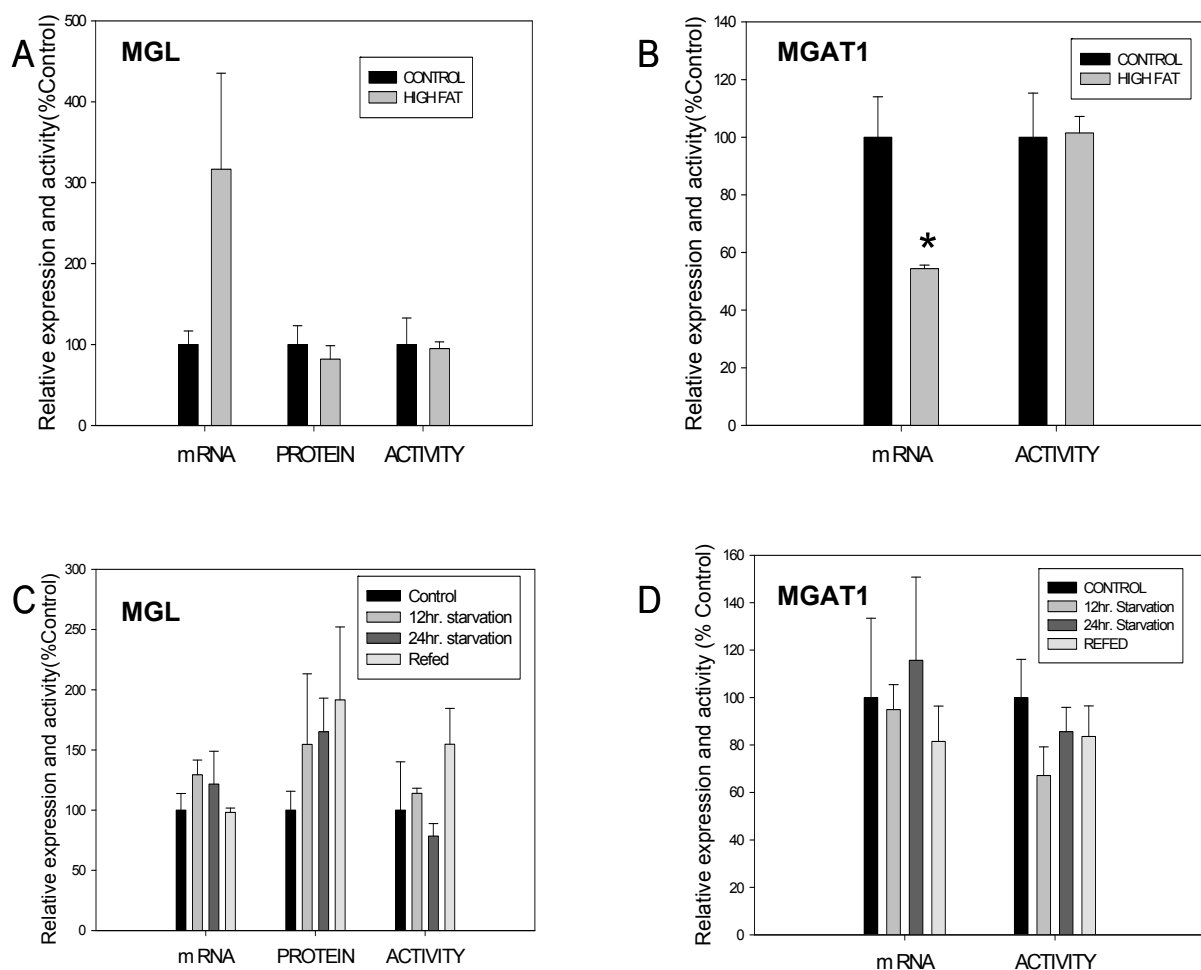
Figure 2-7. Nutritional regulation of MGL and MGAT1 in adipose tissue. (A) MGL regulation in adipose tissue by high fat feeding. MGL activity for the control was 185.4 nmol/min/mg protein. (B) MGAT1 mRNA expression and activity in adipose tissue by high fat feeding. MGAT activity for the control was 2.85 nmol/min/mg protein. (C) MGL regulation in adipose tissue by starvation and refeeding. MGL activity for the control was 363.7 nmol/min/mg protein. (D) MGAT1 regulation in adipose tissue by starvation and refeeding. MGAT activity for the control was 3.41 nmol/min/mg protein. Values are presented relative to the expression and activity of the control group set to 100%. Samples were pooled from two mice to obtain sufficient tissue for analysis, except for those fed the high fat diet, where no pooling was necessary. Data represent mean ± S.E. from n = 8 or n = 4-7 samples per each group for the high fat feeding or the starvation and refeeding study, respectively. *$p < 0.05$.

4. Discussion

It is well known that *sn*-2-MG, a major digestive product of dietary TG, is reesterified to TG in the enterocyte via the MGAT pathway. Recently, we presented evidence of MG hydrolysis by MGL in intestinal epithelium and the human intestinal Caco-2 cell line (16). In the present study, the regulation of two MG metabolizing enzymes, MGAT and MGL, in intestine as well as other tissues, has been explored during ontogeny and during alterations in nutritional status.

For both MGL and MGAT, a dynamic and complex pattern of changes was observed during mouse intestinal development. Discordances between mRNA, protein, and activity levels suggest that post-transcriptional and/or post-translational regulatory events are taking place. At present, the mechanisms underlying the complex regulation of intestinal MGL and MGAT are unknown. One possibility is that enzyme activities may be altered by phosphorylation state, well known to regulate activities of many lipid metabolic enzymes. For example in the liver, it has been shown that the activities of key enzymes catalyzing fatty acid β-oxidation and glycerolipid biosynthesis are regulated reciprocally by their phosphorylation via casein kinase 2 and AMP-activated kinase (170-172). Posttranslational regulation of lipid metabolic enzymes in intestine is entirely unexplored at present. A ProSite consensus sequence search (173) indicates that MGL and MGAT have multiple putative phosphorylation sites by protein kinase C, tyrosine kinase, and/or casein kinase 2. Elucidation of the molecular mechanism of regulation of intestinal enzymes involved in lipid metabolism will provide a more complete understanding of lipid assimilation in the enterocyte.

Levels of MGAT2 protein and activity are greatly elevated during the suckling period, possibly contributing to the efficient absorption of milk fat during development. In contrast, during lactation, the intestinal MGL protein was not detectable despite an increase in MG hydrolytic activity over the same time course (Fig. 2-1-D). We found that a substantial amount of carboxyl ester lipase is present in small intestine during the suckling period. CEL has broad catalytic activity toward neutral lipids, including *sn*-2-position fatty acyl chains (29, 46). It is expressed in pancreas

and mammary gland, and is present in maternal milk (29, 46, 174). Further, internalization of CEL present in the intestinal lumen into enterocytes has been demonstrated (44, 175). Thus, increased MG hydrolysis without MGL protein during suckling might be due to the action of CEL.

In contrast to intestine, the activities of hepatic MG metabolizing enzymes during development are quite consistent with their levels of mRNA and protein expression, suggesting that transcription is the major mechanism controlling hepatic MG metabolism during ontogeny. The 5-10 fold increases in MGL mRNA, protein, and activity during development (Fig. 2-3) parallel the known elevation of hepatic TG hydrolase expression, which is believed to mobilize TG in the liver (176, 177). Indeed, hepatic TG content declines during development in both rat (168, 169) and mouse (Fig. 2-4-D). Thus, the profile for hepatic MGL induction during development suggests that it is likely to play a role in the mobilization of liver TG stores. The elevated hepatic MGAT2 m RNA and activity in early developmental stages suggests an important role for MGAT in hepatic TG synthesis, both in the absence of glycerol-3-phosphate acyltransferase (GPAT) activity in the prenatal period, or along with GPAT activity during suckling (178).

The regulation of MG metabolizing enzymes is tissue-specific, as indicated by several points: a) the apparent transcriptional regulation of liver but not intestinal MGL and MGAT; b) the reciprocal regulation of MG esterification and lipolytic activities observed in the liver (Fig. 2-3 and 2-4) is not found in the intestine (Fig. 2-1 and 2-2); and c) the activities of hepatic MGAT per mg of liver protein appear to be much lower than the levels of MGL, while the opposite is true of intestinal activities. (It is worth noting that these values are not absolute activities, since tissue samples and not purified enzymes were used). Taken together, the tissue-specific differences suggest distinct roles for the MG substrate in intestine and liver.

The present studies demonstrate that nutritional manipulation alters intestinal MG metabolism. Intestinal MGL expression and activity were induced by a high fat diet, but not by starvation (Fig. 2-5-C and 2-5-E), suggesting that upon increased lipid flux to the enterocyte, MG catabolism was stimulated. The physiological reason for increased MG catabolism upon high fat

feeding is unknown, although it may represent a controlling mechanism to regulate lipid assimilation when excessive lipid has been ingested. However, the levels of intestinal MGL activity per mg of protein are approximately 10 times lower than intestinal MGAT activity, suggesting an alternate function, perhaps related to cellular signaling as discussed below.

After 3 weeks of high fat feeding a 3-fold induction of MGAT protein was observed, with minimal change in activity (Fig. 2-5-D). These results are in agreement with those of Cao et. al., found that 4 weeks of high fat feeding (40% kcal) increased MGAT2 protein expression in the small intestine 2 fold, with only a minor (20%) increase in activity (24). It was also consistently found that intestinal MGAT2 mRNA was altered neither during ontogeny nor by nutritional challenge, despite changes in MGAT2 protein and activity. Together with the developmental expression studies, these results support the post-transcriptional and/or post-translational modification of MGAT2 in the intestine.

The high fat diet stimulates liver MGL activity and protein (Fig. 2-6-A). Since high fat feeding has been shown to increase hepatic VLDL secretion (179), the induction of MGL might reflect a role in the mobilization of intracellular TG for lipoprotein secretion. Starvation up to 24 hr, or refeeding, did not alter MGL activity, despite a significant induction in mRNA expression during fasting (Fig. 2-6-C). A 48h fast decreases MGL protein and activity (not shown). The two nutritional control studies thus suggest that hepatic MGL is likely participating in intracellular TG mobilization directed toward secretion in the fed state rather than providing substrate for β-oxidation. Neither high fat feeding nor a starvation-refeeding protocol substantially affected MGAT activity. The clear contrast with the known marked induction by starvation/refeeding of lipogenic genes such as fatty acid synthase and GPAT (163, 164), suggests that hepatic MGAT may have a distinct role relative to other lipogenic enzymes. It has been suggested that the function of hepatic MGAT may be associated with the retention of essential fatty acids by reacylation of sn-2-MG during lipolysis (180). The present results are in keeping with this proposal. The high fat diet used in the present studies contained primarily short chain saturated fatty acids, thus it will be

of interest to determine whether a diet high in essential fatty acids causes as increase in hepatic MGAT levels.

The metabolism of MG in adipose tissue was not substantially affected by nutritional modification. This suggests that the physiological role of MGAT in this tissue may not be directly related to TG synthesis, or, more likely, that the total level of MGAT present is sufficient to effectively esterify the levels of MG substrate present. That starvation did not result in significant changes in MGL levels is perhaps surprising, since an elevation in MG catabolism might have been expected, as MGL is believed to participate in the complete hydrolysis of TG in adipose tissue (95). Interestingly, however, the absence of changes is consistent with what has been found for hormone sensitive lipase (HSL) mRNA and protein expression and activity, which were also not stimulated by 12 h or 24 h fasting. Indeed, no HSL stimulation was found until 3 days of starvation in the rat, although the serum free fatty acid level doubled within the first day of fasting (181). The mechanisms contributing to the starvation-induced elevation of circulating free fatty acid in the absence of induction of HSL and MGL need to be elucidated. It is possible that the recently identified adipose tissue TG lipase (ATGL, or desnutrin) (182-184) may underlie this fatty acid elevation, as Sul and coworkers have shown that desnutrin gene expression is induced during starvation (182).

The function of intestinal MGL appears to oppose the typical metabolic fate of *sn*-2-MG, esterification to DG and ultimately TG. As discussed above, tissue-specific functions of MGL are likely. In adipose tissue, the physiological function of MGL in lipid metabolism is thought to be the complete hydrolysis of TG following the action of HSL and ATGL (95, 96). For liver MGL, the present studies suggest involvement in TG mobilization for secretion. Another intriguing functional aspect of MGL has been found recently in the central nervous system. MGL has been proposed to be a key enzyme modulating endocannabinoid signaling via hydrolysis of *sn*-2-arachidonoyl glycerol, an endogenous agonist of the cannabinoid receptors, CB1 and CB2 (99, 100). It has been reported that CB1 is present in the enteric plexus of the gastrointestinal tract

(155, 156), and endocannabinoid signaling has been proposed to function in gastroprotection against inflammation, control of intestinal motility, and secretory processes (158, 159). Thus, a potential signaling function for intestinal MGL should be considered.

The physiological significance of *sn*-2-MG metabolism in the small intestine has been indirectly demonstrated by the recently reported anti-obesity effect of 1, 3-DG feeding (185-188). Although the mechanisms underlying these effects are not known, we hypothesize that reduced *sn*-2-MG supply in the small intestinal epithelium, resulting from the lack of *sn*-2-acylated substrate, may lead to the altered lipid metabolism observed in 1, 3DG-fed mice. It will be of interest to examine how manipulation of intestinal MG metabolizing enzymes will affect TG reesterification, chylomicron secretion, and, perhaps, whole body energy homeostasis.

In summary, MG metabolism undergoes dramatic changes in both intestine and liver during ontogeny, and is modulated by high fat feeding. Intestinal MGL in particular is significantly elevated by a high fat diet, suggesting a potential function for MGL in dietary lipid assimilation at the substrate and/ or regulatory level.

Chapter 3.

Function of Intestinal Monoacylglycerol Lipase (MGL):

Over-expression of Monoacylglycerol Lipase (MGL) in Mouse

Small Intestine Results in an Obese Phenotype

1. Abstract

We recently demonstrated that, in addition to the well known anabolic metabolism of intestinal monoacylglycerol (MG), MG hydrolytic activity and expression of the MG lipase (MGL) gene were present at low levels in rodent small intestine. The function of small intestinal MGL is unknown. In the present studies, we generated transgenic mice (iMGL mice) that over-expressed MGL specifically in small intestine using the intestinal fatty acid binding protein promoter. Marked induction of transgenic MGL mRNA was found in transgenic animals, and intestinal specific expression of the transgene was confirmed using Northern and Western analysis and MGL activity measurements. Following 3 weeks of high fat feeding (40% Kcal), body weight gain and total fat pad weight were significantly increased in iMGL mice compared to non-transgenic littermates. DXA measurements showed that body fat mass was significantly higher in the iMGL mice whereas lean mass was not altered. Triacylglycerol (TG) content of intestinal mucosa and liver were also increased in iMGL mice. Plasma TG levels in iMGL mice were high but free fatty acid and total cholesterol levels were not changed. The metabolism of ^{14}C-oleate and ^{3}H-monoolein in small intestinal mucosa were not substantially altered, although less labeled MG remained following in vivo incubation. We determined the levels of individual MG species in intestinal mucosa and found that most were lower in iMGL mice, likely due to the action of the MGL transgene. Food intake data showed that the iMGL mice were hyperphagic. In addition, iMGL mice had reduced energy expenditure. Based on this phenotype, we hypothesize a role for intestinal MGL in whole body energy balance, possibly via regulation of food intake as well as metabolic rate.

2. Introduction

Dietary triacylglycerol (TG) is hydrolyzed to two fatty acids and *sn*-2-monoacylglycerol (MG) by pancreatic lipase in the small intestinal lumen (28). Both hydrolysis products are absorbed as monomers across the apical side of the intestinal epithelial cell (28, 58, 60). After absorption, *sn*-2-MG is rapidly reincorporated into TG in the endoplasmic reticulum (ER), providing a backbone for TG re-esterification via the monoacylglycerol acyltransferase (MGAT) pathway. Unlike other tissues, the MGAT pathway in small intestine plays a key role in TG re-synthesis during fat absorption, as more than 80 % of postprandial TG formation is catalyzed by this pathway (76, 77). Sequential acylation is initiated by MGAT, and completed by diacylglycerol acyltransferase (DGAT) enzymes; recently, genes encoding for both these enzymes have been identified (78-80, 83, 84). MGAT1 was cloned first, and was found to be expressed in various tissues such as adipose tissue, kidney, and testis, but not in small intestine where the highest MGAT activity levels are present (78). This prompted the identification of a second isoform, MGAT2, which is exclusively expressed in rodent small intestine (79,80).   In humans, three MGAT genes have been identified and two distinct forms, hMGAT2 and 3, are expressed in the gastrointestinal tract (79, 81). Two DGAT genes (DGAT1 and DGAT2) have also been identified and both are abundantly expressed in rodent small intestine (83, 84). The relative contribution to TG reesterification and the precise functions for each isoform of DGAT in the enterocyte remain to be elucidated.

Intestinal MG esterification has been well characterized as part of the dietary lipid assimilation process (28). In addition, MG hydrolysis in small intestine was reported in the 1960' s (91) and the partial purification of MG lipase (MGL; EC 3.1.1.23) from rat intestinal mucosa was attempted (91, 92). It was also shown that the majority of MGL activity was found in the microsomal fraction of the intestinal mucosa, suggesting localization to the endoplasmic reticulum (91). Recently we provided further evidence for the hydrolysis of MG in the enterocyte, as well as the presence of MGL gene expression, supporting a catabolic process for MG in small intestinal

epithelium (16). Nevertheless, there has been no further functional investigation of this enzyme in the intestinal epithelium. Thus, despite the large quantity of MG absorbed into the proximal small intestine, the function of MG hydrolysis in the enterocyte is unknown.

Holm and her colleagues cloned the MGL cDNA by screening a mouse adipocyte cDNA library and identified the residues of a canonical lipase catalytic triad (93). MGL mRNA transcript has been found in several tissues including liver, testis, kidney, adipose tissue, and skeletal muscle (93), and as noted above, we found MGL expression at low levels in the small intestine (16). MGL seems to have various functions depending on the tissue. In adipose tissue, the physiological function of MGL in lipid metabolism is thought to be the complete hydrolysis of TG following the action of hormone sensitive lipase and desnutrin (also known as adipose tissue TG lipase, ATGL), which produces *sn*-2-MG and fatty acids (95, 96). MGL cleaves *sn*-2-MG as efficiently as it does *sn*-1(3) MG, allowing complete breakdown of this intermediate to glycerol and fatty acid. Another functional aspect of this enzyme has been described in the brain, where MGL acts as a primary regulator of *sn*-2-arachidonoyl glycerol (2-AG) signaling action (99). 2-AG is a monoacylglycerol believed to work as an endogenous ligand for the cannabinoid receptors, modulating neuronal activity in the central nervous system (99, 149). One of the main functions of the cannabinoid system is the regulation of food intake by either central or peripheral actions (101, 142, 152, 189). Therefore, controlling neuronal signaling pathways might be another consideration for the function of MGL in the intestine.

The action of MGL in the intestine appears to oppose the typical metabolic fate of intestinal *sn*-2-MG, namely esterification to DG and ultimately TG, and we found that in adult mouse intestine there was, in fact, relatively low MG lipolytic activity compared to its acylation (190). As discussed above, MGL function is likely to be tissue-specific. In an effort to understand the function of intestinal MGL, we generated transgenic mice (iMGL mice) that over-expressed MGL specifically in small intestine using the intestinal fatty acid binding protein (IFABP) promoter, and investigated the effects on intestinal lipid metabolism as well as whole body energy

homeostasis. The major phenotype of the iMGL transgenic mice compared to wild type littermates, after 3 weeks of a high fat (40% kcal) diet, was a significant increase in body weight gain and body fat accumulation accompanied by hyperphagia, as well as reduced energy expenditure. These results suggest that alteration of intestinal MG metabolism greatly affects total body energy balance. We hypothesize a role for intestinal MGL in whole body energy homeostasis, possibly via regulation of food intake and metabolic rate.

3. Experimental procedures

Materials

[^{14}C] *sn*-2-monoolein (oleoyl-1-[^{14}C], 55 mCi/ mmol) and [^{3}H] *sn*-2-monoolein (oleoyl-9, 10-[^{3}H (N)], 60 Ci/ mmol) were purchased from American Radiolabeled Chemicals, Inc. (St. Louis, MO). [1-^{14}C] oleate (55 mCi/ mmol) was purchased from Perkin Elmer Life Science (Boston, MA). Unlabeled *sn*-2-monoolein was obtained from Doosan Serdary Research Laboratories (Toronto, Canada). The 3% borate impregnated thin layer chromatography (TLC) plates were purchased from Analtech (Newark, DE). Anti-peptide antibody against the N-terminal region of mouse MGL was a generous gift from Dr. Daniele Piomelli (99) (UC Irvine, CA). β-actin antibody was purchased from Sigma (St. Louis, MO).

Generation of the IFABP/MGL recombinant vector

The transgene for intestinal specific overexpression of MGL is diagrammed in Fig. 3-1-A. The plasmid containing the rat IFABP promoter (region -1178 to +28 nucleotides of the rat IFABP gene) (191). was generously provided by Dr. Jeffry Gordon (Washington U., St. Louis MO). The mouse MGL coding region (935bp) was obtained by RT-PCR using mouse adipose tissue RNA, and then subcloned into the IFABP vector using BamH1 and Hind3 sites. Subsequently, in order to achieve maximal induction of transgene expression , SV40 poly A and intron sequences (1.6kb), a gift from Dr. Jeffry Ceci (U.of Texas Medical Branch, Galveston TX) (192), were ligated to the 3' end of the MGL coding region using Hind3 and Xho1 sites. The 3.8Kb transgene was liberated by restriction enzyme digestion by Xho1, Xba1, and Bgl1. The additional Bgl1 digestion was necessary for better separation of the 3.8 Kb transgene from other digested plasmid sequences.

Generation of transgenic mice

The linearized transgene construct was injected into pronucleii of fertilized eggs from C57/BL6J females that mated with hybrid males (C57/BL6J X SJL). The fertilized eggs following pronuclear injection were implanted into surrogate females. 12 founders were identified and mated with C57/BL6J to produce F1 mice, used to check transgene expression and for further experimentation. Marked induction of the transgenic MGL transcript was found in 3 transgenic founders (#415, #361-1, and #361-2). The F1 generation from the #415 founder was used for most of the subsequent studies, unless otherwise specified.

Genomic DNA analysis in transgenic mice

Initial transgene detection among the potential founders was done by PCR analysis of genomic DNA samples from tail biopsies. Primers were designed so that the PCR reaction produces a unique 400bp junction fragment spanning the middle of the MGL coding region and part of the SV40 poly A sequence in transgenic animals: forward 5'-GAG TCA GGA CAA AAC ACT CAA GAT GTA -3', reverse 5'-ACT AGA TGG CAT TTC TTC TGA GCA AAA C-3' (Fig. 3-1-B). Southern blot analysis was performed in order to verify the number of copies and the integrity of the transgene in the mouse genome. 25μg of genomic DNA was digested with BamH1, separated by 1% agarose gel, and transferred onto nylon membranes (GE Healthcare, Piscataway, NJ). Integrated recombinant DNA was detected by [^{32}P] labeled probes for partial sequences of a) SV40 poly A signal, b) IFABP promoter region, or c) the junction region between MGL coding region and SV 40 poly A sequence. 1-100 copies of transgene construct were mixed with wild type genomic DNA for a copy standard to determine the copy number of each transgenic line by Southern blot analysis (Fig. 3-1-C).

Animals, diets, and tissue collection

Animals were maintained on a 12 hr light and dark cycle and fed a regular chow diet (Purina Mouse Chow 5015, Purina Co., St. Louis, MO) ad libitum after weaning. Male mice aged ~

3 months old were housed two per cage, and fed with purified rodent diet consisting of 40% fat by calories from coconut oil, rich in short chain saturated fatty acids (D12327, Research Diets, New Brunswick, NJ), for 3 weeks ad libitum. Food intakes and body weights were monitored once a week and body composition was measured using the Piximus (Perkin Elmer Life Science, Boston, MA) mouse DXA instrument at the end of the feeding trial. Animals were anesthetized prior to either metabolism studies or tissue collection. All tissues were immediately frozen in ethanol /dry ice and kept at -70ºC.

Northern blot analysis for transgenic mRNA detection

Tissues were homogenized in 5X volume (5 ml per 1g of tissue) of Solution D (4 M Guanidinium thiocyanate, 25 mM Na Citrate, 0.1 M 2-mercaptoethanol) using several strokes of a Polytron. Total RNA was purified by phenol extraction. Poly A$^+$ RNA was obtained as described (190). 40μg of total RNA or 1ug poly A$^+$ RNA were loaded onto a 1% agarose gel, separated by electrophoresis, and transferred onto nylon membranes (GE Healthcare, Piscataway, NJ). Full length coding regions of mMGL cDNA were labeled with [^{32}P] (Perkin Elmer Life Science, Boston, MA) using the Random Prime labeling system (GE Healthcare, Piscataway, NJ). Membranes were pre-hybridized for 1 hr and hybridized for 2-3 hr at 65 ºC using Rapid-hybridization solution (GE Healthcare, Piscataway, NJ). Blots were washed twice at room temperature with 2×SSC, 0.1% SDS for 15 min. An additional high temperature (65 °C) wash with 0.1×SSC, 0.1% SDS for 30 min was completed before exposing the blots to a PhosphorImager screen. Quantification was done using the Molecular Dynamics STORM scanner and ImageQuaNT software (Molecular Dynamics, Sunnyvale, CA).

Western blot analysis for MGL protein expression

Tissues were homogenized in 10 volumes of homogenization buffer on ice for 30 sec. using a Wheaton tissue homogenizer (Wheaton Science, Millville, NJ), and crude tissue

homogenates were centrifuged at 600×g for 10 min. at 4 ºC to remove unbroken cell debris. Homogenization buffer contained 50 mM Tri-HCl and 0.32 M sucrose (pH 8) with 0.5% (v/v) protease inhibitors (Sigma. Cat. # 8340). Protein concentration was determined by the Bradford assay (167). 50 µg of total cell protein were loaded onto 12% polyacrylamide gels and separated by SDS-PAGE. The proteins were transferred onto PVDF membranes using a semi-dry transfer system (Bio-Rad, Hercules, CA) for 1 hr at 20 V. All membranes were incubated in a 5% nonfat dry milk blocking solution overnight at 4ºC and then probed with primary antibody for 1 hr. Dilution of the anti-mMGL antibody was 1:5,000. After washing three times, blots were incubated with anti-rabbit IgG-horseradish peroxidase conjugate at 1:10,000 dilution for 1 hr and then developed by chemiluminescence (ECL reagent, GE Healthcare, Piscataway, NJ). Blots were stripped and reprobed with mouse β-actin antibody (Sigma, St. Louis, MO) to check the integrity of the sample and as a loading control. Quantification of protein bands was done using Image J software (NIH).

In vitro MGL assay

MGL activity was determined by measuring the release of fatty acid from *sn*-2-MG as described previously (190). [^{14}C] *sn*-2-monoolein (oleoyl-1-[^{14}C], 55 mCi/ mmol) was mixed with unlabeled *sn*-2-monoolein (Doosan Serdary Research, Toronto, Canada) to obtain the desired concentrations. The mixture of [^{14}C] radiolabeled and unlabeled *sn*-2-monoolein was dried under N_2 gas, and 0.125 M Tri-HCl buffer containing 1.25% BSA was added. Substrate emulsions were prepared by brief sonication (1 min) on ice. 100µg of each tissue sample was introduced in 50µM substrate in a total volume of 0.5ml and the reaction was carried out for 10 min at 23ºC. Lipid extraction and TLC separations were done as described (190).

In vivo fatty acid and sn-2-MG metabolism studies

The metabolic fate of dietary fatty acid and *sn*-2-MG in small intestine were determined in vivo using intra-duodenal radiolabeled lipid administration as described (17). Mice were

anesthetized with a mixture of ketamine/xylazine/promazine (80/100/150mg/kg, respectively) via intraperitoneal injection prior to lipid administration. Less than 40 nmol of each labeled lipid, either [^{3}H] *sn*-2-monoolein or [1-^{14}C] oleic acid, was administrated via cannula to the mouse duodenum as a mixture with a 10 mM sodium taurocholate solution. Following 2 min, mice were sacrificed, and the entire small intestine from pylorus to cecum was immediately excised. The intestine was rinsed twice with saline, and then the mucosa was harvested by scraping. Tissue was homogenized immediately with 10X volume of 1X PBS solution. Protein concentration was determined by Bradford assay (167). Tissue lipids were extracted using the Folch method (193). Lipid extracts were kept at – 20°C until TLC analysis was performed. Lipid extracts were spotted on standard silica gel plates (Sigma, St. Louis, MO) and separated by a solvent system of hexane/ethyl ether/ acetic acid, 70:30:1, v/v. For [1-^{14}C] oleic acid, the plates were exposed to a PhosphorImager screen to visualize labeled lipids. Quantification of each lipid fraction was analyzed using ImageQuaNT software (Molecular Dynamics, Sunnyvale, CA). For [^{3}H] *sn*-2-monoolein metabolism, TLC plates were scraped and counted using a scintillation counter (Perkin Elmer Life Science, Boston, MA).

Fecal fat analysis

Fecal fat content was estimated gravimetrically as described by Newberry *et. al.* with minor modification (194). Briefly, 0.5g feces was soaked with 1ml of water overnight, and 5ml of chloroform/methanol (2:1) solution was added and the sample was homogenized for 15 sec. using a Wheaton tissue homogenizer (Wheaton Science, Millville, NJ); an additional 15 ml of chloroform/methanol (2:1) was added and vortex mixed. Lipid extract was collected through filter paper and dried under nitrogen gas. Fecal fat weight was measured in pre-weighed glass vials. Percent fecal fat was calculated based on total fecal weight.

Fatty acid oxidation

Intestinal FA oxidation was measured as described previously (17). Briefly, tissue homogenate was diluted to 1mg/ml with 1x PBS and 1 ml was placed in a 15mL disposable plastic tube. A piece of tissue paper soaked in 1 M benzethonium hydroxide in a 0.5mL Eppendorf tube was then placed in the 15mL tube to trap $^{14}CO_2$. 0.3mL of 3M perchloric acid was added, and samples were capped tightly and incubated overnight at 37º C with gentle shaking. Following overnight incubation, the acidified sample was vortex mixed, centrifuged at 2,800 rpm for 10 min, and radioactivity of the supernatant and tissue paper were measured. Radioactivity of the supernatant (acid-soluble products, ketones and TCA intermediates) plus tissue paper (CO_2) was considered as total FA oxidation. Data are presented as % FA oxidation, which was calculated as the total FA oxidation (radioactivity from supernatant plus tissue paper) divided by the radioactivity found in 1 mg of tissue homogenate.

Tissue TG

To determine tissue TG content, intestinal mucosa, liver, and muscle lipid extracts (193) were spotted onto TLC plates with 2µg to 100µg of lipid standards to quantify the TG content in each tissue, separated as above, and visualized by iodine staining. Quantification was performed using Image J software (NIH).

Blood chemistry

Serum TG, free fatty acid, and total cholesterol levels were determined using colorimetric assay kits (Wako, Richmond, VA). Following 3 weeks of high fat feeding as described above, the measurements were done either in the fed state, where food was present throughout the dark period and the experiment was typically done in the morning (9am – 11 am), or following an overnight fast, where food was withdrawn at the beginning of the dark period and the experiment was performed the next morning. Mice were anesthetized and blood was collected from the

abdominal artery, and then immediately centrifuged to obtain serum. Fasting blood glucose levels were measured using the Accu-Chek (Roche Diagnostics, Indianapolis, IN) glucose meter from mouse tail snips.

Quantitative RT-PCR

Relative mRNA expression of several genes involved in lipid metabolism in the small intestine was analyzed by quantitative RT-PCR using SYBR Green chemistry. Preparation of RNA samples and q PCR reactions were performed as described previously (190). Briefly, total RNA was prepared by GTC extraction, and samples were further purified using the RNeasy clean up kit (Qiagen, Valencia, CA) along with DNase 1 treatment. Reverse transcription was performed using 1 μg of total RNA, random primer, RNase inhibitor and AMV reverse transcriptase (Promega Madison, WI) in a total volume of 25 μl. Primer sequences were retrieved from Primer Bank (Harvard Medical School QPCR primer database), and are listed in Table 3-1. Efficiencies of PCR amplification for β-actin and the gene of interest were tested during preliminary experiments and similar PCR efficiencies were confirmed. Real time PCR reactions were performed in triplicate using an Applied Biosystems 7300 instrument. Each reaction contained 80 ng of cDNA, 250 nM of each primer, and 12.5 μl of SYBR Green Master Mix (Applied Biosystems, Foster City, CA) in a total volume of 25 μl. Relative quantification of expression was calculated using the comparative Ct method normalized to β-actin.

LCMS analysis

MG levels in small intestinal mucosa were estimated by LCMS analysis using a Dionex UltiMate 3000 HPLC (Dionex, Sunnyvale, CA, USA) coupled to an Applied Biosystems 4000Q-TRAP® mass spectrometer (Applied Biosystems, Ontario, Canada). Tissue lipids were extracted by the Folch method, dried down, and reconstituted in isooctane: tetrahydrofuran (9:1,

Table 3-1. Q-PCR primer sequences

β-ACTIN	Forward 5'-GGC TGT ATT CCC CTC CAT CG-3'
	Reverse 5'-CCA GTT GGT AAC AAT GCC ATG T-3'
MGAT2	Forward 5'-TGG GAG CGC AGG TTA CAG A-3'
	Reverse 5'-CAG GTG GCA TAC AGG ACA GA-3'
ER GPAT (GPAT 3)	Forward 5'-TAT CCA AAG AGA TGA GTC ACC CA-3'
	Reverse 5'-CAC AAT GGC TTC AAC CCC TT-3'
DGAT1	Forward 5'-TGT TCA GCT CAG ACA GTG GTT-3'
	Reverse 5'-CCA CCA GGA TGC CAT ACT TGA T-3'
DGAT2	Forward 5'-TTC CTG GCA TAA GGC CCT ATT-3'
	Reverse 5'-AGT CTA TGG TGT CTC GGT TGA C-3'
PPARα	Forward 5'-TCG GCG AAC TAT TCG GCT G-3'
	Reverse 5'-GCA CTT GTG AAA ACG GCA GT-3'
CB1	Forward 5'-GGG CAC CTT CAC GGT TCT G-3'
	Reverse 5'-GTG GAA GTC AAC AAA GCT GTA GA-3'

v/v), such that extracted lipids from 2 mg protein were diluted in 1ml of solvent. 1ng of mononbonanoin was spiked into 5µl of sample to use as an internal standard. 4 µl of extract were injected into a Waters (Milford, MA, USA) Spherisorb® S5W 4.6 x 100 mm silica column with a Spherisorb® S5W 4.6 x 10 mm guard cartridge, and eluted using a modified version of the tertiary normal phase solvent gradient described by Homan and Anderson (195). The autosampler was kept at 20 ºC and the column oven at 45ºC. The flow rate was 1 ml/minute except from 6 to 10 minutes, when it was 0.4 ml/minute. Ionization was carried out with the PhotoSpray™ ion source operated in positive ion mode. Toluene was the dopant and was pumped into the source using a Dionex AXP-MS pump. The flow rate of the toluene was 100 µl/minute except from 6 to 10 minutes, when it was 40 µl/minute. Nitrogen was used for all gases and was produced by an AirGen A320DR nitrogen generator (Peak Scientific Instruments Ltd., Bedford, MA, USA). The MS parameters were: curtain gas, 15; collision gas, 4; ion source gas 1, 40; ion source gas 2, 20; nebulizer temperature, 450° C; transfer voltage, 750 V; interface heater, on; entrance potential, 10; collision cell exit potential, 10. Monoacylglycerols were measured using Multiple Reaction Monitoring with dwell times of 100 milliseconds for all compounds. A standard curve containing 50 pg to 20 ng (11 values, 10 µl/injection) of each monoacylglycerol was run prior to and immediately after the sample lipid extracts. The peaks corresponding to each analyte were integrated and concentrations were calculated using Analyst 1.4.2 software in Windows XP.

Energy expenditure measurement

The metabolic rates of animals were measured by indirect calorimetry, using the PhysioScan instrument (AccuScan Instruments Inc.) at the Mouse Metabolic Phenotyping Center at the University of Cincinnati. Following 3 weeks of high fat feeding as described above, animals (n=8 per each group) were sent to the metabolic core, and measurements were performed in the fed state following a 10 day acclimation during which they were fed the same high fat diet. Oxygen consumption (VO_2) and carbon dioxide (VCO_2) production were continuously monitored by

PhysioScan software every second over a 24 hr. period. Respiratory quotient (RQ) and energy expenditure were calculated based on the VO_2 and VCO_2 values, as described by Weir with minor modification (196).

4. Results

Generation of transgenic mice overexpressing murine MGL specifically in small intestine using the IFABP promoter - Following pronuclear injection of the recombinant IFABP/MGL construct, 101 potential founders were obtained from surrogate females, and transgenic founders were initially identified by PCR analysis as described above (Fig. 3-1-B). 12 founders were identified, and these were bred with C57BL/6 mice to establish each transgenic line. Southern blot analyses were performed with genomic DNA samples from each founder and their offspring to check the copy number and the integrity of transgene integration in the mouse genome. A diagram and example of the Southern analysis are depicted in Fig. 3-1-C. 25µg of genomic DNA were digested with BamH1, and probed with partial SV 40 poly A sequence (thick bars) to detect repeated 2kb fragments (thin bars). The blot demonstrates a copy number standard (right side) with samples from several founders (left side). The expected 2kb bands were detected in the #361, #415, #401, and #359 founders, with extra bands from the 3' end of the transgene insertion into the genome. A less than 2kb sized band was detected in the #109 line without a 2 kb band, possibly due to a single integration. The #370 sample, a non-transgenic littermate, was used as a negative control for the analysis. Copy numbers varied in the different lines, from a single copy to > 50. The # 415 transgenic line, used for subsequent studies, has more than 50 copies of intact recombinant MGL DNA inserted. Among the 12 founders, two female founders (#368 and #384) were infertile, and transgene integration in the #374 line was not intact. One of the founders (#361) had multiple insertions of the transgene, confirmed by Southern analysis, so two separate lines were established from the #361 founder. Thus, 10 transgenic lines were established, and these were checked for MGL expression in the small intestine.

Intestinal specific overexpression of MGL - Northern blot analysis, probed with a full length mMGL cDNA, demonstrated a robust induction of transgenic MGL mRNA in the #415, #361-1 and #361-2 lines, whereas no transgenic expression was found in their wild type littermates, as

Figure 3-1

A

B

#415 #416#417#418#419#420#421
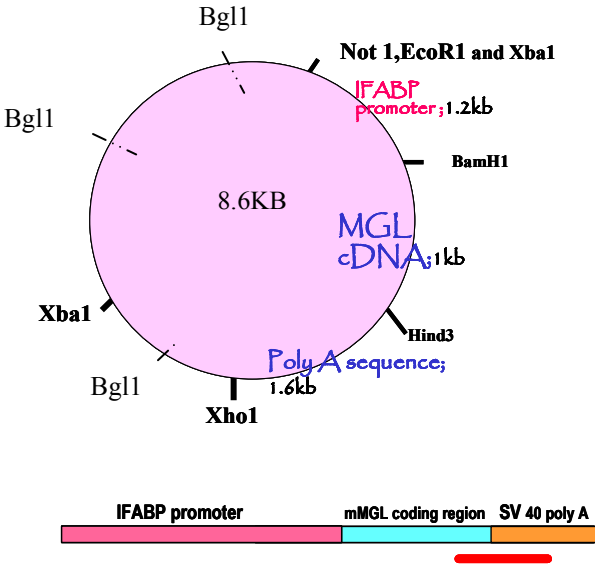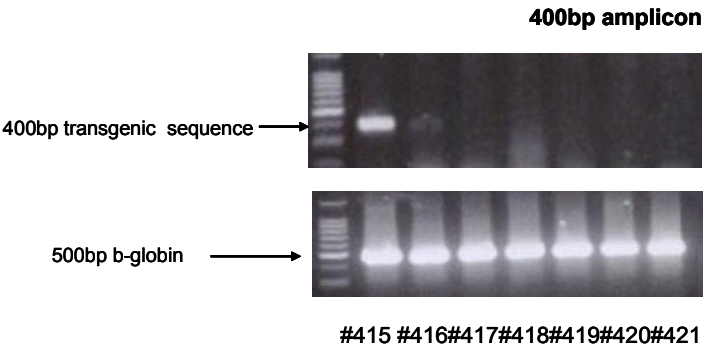
C
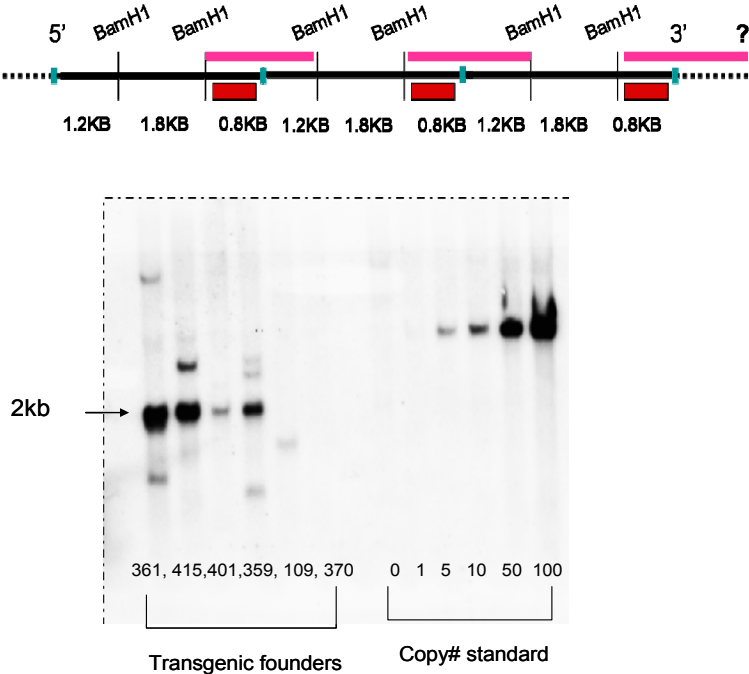
Figure 3-1. Generation of transgenic mice (iMGL) overexpressing MGL specifically in small intestine. (A) Construct of the IFABP promoter/MGL recombinant vector. (B) PCR screening for transgenic animals. A unique 400bp sequence only present in transgenic animals was the target for amplification. Bottom gel shows β-globin amplification, used for checking the integrity of the genomic DNA samples. Numbers on the bottom indicate individual potential founders. (C) DNA analysis of various transgenic founders by Southern blotting. Top diagram describes the design of a Southern analysis. Partial sequence of 0.8kb region (thick bars) was used as a probe to detect a 2kb sequence (thin bar) present in the transgene. Bottom blot shows the expected 2kb band with various copy numbers in several transgenic lines along with their extra bands. (unpredictable sizes from 3'end insertion into the mouse genome. Right side of blot shows copy number standard from 0 to 100.

expected (Fig. 3-2-A). Endogenous MGL transcript, corresponding to the 4kb band, was barely detectable in these adult small intestine samples by Northern analysis, in agreement with our previous results (190). The results indicate that overexpression of MGL derived from the IFABP promoter was marked compared to endogenous expression levels in the small intestine. The F1 generation from the #415 male founder was used in subsequent studies. Tissue specific expression of the transgene was confirmed by Northern analysis. Transgenic 2kb mMGL mRNA was found only in the small intestine (Fig. 3-2-B, lane 2), not in other organs, whereas brain, adipose, liver, and stomach showed only the 4Kb endogenous transcript, but not transgenic mRNA (Fig. 3-2-B), demonstrating intestinal specific expression of the MGL transgene. MGL protein levels in small intestine were determined by Western analysis and enzyme activities were measured as described in Experimental procedures, following 3 week high fat feeding. Significant increases in MGL protein (Fig. 3-2-C) and activity levels in the small intestine were found in the transgenic animals, as shown in Fig. 3-2-D.

Normal metabolic fates of dietary lipids in iMGL small intestine– To address the impact of MGL overexpression on intestinal lipid metabolism, the metabolic fates of dietary fatty acid and *sn*-2-MG were analyzed by intraduodenal injection of radiolabeled ^{14}C-oleic acid or ^{3}H-monoolein in vivo. No differences in the percentage of metabolites of ^{14}C-oleic acid were found in iMGL mice. In agreement with previous results, fatty acids were primarily incorporated into TG (70%), with lesser amounts used for PL synthesis (10%) or other intermediates (Fig. 3-3-A). For ^{3}H-monoolein administration, only the percent MG was less in iMGL mice compared to wild type (wild type; 4.5 ± 0.6 % vs. iMGL; 2.76 ± 0.31 %, $p < 0.05$). No further changes in the acute metabolism of MG were found, similar to the results for ^{14}C-oleic acid metabolism (Fig. 3-3-B). The reduced MG levels following ^{3}H-monoolein injection are likely due to MGL overexpression in transgenic animals. To determine whether intestinal MGL overexpression affects quantitative TG esterification, the acute (2 min) incorporation of radioactive ^{14}C-oleate or ^{3}H- monoolein into TG

Figure 3-2
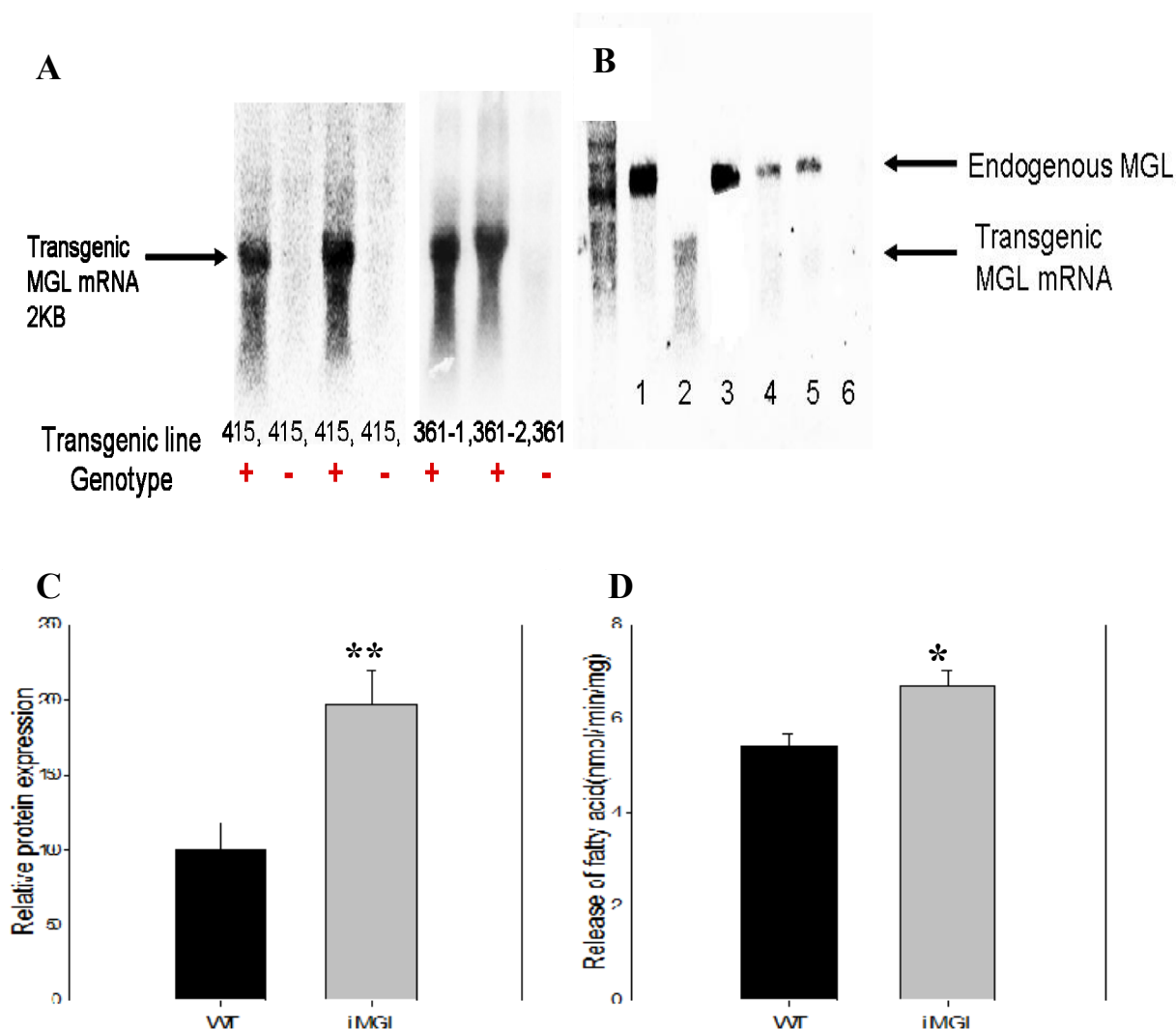
Figure 3-2. Tissue specific overexpression of transgenic MGL mRNA. (A) Overexpression of transgenic MGL transcript (2kb) in mouse small intestine. 40μg of total RNA samples were loaded onto each well, and probed with [^{32}P] labeled full length coding region of mMGL cDNA. (B) Intestinal specific expression of transgenic MGL transcript. 1μg of poly A$^+$ RNA samples were loaded onto each well, and probed with mMGL cDNA. Lane 1, Brain; lane 2, Small intestine; lane 3, Adipose tissue; lane 4, Liver; lane 5, Stomach; lane 6, Cecum. Upper bands found in lanes 1, 3, 4, and 5 corresponded to the 4kb endogenous MGL transcript, and lower band shown in lane 2 was the 2kb transgenic MGL transcript. (C) Relative MGL protein expression in iMGL versus wild type small intestine. Values are presented relative to the expression of the wild type littermates set to 100%. Data represent mean ± S.E. n= 5-8 per group. (D) MGL activity in iMGL versus wild type small intestine. n= 5-8 per group, *$p<0.05$, **$p<0.01$ versus wild type littermates.

Figure 3-3

A **^{14}C-oleic acid metabolism**

B **^{3}H-monoolein metabolism**

C

D

E

F
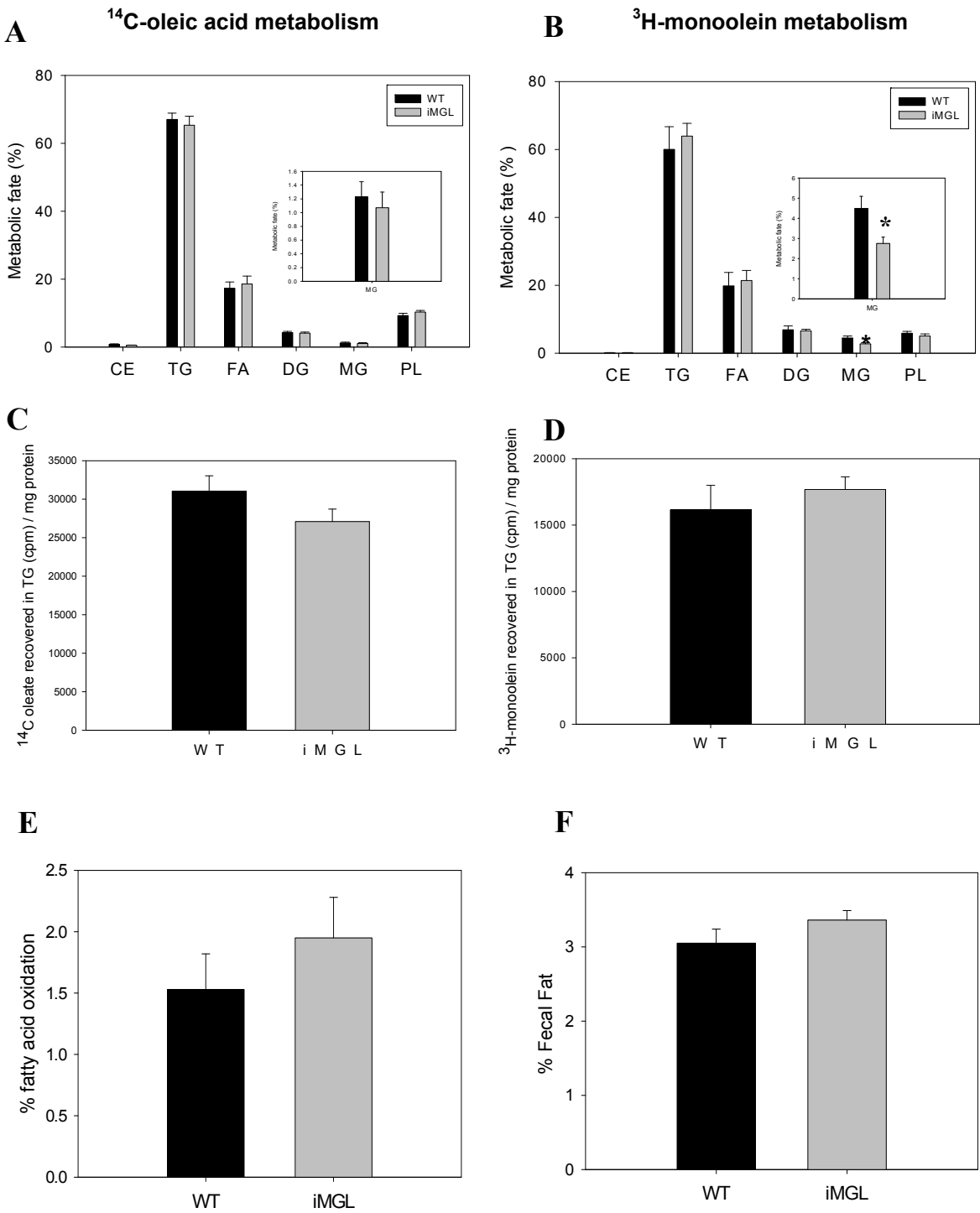
Figure 3-3. Metabolic fates of dietary fatty acid and monoacylglycerol in iMGL mice small intestine. Metabolism studies were conducted in vivo by administration of radiolabeled lipids in mouse duodenum, and metabolites were assayed as described in Experimental Procedures. (A) Metabolic fate of dietary ^{14}C-oleic acid in iMGL mice small intestine. Data are presented as the % of each metabolite relative to total metabolites. Inset shows an enlarged scale for MG (WT; n= 10, iMGL; n= 16). (B) Metabolic fate of dietary ^{3}H-monoolein in iMGL mice small intestine. Data are presented as the % of each metabolite relative to total metabolites. Inset shows an enlarged scale for MG (WT; n= 5, iMGL; n= 9). (C) ^{14}C oleate incorporation into TG (cpm/ mg protein) (WT; n= 10, iMGL; n= 16). (D) ^{3}H monoolein incorporation into TG (cpm/ mg protein) (WT; n= 5, iMGL; n= 9). (E) Percent fatty acid (^{14}C oleate) oxidation in iMGL mice small intestine (WT; n= 10, iMGL; n= 18). (F) Fecal fat analysis. Fecal fat content is presented as the % of stool weight (WT; n= 6, iMGL; n=5). Data represent mean ± S.E. * $p < 0.05$ versus wild type littermates.

was estimated. No differences in radioactive lipid incorporation were found (Fig. 3-3-C and D), suggesting that acute TG esterification was not affected by MGL overexpression in the small intestine. Fatty acid oxidation was also determined following the 2 min intraduodenal administration in vivo, and the percent of ^{14}C-oleic acid oxidized to CO_2 plus acid soluble metabolites was not statistically different in iMGL mice and wild type littermates (Fig. 3-3-E). To determine whether lipid absorption was altered in iMGL mice, we measured the percent fecal fat content, which was estimated gravimetrically based on total fecal weight. The results showed that fecal fat content in iMGL mice was similar to that of the control group, indicating that the efficiency of dietary fat absorption in iMGL mice was not altered (Fig. 3-3-F).

Decreased MG species levels in iMGL mice small intestine- Quantification of each MG species in iMGL mice small intestine compared to wild type littermates was done using LCMS analysis as described in Experimental Procedures. Most of the MG species were significantly lower (20-50%) in iMGL mice, except monolinolenin and monopalmitolein, though there was a trend for decreased monolinolenin levels that did not reach statistical significance (Fig. 3-4). The results are consistent with the broad substrate specificity of MGL (91, 197-199). Other lipid species in iMGL mice small intestine were examined using TLC analysis. TG levels were significantly increased (Fig. 3-5-E), as well as fatty acid content (wild type; 39.56± 6.88 vs. iMGL; 78.24 ± 10.40 µg/mg protein, $p <$ 0.01), whereas phospholipid levels were not significantly changed according to genotype (wild type; 0.46± 0.09 vs. iMGL; 0.51 ± 0.05 mg/mg protein, $p = 0.66$).

Increased adiposity in iMGL mice – **i**MGL animals were viable and healthy. No abnormalities or distinguishable phenotypes were observed during growth. Animals were fed a high fat diet for 3 weeks when they were 3 months old, and phenotype analyses were performed after the feeding trial. There was no significant difference in baseline body weight according to genotype (wild type; 29.09 ± 0.52g vs. iMGL; 30.41 ± 0.49g, $p = 0.07$). Following 3 weeks of high fat feeding, however,
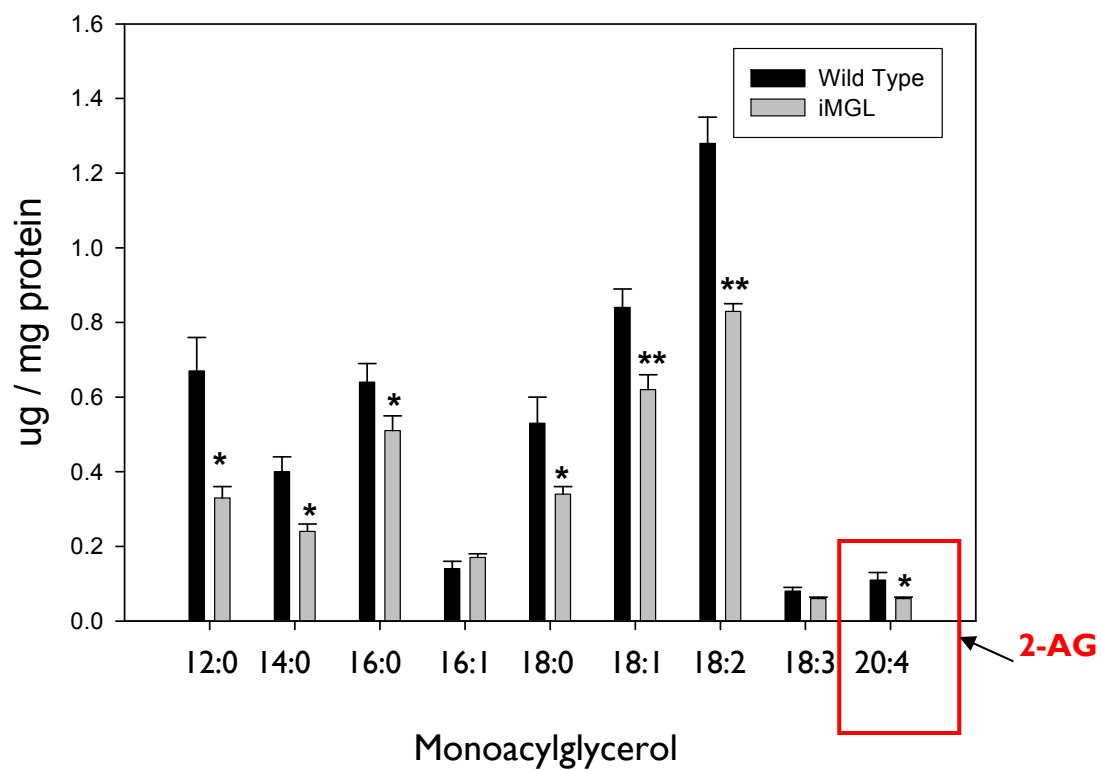
Figure 3-4

Figure 3-4. Comparison of MG levels in iMGL mice small intestine by LCMS analysis.
(WT; n= 7, iMGL; n= 8). Data represent mean ± S.E. * $p < 0.05$, ** $p < 0.01$ versus wild type littermates.

weight gains in the iMGL mice were significantly higher than those of wild type littermates (wild type; 3.83± 0.37g vs. iMGL; 5.45 ± 0.32g, $p < 0.01$) (Fig. 3-5-A). Another transgenic line (#361-1 line) also showed a similar trend, with higher body weight gain relative to their wild type littermates (data not shown). In addition, the accumulation of body fat was higher in iMGL (Fig. 3-5-C). The % body fat was significantly higher and adipose tissue mass was double in iMGL mice compared to wild type mice following 3 weeks of high fat feeding (Fig. 3-5-B and C). Ventral views of iMGL mice and their littermate controls also clearly demonstrated the increased adiposity in iMGL mice; representative images are shown in Fig. 3-5-D. Ectopic fat deposition was found in liver and small intestine. TG content in these tissues were significantly elevated (Fig. 3-5-E and F), but muscle TG level was not different (Fig. 3-5-G). Serum lipid and fasting blood glucose levels of iMGL mice were compared to those of littermate controls. Serum TG levels in iMGL mice were significantly higher in the fed state, but not in the fasting condition (Table 3-2). There were no differences in other serum parameters according to genotype (Table 3-2).

Increased Food intake and decreased energy expenditure in iMGL mice – Cumulative food intakes during the high fat feeding trial were measured and average daily food intake per mouse was calculated. A significant increase in the food intake of iMGL mice was found compared to littermate controls (wild type 3.34± 0.08 g/day vs. iMGL; 3.87 ± 0.14 g/day, $p < 0.01$) (Fig. 3-6-A), indicating that the iMGL mice were hyperphagic. This hyperphagic behavior was observed, even in the first week of feeding and was sustained throughout the entire 3 week feeding period (Fig. 3-6-B). Metabolic rates of iMGL and wild type mice were monitored for 24hr. by indirect calorimetry. There were significant decreases in both oxygen consumption (VO_2) and carbon dioxide production (VCO_2) over the entire time course, both in the dark phase and the light phase (Fig. 3-6-C, and D). Respiratory quotient (RQ) values in both genotypes were similar (WT 0.78± 0.01/ iMGL; 0.78± 0.01, $p = 0.72$), indicating no alternation in fuel selection in iMGL mice (Fig. 3-6-F). Energy expenditure, calculated based on VO_2 and VCO_2, showed a small but significant 9%

Figure 3-5

A

B

C

WT

iMGL

D

E

F

G
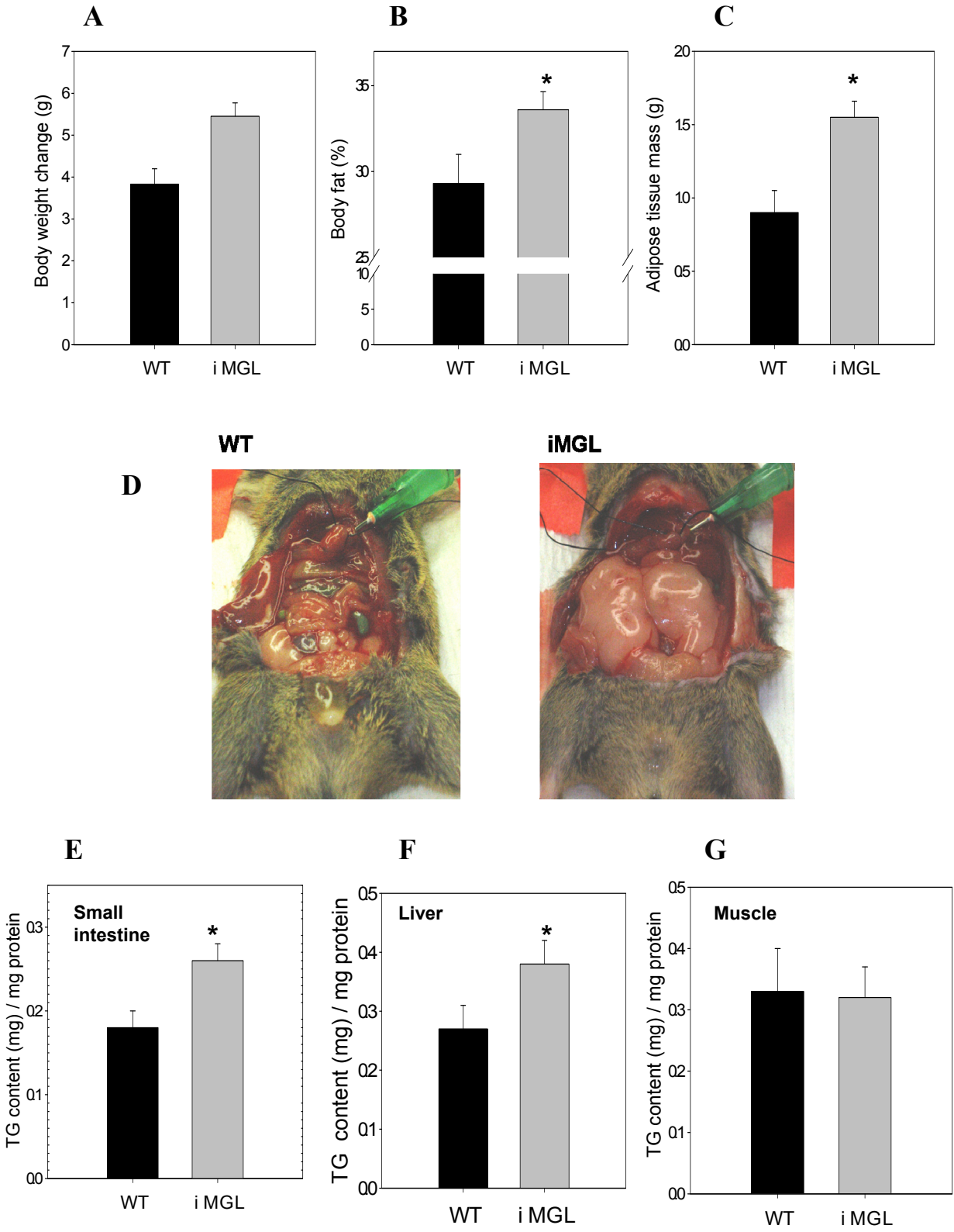
Figure 3-5. Increased adiposity in iMGL mice after 3 weeks of a high fat (40% kcal) diet. (A) Body weight changes (WT; n= 41, iMGL; n=57). (B) % body fat determined by DXA measurement (WT; n= 24, iMGL; n=49). (C) Fat pad weight (total of epididymal, peri-renal, and mesenteric-omental depots) (WT; n= 15, iMGL; n=28). (D) A ventral view of a representative iMGL mouse and a wild type littermate. (E) TG content in intestinal mucosa (WT; n= 9, iMGL; n=14). (F) TG content in liver (WT; n= 6, iMGL; n=13). (G) TG content in muscle (WT; n= 8, iMGL; n=16). Data represent mean ± S.E. * $p < 0.05$, ** $p < 0.01$ versus wild type littermates.

Table 3-2 Serum lipid and glucose levels

		Wild Type	iMGL
TG (mg/dL)	Fed	79.71 ± 5.93	104.60 ± 10.38*
	Fasting	45.68 ± 5.26	34.16 ± 1.60
Cholesterol (mg/dL)	Fed	178.24 ± 11.41	178.27 ± 8.25
	Fasting	114.65 ± 11.31	113.27 ± 10.90
Fatty acid (mM)	Fed	2.74 ± 0.18	2.51 ± 0.07
	Fasting	0.83 ± 0.20	0.79 ± 0.23
Glucose (mg/dL)	Fasting	159.38 ± 7.83	146.82 ± 9.96

* $p < 0.05$ versus wild type

Figure 3-6
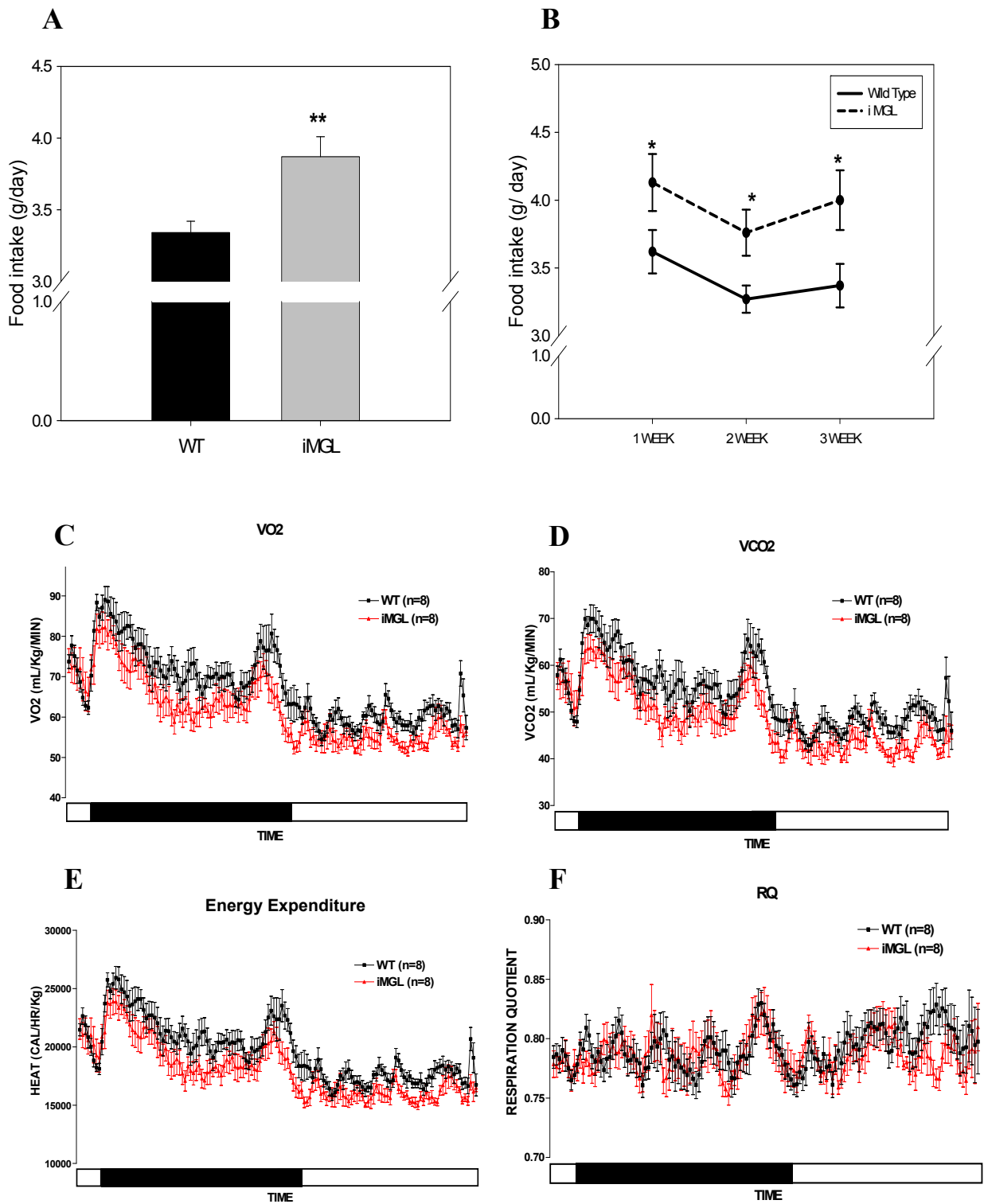
Figure 3-6. Increased food intake in iMGL mice. (A) Average daily food intake per mouse over the 3 week high fat feeding trial (WT; n= 15, iMGL; n=20). (B) Time course of average daily food intake per mouse for each week (WT; n= 15, iMGL; n=15). (C) Time course of oxygen consumption during 24 hr. Values are expressed as ml/kg/min (WT; n= 8, iMGL; n=8). (D) Time course of CO_2 production during 24 hr. Values are expressed as ml/kg/min (WT; n= 8, iMGL; n=8). (E) Time course of Energy expenditure during 24hr. calculated based on VO_2 and VCO_2. Values were expressed as calorie/ hour/ kg body weight (WT; n= 8, iMGL; n=8). (F) Time course of respiratory quotient (RQ) values. (WT; n= 8, iMGL; n=8). On the X axis, the black bar represents the dark period and the white bar is the light period. All indirect caloriemtry measurement were collected every second for 24 hr. Data represent mean ± S.E. * $p < 0.05$, ** $p < 0.01$ versus wild type littermates.

decrease in iMGL mice (Fig. 3-6-E). Thus, the calculated average metabolic rate over the 24 hr measurement was less in iMGL mice (WT; 19,671± 501 Cal/hr/kg, iMGL; 18,073± 467 Cal/hr/kg, $p < 0.05$). These observations suggest that both increased food intake and decreased metabolic rate contribute to the increased adiposity in iMGL mice.

Expression of genes involved in intestinal lipid metabolism in iMGL mice – The expression levels of major lipogenic genes in small intestine were measured by Q-PCR analysis. There was no compensatory increase of lipogenic gene expression in response to MGL overexpression. In fact, MGAT2 and ER GPAT (GPAT3), encoding for the enzymes which initiate TG reesterification in small intestine, were modestly but significantly downregulated in iMGL mice (Fig. 3-7-A). Expression of PPAR α, known to regulate many genes in intestinal lipid metabolism including DGAT and LFABP, and also to mediate the anorexic effect of oleolyethanolamine (OEA) (133), was not altered in iMGL mice (Fig. 3-7-B). DGAT1 and DGAT2 levels were unaltered as well. CB1 expression in submucosal and myenteric plexuses innervating intestinal muscle layers has been demonstrated previously (138, 157), but mucosal expression has not been reported. We were able to detect mucosal CB1 expression by qPCR analysis (Fig.3-7-B). Preliminary analysis for the direct comparison of CB1 expression level in mucosa indicated that CB1 levels in mucosa were 5 fold lower compared to intact intestine (data not shown). Interestingly, CB1 expression in both intestinal mucosa and the entire intestine were modestly, but significantly downregulated (35-40%) in iMGL mice, consistent with the decreased level (45%) of its ligand, 2-AG (Fig. 3-4 and 3-7-B).

Figure 3-7
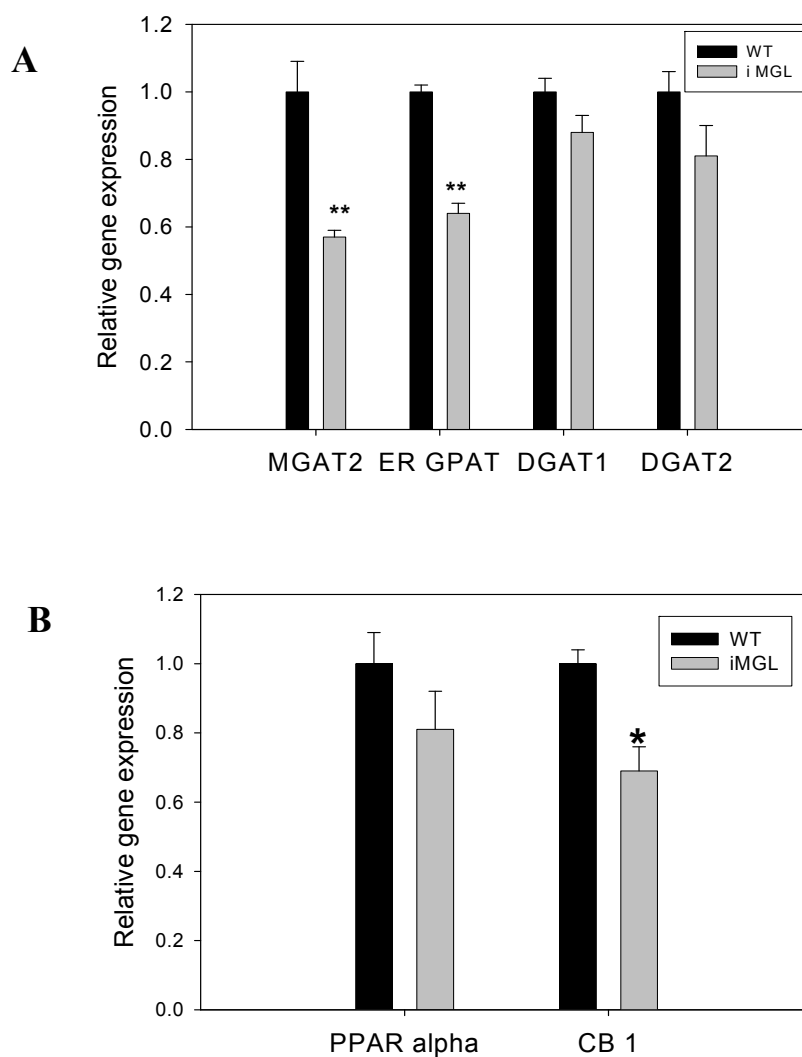
Figure 3-7. Gene expression in iMGL mice small intestine. Relative gene expression was determined by Q-PCR. Reaction conditions and primers are as described in Experimental Procedures and Table 3-1. (A) Relative mRNA expression of lipogenic genes in iMGL mice intestinal mucosa. (B) Relative mRNA expression of PPAR α and CB1 (WT; n= 6, iMGL; n= 6). Values are presented relative to the expression of the wild type littermates set to 1. Data represent mean ± S.E. * $p < 0.05$, ** $p < 0.01$ versus wild type littermates.

5. Discussion

The hydrolysis of *sn*-2-MG in intestinal epithelium has been reported (16, 91, 92) and recently MGL expression and its regulation in rodent small intestine have been described (16, 190). Nevertheless, the physiological role of MGL in the small intestine is entirely unknown. To address the functional significance of intestinal MGL, we generated transgenic mice overexpressing mouse MGL specifically in the small intestine under the control of the IFABP promoter, which directs expression to the small intestine villus cells, exclusively. Intestinal specific expression of transgene was successfully achieved as intended without unexpected promoter leakage, and marked induction of transgenic MGL mRNA was found in the iMGL intestinal mucosa. Despite apparent overexpression of transgenic MGL message, the corresponding protein and activities were under detectable levels in chow fed mice. However, following the high fat diet, MGL protein and activity levels in iMGL mice were significantly higher than their littermate control. This observed effect of the high fat diet may be mediated by post-transcriptional regulation, perhaps via MGL protein stability, but not likely due to the IFABP promoter since a high fat diet does not affect transcriptional efficiency of the IFABP promoter (23). These differences in mRNA, protein, and activity levels found in iMGL mice further support the possibility for post-transcriptional and post-translational regulation of MGL expression, as discussed in chapter 2.

Obesity in the iMGL mice was clearly demonstrated, in that the increased body weight resulted from a marked increase in % body fat and adipose tissue mass. Further, ectopic TG accumulation was found in liver and intestinal mucosa, and the iMGL mice displayed postprandial hypertriglyceridemia as well. This obese phenotype was unexpected, since the action of MGL would seem to be opposite to the well known MG absorption and assimilation process, with esterification catalyzed by MGAT2 (24, 28, 79, 80). We had speculated that the overexpression of MGL might counteract this predominant MGAT pathway, resulting perhaps in reduced intestinal TG production and a lean phenotype when animals were exposed to a high fat diet. Contrary to such expectations, the iMGL mice were obese. Fat absorption was quantitatively normal, and the acute

intestinal metabolism of MG and FA were not significantly altered. Plasma TG levels in the fed state were even higher in iMGL than in wild type animals. Also, there was no compensatory increase in lipogenic gene expression in the small intestine to explain this obese phenotype; indeed MGAT2 and GPAT3 were moderately downregulated. Only MG levels were significantly reduced, likely due to increased MG hydrolysis secondary to overexpression of MGL, but lipid absorption and TG resynthesis were intact.

Although the mucosal TG accumulation found in iMGL mice intestine is likely due to the ectopic fat accumulation accompanying the obese phenotype, delayed TG secretion from the intestine can not be ruled out, since neutral lipid storage in intestinal mucosa has been well characterized as a part of secretion defects (25, 69, 200). Abetaliproteinemia, the hereditary defect in microsomal TG transfer protein (MTP) is the well known example (200). In addition, DGAT1^{-/-} and MGAT2 [-/-] mice displayed a diminished postabsorptive chylomicronemia along with mucosal lipid accumulation. Nevertheless, total quantitative dietary fat absorption was normal in both mice, even when fed a high fat diet, and the acute incorporation of radiolabeled oleic acid into TG were also intact (25, 201), indicating that delayed lipid secretion did not significantly affect overall fat absorption. Furthermore, their lean phenotype was likely caused by a significant increase in metabolic rate, not the delayed lipid secretion from the enterocyte. Future studies will examine chylomicron secretion in iMGL mice to fully understand the mucosal lipid accumulation, however it is unlikely involved in the marked perturbation of energy homeostasis found in iMGL mouse, for the following reasons. First of all, iMGL mice showed a postprandial hypertriglyceredemia, which is hard to reconcile with a diminished chylomicronemia. Secondly, total quantitative lipid absorption and TG esterification were not compromised in iMGL mouse intestine, as mentioned above. Finally, a delayed TG secretion can not account for the obese phenotype in iMGL mice.

The percent recovery of radioactivity in the MG fraction 2 min following intraduodenal administration of radiolabeled *sn*-2-monoolein was 35% lower compared to the littermate controls. Consistent with this observation, the absolute amounts of almost all of the individual MG species

were lower in iMGL intestinal mucosa, with decreases ranging from 20-50%, providing clear evidence for increased MGL activity upon transgene overexpression. Among the nine MG species analyzed, only two, monolinolenin and monopalmitolein did not show statistically significant decreases; the monolinolenin level trended lower, and monopalmitolein levels did not vary between iMGL and wild type mucosa. MGL has been shown to have broad substrate specificity in terms of acyl chains, hydrolyzing both short and long chain and saturated and unsaturated fatty acyl chain moieties, as well as sn-2 and sn-1 monoacylglycerol isomers (91, 197-199). Several studies have shown a higher hydrolysis rate for the 2-AG substrate compared to monoolein and monopalmitin (202-204). However, an opposite result was reported by Dinh $et\ al.$, who reported faster hydrolysis of monoolein relative to monoarachidonoylglycerol in HeLa cells following adenovirus transfection of MGL (99). The present results showed a larger decrease in monoarachidonoylglycerol (45%) than in monoolein (26%) and monopalmitin (20%), consistent with preferential hydrolysis of 2-AG. It is worth noting that the 2-AG levels found in the present study were approximately 30 nmol/g tissue in the wild type mouse, in agreement with a previous report (44nmol/g tissue) (158). Brain 2-AG levels have been shown to be in the range of 2-14 nmol/g tissue depending on the specific region (205). Adipose tissue 2-AG levels were reported to be 1-2.5 nmol/g tissue (151). Levels in other tissues such as liver, spleen, and lung are 0.78-1.17nmol/g tissue (205). Thus, intestinal 2-AG levels are quite high compared to other organs, presumably due to their dietary source. The physiological efficacy of 2-AG has been well established as a ligand for the EC signaling system, whereas other MG species are unable to bind to the CB receptors (140, 206) and currently there is no evidence for MG species other than 2-AG, as signaling mediators. However, Ben-shabt $et.al.$ reported that 2-monopalmitin and 2-monolinolein potentiate 2-AG binding to the CB1 receptor (206), suggesting a possible indirect role in signaling.

Despite the apparently normal intestinal MG metabolism, the overexpression of MGL in the small intestine and the reduced mucosal 2-MG levels were correlated with profound affects on whole body energy balance. The underlying mechanisms by which altered MG levels in iMGL

small intestine affects both appetite and metabolic rate, resulting in an obese phenotype, are not presently known. Indeed, the results are opposite of what might be expected given the known effects of 2-AG in the EC signaling system. The monoacylglycerol 2-AG is a ligand for CB receptors, and a main function of this signaling system is in appetite regulation, either through central or peripheral nervous systems (101, 142, 152). Ligand binding to the CB receptor results in increased food intake (101, 189). MGL is the key enzyme responsible for deactivating 2-AG signaling by hydrolysis of 2-AG in brain (99, 149). Thus, MGL hydrolysis of 2-AG in the brain results in diminished activation of CB receptors, which leads to anorexic effects (99-101). Nevertheless, food intake was significantly increased in the iMGL mice. The hyperphagic phenotype in iMGL mice is hard to reconcile with the currently understood actions of the EC system.

Energy expenditure in iMGL mice was decreased significantly, providing another mechanism for development of the obese phenotype. Again, the EC system has been suggested to regulate energy expenditure, in addition to its well established function in appetite control (101, 207). Treatment of diet induced obese mice with rimonabant, a potent and selective CB receptor antagonist, caused a sustained decrease in body weight and adiposity with only a transient hypophagia (208). Further, Liu et.al. provided more direct evidence, showing that 7 days of rimonabant treatment in genetically obese ob/ob mice significantly increased VO_2 consumption compared to vehicle treated ob/ob mice (207). Thus, if the EC system in iMGL mice is not intact, this may give rise to changes in metabolic rate.

Altered metabolic rate has been shown to contribute to an obese phenotype in various enterocyte lipid metabolism knock out and transgenic animal models, contributing to changes in body weight and adiposity. For example, increased energy expenditure in DGAT1$^{-/-}$ mice has been suggested as a potential mechanism for their resistance to diet induced obesity (86). Similarly, in MGAT2$^{-/-}$ mice, a higher metabolic rate and lower weight gain were observed under a high fat feeding regimen (201). Thus, there is precedence for a linkage between intestinal lipid metabolism

and whole body energy expenditure. The mechanisms underlying altered metabolic rate in iMGL mice, as in the DGAT1$^{-/-}$ and MGAT2$^{-/-}$ models, remain to be elucidated. There was no difference in RQ according to genotype. We had initially speculated that iMGL mice might burn less lipid for fuel utilization, since they have greater fat mass. However, the RQ results suggest no selectivity in fuel utilization in iMGL mice, but rather less quantity used for energy yield regardless of fuel type.

Both central and peripheral actions of endocannabinoid (EC) signaling mediate orexigenic behavior (101, 142, 152, 189). For example, administration of cannabinoid into the hypothalamus triggers hyperphagia (143-145). During fasting, 2-AG levels in the hypothalamus are increased and returned to normal levels upon feeding (145, 146). The EC system in intestine also exerts a hyperphagic effect, shown to be mediated by changes in anandamide (AEA) levels (152, 157, 209). AEA is considered to be a major endogenous ligand for the CB receptors, along with 2-AG (100, 139). Food deprivation significantly increased AEA levels in the small intestine (152). In addition, CB1 receptor expression in the vagus afferent nerve termini innervating the gastrointestinal tract is also regulated by feeding status, with expression upregulated by starvation and downregulated upon feeding (160). In contrast to AEA, the significance of intestinal 2-AG in EC signaling in appetite regulation has not been well investigated. Petersen *et.al* reported that the 2-AG level in rat intestine was not significantly changed after 24 hr food deprivation, although there was a non-significant trend toward an increase in 2-AG level upon starvation (209). Thus, the role of intestinal 2-AG in feeding regulation remains to be elucidated. As Storr and Sharkey speculated (157), two distinct pools of 2-AG may be present in the intact small intestine, one serving a signaling function and the other much larger pool for the bulk lipid metabolic pathway. The cell type and spatial localization of these putative pools is not known. Perhaps the reciprocal regulation of the two pools, if any, could provide a piece of the puzzle to understand the present results. For example, the decreased mucosal 2-AG level in iMGL mice may trigger an increase in biosynthesis of 2-AG in nerve termini, causing activation of EC signaling in the small intestine and, finally, leading to an orexigenic effect in iMGL mice.

The gaps in our knowledge of the EC system, MGL, and 2-AG in the intestine include the following: 1) As noted above, changes in intestinal 2-AG levels based on feeding status are still ambiguous, awaiting a definite assessment; 2) Is the change in eating behavior of iMGL mice directly via alteration of the EC system, or is it mediated by changes in other satiety signals such as oleolyethanolamin (OEA), an anorexic lipid mediator found in small intestine (210). 3) Are there different pools of 2-AG, based either on cell type, in different layers of the intestine and/ or at the subcellular level? 4) How does mucosal expression of MGL affect EC signaling, which is believed to be present in nerve terminals innervating the intestinal muscle layer? 5) Are other gut peptide and hormones involved in the observed effect of MGL overexpression? As mentioned in chapter 1, many gut peptides exert their appetite and metabolic regulation via crosstalk between gut and brain, and there is growing evidence for the interaction between signaling systems. For example, the EC system interacts with ghrelin and CCK signaling (160, 211). In vagal afferent neurons, CCK administration attenuated the CB1 induction caused by starvation, and CCK antagonist treatment prevented loss of CB1 expression resulting from refeeding (160). Also, the administration of ghrelin blocked the downregulation of CB1 by refeeding (211). Thus, the underlying mechanisms for obesity in the iMGL mouse should be considered broadly, not solely focusing on the EC signaling cascades. While these and other questions remain, these studies are the first to demonstrate that alteration of intestinal MG levels significantly affects whole body energy homeostasis, primarily via changes in food intake and energy expenditure, providing a new insight for intestinal MGL as a regulator of energy balance.

In summary, we found a clear metabolic perturbation in mice overexpressing MGL specifically in the small intestine, demonstrating a physiological significance for intestinal MGL. Increased adiposity secondary to hyperphagia and hypometabolic rate in iMGL mice suggests that intestinal MGL might be envisioned as a new metabolic regulator controlling whole body energy homeostasis. Detailed molecular mechanisms need to be elucidated and such studies will likely

lead to another avenue for understanding intestinal MG, in addition to its role in dietary lipid absorption.

Chapter 4.

General Conclusions and Future Directions

One third of the dietary TG hydrolysis products in the intestinal lumen is *sn*-2-MG. Following its absorption into the enterocyte, *sn*-2-MG provides a backbone for TG reesterification via the MGAT pathway, the predominant TG synthetic pathway in the intestinal epithelium. Not only is the highest MGAT activity found in the small intestine, but also the presence of multiple genes encoding for MGAT activities in this tissue indicates its critical role in lipid absorption, as discussed in chapter 1. Nevertheless, the small intestine also exhibits a catabolic process for *sn*-2-MG with the expression of the MGL gene, however its function in enterocytes is currently unknown. Thus, the metabolism of intestinal *sn*-2-MG is likely to be complex, with diverse metabolic fates and functions, rather than simply serving as an intermediate in TG assimilation.

Despite the abundance of diet-derived *sn*-2-MG, the regulation of MG metabolism in the small intestine has not been explored in depth. Therefore, the aim of this thesis was to understand the regulation and function of the two MG metabolizing enzymes in the small intestine, MGL and MGAT2 and, further, to elucidate the impact of intestinal MG metabolism on whole body energy balance.

The regulation of intestinal MG metabolizing enzymes during development and by nutritional status.

mRNA expression, protein expression, and activities of the two known MG metabolizing enzymes, MGL and MGAT2, were examined in C57BL/6 mouse small intestine, as well as liver and adipose tissues, during development and under nutritional modifications. Results demonstrate that MG metabolism undergoes tissue-specific changes during development. Hepatic MGL mRNA, protein and activity all increased 5-10 fold during development, whereas MGAT2 mRNA and activities decreased, suggesting a reciprocal regulation occurring primarily via transcriptional mechanisms. In contrast, intestinal regulation during ontogeny was complex, exhibiting discordances in changes of mRNA, protein, and activity.

Based on these discordances, post-transcriptional or translational regulation of expression was suggested for the two MG metabolizing enzymes in the small intestine during mouse ontogeny. As discussed in chapter 2, both enzymes have putative phosphorylation sites for various kinases (Fig.4-1). It will be of interest to explore 1) whether MGAT and MGL are phosphorylated, and at what sites; 2) under what physiological conditions phosphorylation or dephosphorylation occur; 3) how phosphorylation status affects enzyme activities; and 4) whether there is tissue specific regulation or reciprocal regulation of the two MG metabolizing enzymes by certain kinases. In addition to phosphorylation, both enzymes also have several putative N-myristoylation sites, and MGL has an N-glycosylation site as well, further suggesting possibilities for other types of post-translational modification (Fig.4-1) (173).

Intestinal MGL activity increased rapidly after birth and was maintained throughout adulthood, whereas protein expression in the suckling period was under detectable levels. Thus, *sn*-2-MG hydrolysis during this time period may be mediated by other lipases. Carboxyl ester lipase (CEL), which is known to have *sn*-2-MG hydrolytic activity was suggested as one of the candidates, and as shown in Fig. 2-1-E, a considerable amount of CEL is in fact expressed in suckling small intestine, suggesting an involvement of CEL in MG hydrolysis. In addition to CEL, enterocytes express pancreatic lipase (PTL) and hormone sensitive lipase (HSL) as well (51,52), and these might also contribute to MG breakdown during lactation. However PTL is not expressed until weaning (212), and both HSL and PTL have only limited catalytic activity toward *sn*-2-MG (28,95). Perhaps, there might be an as-yet unknown, novel lipase possessing MG hydrolytic activity. Exploring new candidate genes for intestinal MG hydrolysis will be an additional aspect for future studies.

In addition to an obvious discordance found in MGL protein and activity levels in the suckling intestine, another disparity for intestinal MGL regulation during ontogeny was found in the relative mRNA and protein levels in prenatal versus adult stages. Relative transcript levels in adults are considerably lower than those in the prenatal stages, but protein levels were opposite

Figure. 4-1

A
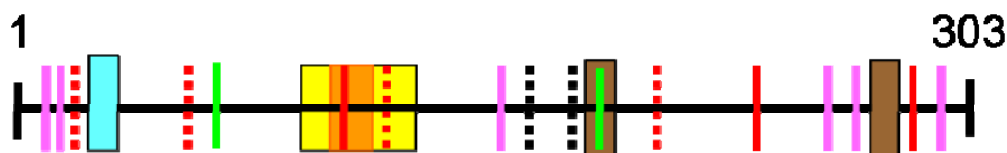
Figure 4-1-A. mMGL protein domain analysis. Prosite analysis (173) was used for the protein domain search and putative TM domain analysis was done using TMpred (213) and HMMTOP (214) algorithms.

 Red: amino acids comprising catalytic triad (102, 239,269)
Blue: lipase consensus (HG dipeptide; 49,50)
Orange: lipase consensus ,GXSXG serine active site (116-125)
Yellow: Putative TM domain (115-139)
Green: CK2 phosphorylation (83-86, 189-192)
Pink color: PKC phosphorylation (6-8, 40-42, 158-160, 253-255, 260-262)
Brown: Tyrosine kinase phosphorylation (186-194, 262-268)
Black dashed line: N-glycosylation (173-176, 187-190)
Red dashed line: N-myristoylation (39-44, 81-86, 124-129, 204-209)

B
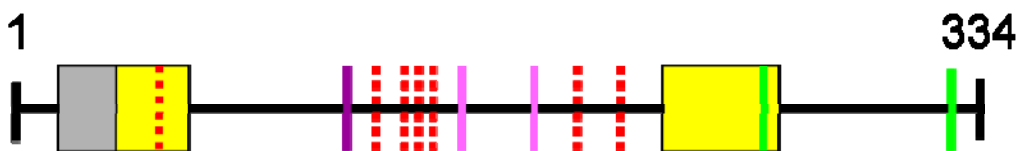
Figure 4-1-B. mMGAT2 protein domain analysis. Prosite analysis (173) was used for the protein domain search and putative TM domain analysis was done using TMpred (213) and HMMTOP (214) algorithms.

 Gray: Putative lipid binding domain (21-36)
Purple: HPHG conserved sequence in DGAT2 family (107-110)
Yellow: Putative TM domain (24-43, 209-227)
Green: CK2 phosphorylation (225-228, 297-300)
Pink: PKC phosphorylation (163-165, 173-175)
Red dashed line: N-myristoylation (40-45, 111-116, 116-121, 158-163, 159-164, 178-183, 187-192)

(Fig. 2-1), implicating potential regulatory processes occurring either in protein or in mRNA stabilities. Interestingly, mouse MGL mRNA contains a very long 3'untranslated region (UTR). The average rodent 3'UTR length is about 400bp (215), whereas MGL has an extensively long 2580 bp 3'UTR sequence in the total 4kb mRNA sequence. It is well known that one of the main functions of the 3' UTR is regulating mRNA stability and translation efficiency (215). Therefore, future studies could address an analysis of the MGL 3' UTR sequence, for example, analyzing the AU rich elements (AREs). Such stretches, consisting mainly of adenine and uridine nucleotides, are known to affect mRNA stability; they can either stabilize or destabilize the mRNA depending on the protein bound to it (216). Since our functional analysis of intestinal MGL (Chapter 3) provided evidence for its potential role in energy balance, and MGAT2 function in lipid absorption is well known, the modulation of expression and activities of these two enzymes could be useful targets for obesity treatment.

Results of the developmental regulation studies strongly suggested the tissue specific regulation and functions of MGL as well as MGAT2, as follows: 1) Reciprocal regulation of the two enzymes was only found in liver, but not in the small intestine. 2) Hepatic MGL activity in the adult was about 20 fold higher than that in the small intestine whereas hepatic MGAT activity in the adult was about 20 fold less than intestinal MGAT activity. 3) Apparent transcriptional regulation was observed in liver, but more complex regulatory mechanisms were suggested in intestine. In addition, further evidence for tissue specific functions come from the different pattern of MGL subcellular localization in each tissue, observed in preliminary studies. As shown in Figure 4-2, intestinal MGL protein was only detected in the membrane fraction, whereas hepatic MGL expression was not restricted to membranes, but was also present in the cytosolic compartment. Putative transmembrane (TM) domains of MGL were predicted by several algorithms, producing variable results. SOSUI (217) and TMHMM (218) analyses suggest MGL as a soluble protein whereas 1 to 3 TM domains were predicted by TMpred (213) and HMMTOP (214) algorithms, indirectly suggesting that diverse localization of MGL might be possible, as we found in liver.

Figure. 4-2
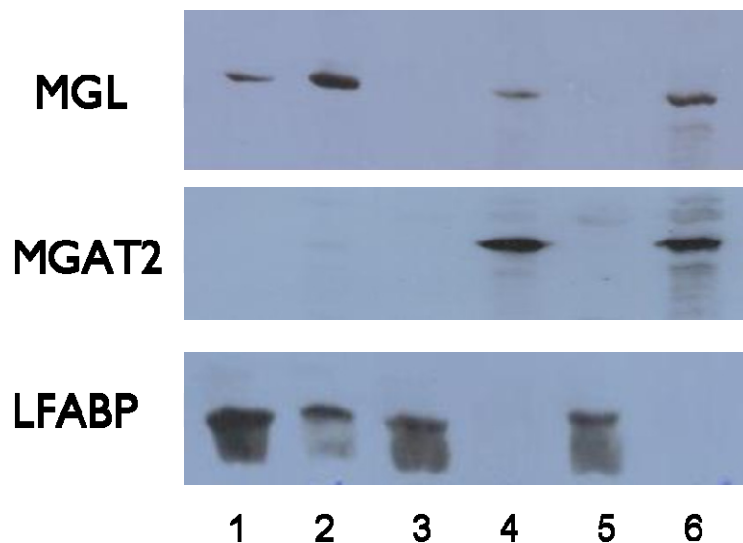
Figure 4-2. Subcellular localization of mMGL in liver and small intestine. Total membrane and cytosolic fractionation were prepared by ultracetrifugation (100,000 xg). 50μg of tissue protein were loaded onto each lane and probed with anti- m MGL, m MGAT2, and LFABP antibodies. Lane 1, Liver cytosol; lane 2, Liver membrane; lane 3, Intestine cytosol; lane 4, Intestine membrane; lane 5, Intestine cytosol; lane 6, Intestine membrane

Predicted TM domains are indicated in Fig. 4-1. More defined localization studies for MGL, both at the subcellular level as well as in intestinal epithelium (crypt to villus and proximal to distal axes) needs to be investigated to help understand its function. Overall, its distinct pattern of regulation, levels of enzyme activity, and preliminary localization data indicate the tissue specific function of MGL in the small intestine. As discussed in chapter 2, hepatic MGL function is likely related to TG mobilization for VLDL secretion. In contrast, intestinal MGL is envisioned as a modulator of energy metabolism, presumably via regulating signaling pathways as discussed in chapter 3 and below.

The function of intestinal MGL in small intestine and in whole body energy homeostasis

In our nutritional modification studies, a significant induction of intestinal MGL was observed following three weeks of high fat feeding (40% kcal) relative to low fat feeding (10% kcal), but little change was observed upon starvation. Based on this observation, we speculated that intestinal MGL might function as a regulator for dietary lipid assimilation by counteracting MGAT activities, when enterocytes are exposed to excessive dietary fat. In order to address MGL function in the small intestine directly, the targeted overexpression of the MGL gene in mouse small intestine was carried out using the IFABP promoter, which directs expression to the small intestine villus cells, exclusively. Marked induction of transgenic MGL mRNA was found in the iMGL transgenic animals and intestinal specific expression of the transgene was confirmed. The impact of this genetic manipulation on intestinal lipid metabolism and whole body energy balance were examined. The major phenotype of transgenic mice compared to wild type littermates following the high fat diet includes a significant increase in body weight gain accompanied by marked body fat accumulation and hyperphagia. Further, a significant decrease in metabolic rate was observed in transgenic animals, implying that impaired intestinal MG metabolism greatly affects whole body energy balance.

The overexpression of MGL in small intestine was expected to result in a lean phenotype upon high fat feeding since MGL action appears to be opposite to MGAT activity. Surprisingly, an unexpected phenotype was observed as described above. Results described in chapter 3 clearly suggest that intestinal MGL is participating in the regulation of energy balance. Nevertheless it may not be mediated at the substrate level by counteracting MGAT as we hypothesized. Quantitative total lipid absorption in small intestine was normal, and TG reesterification from the major luminal TG hydrolysis products, FA and MG, was intact in iMGL mice intestine, suggesting that MGL overexpression minimally affects lipid assimilation pathways in the enterocyte. Significant differences were found only in MG levels; cellular MG levels as well as recovery of radioactivity in the MG fraction following intraduonenal labeled MG administration, were both reduced. As discussed in chapter 3, an intriguing relationship between MG levels and energy metabolism has been shown to be mediated by the EC system, and noticeably decreased 2-AG levels as well as CB1 receptor expression in intestinal epithelium of iMGL mice were observed. Thus, we are proposing that the observed impaired energy homeostasis in iMGL mice may be mediated by alterations in gut-brain signaling, presumably via altered EC regulation.

Hyperactivity of the EC system results in hyperphagic behavior and increased adiposity, and MGL works to terminate EC signaling by breaking down MG, an endogenous substrate for CB receptors (91,101). Here we have a paradox in that MGL induction in the small intestine caused a phenotype associated with EC system activation rather than termination. As discussed, only limited knowledge is available concerning intestinal EC signaling, and a precise mechanism to reconcile this apparent discrepancy is currently unknown. The present studies demonstrate changes in intestinal epithelium; MGL overexpression and decreases in 2-AG level occur in the mucosa, likely in the enterocytes. In contrast, CB1 expression in intestine has shown to be predominantly located in the myenteric and submucosal plexus in muscle layers, though CB1 expression in villus nerve fibers has not been studied well (Fig.4-3). Many unanswered questions need to be explored in order to elucidate this paradox.

Figure. 4-3
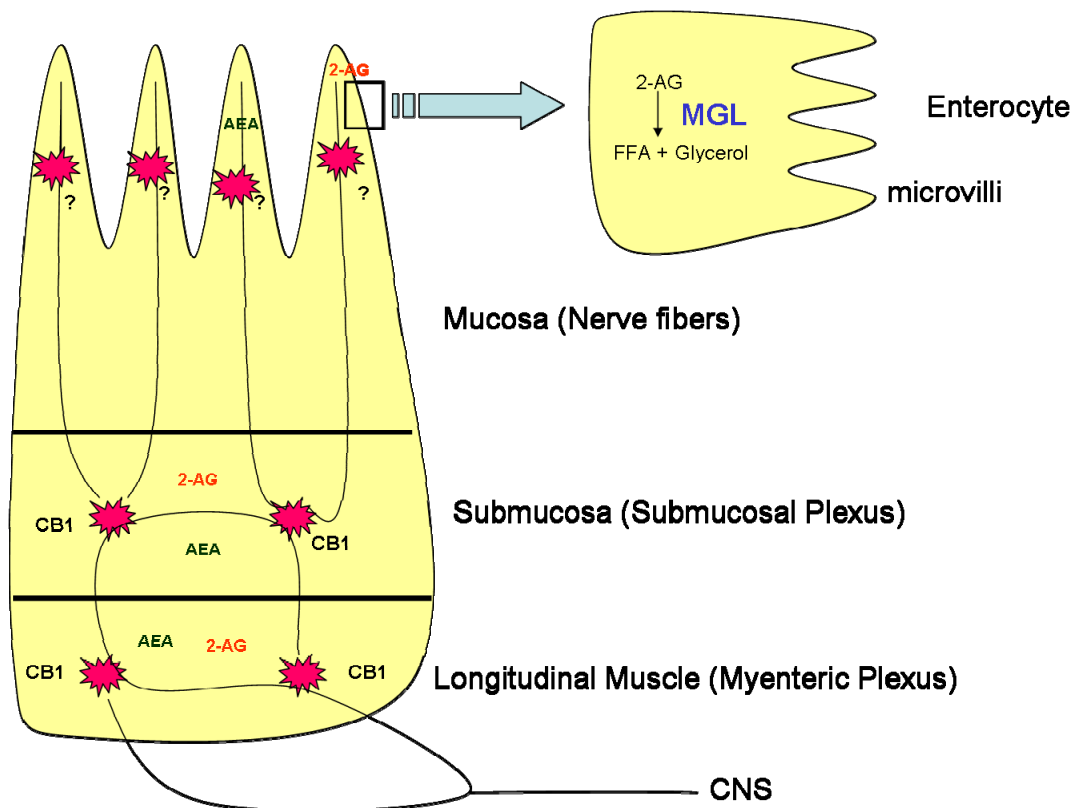
Figure 4-3. Schematic diagram of cannabinoid signaling in the small intestine.
CB1 expression was detected in the myenteric and submucosal plexuses of the gastrointestinal tract (155,156), and the two major endocannbinoids, 2-AG and AEA, are present in the small intestine (140,157). A significant increase in anandamide (AEA) levels in the small intestine was reported during starvation (152), and it has been shown that fasting increased and feeding decreased CB1 expression in the vagus afferent nerve termini innervating the gastrointestinal tract (160). In contrast to AEA, the significance of intestinal 2-AG and MGL in EC signaling and appetite regulation has not been well investigated. Current studies showed that mucosal overexpression of MGL and decreased 2-AG level significantly affect whole body energy balance via hyperphagia and decreased metabolic rate in iMGL mouse. The precise action of the intestinal EC system in either mucosal or muscle layers, and their interaction, if any, needs to be addressed to understand the mechanisms underlying the obese phenotype in the iMGL mouse.

For example, 1) Is diet-derived 2-AG present in the intestinal epithelium able to activate the EC system? If it is, how is 2-AG able to be transported out of the enterocytes and travel to the muscle layer CB1 receptors? 2) Are CB1 receptors present in the termini of villus nerve fibers as well as in the submucosal plexus? 3) Are there separate pools of 2-AG (dietary versus endogenous, or epithelial versus neuronal) and are there any interactions between the pools? 4) Endogenous 2-AG generation in neurons is primarily carried out by diacylglycerol lipase (DGL) (100, 219), thus examining DGL expression in iMGL mice might be of interest. 5) Other gut satiety hormones are known to interact with the EC system. Burdyga *et. al.* reported a reciprocal regulation of CCK and CB1 expression in vagus nerve (160), and ghrelin administration prevented CB1 downregulation caused by refeeding (211). Thus, the analysis of other satiety hormones in iMGL mice may offer valuable clues for addressing the mechanisms underlying their phenotype.

It has been shown that the activation of the EC system triggers an inhibition of cyclic adenosine monophosphate (cAMP) production followed by subsequent stimulation of several signaling cascades including MAP kinases, PI3/PKB and MEK/ERK pathways (220-222). Examining downstream signaling cascades of the EC system in the intestine would be another approach to elucidate how iMGL and EC signaling may be linked. In addition, it should not be ruled out that peripheral (intestinal) changes in 2-AG levels may affect brain EC signaling. Berger *et.al* showed that dietary supplementation of EC precursors such as arachidonic acid and docosahexaenoic acid significantly increased anandamide levels in the brain (223). Perhaps, increased long chain fatty acid release by intestinal MGL might trigger EC synthesis in the brain, consequently resulting in hyperphagia. Investigating the central EC system, for instance by measuring EC levels and expression of CB1 in iMGL mice, would begin to address the existence of indirect mechanisms, if any, causing the observed phenotype of the iMGL mouse.

Adiposity in iMGL mice seems primarily due to the hyperphagia, but the decreased metabolic rate is likely to be another contributing factor. Many satiety hormones exert dual

mechanisms for controlling energy balance by altering both food intake and energy expenditure. The best known example is the *ob/ob* mice, where leptin deficiency results in an excessive body fat accumulation mainly via hyperphagia, but independent actions of leptin on energy expenditure have been demonstrated as well (224-227). Levin *et.al.* showed that body weight loss by leptin injection in *ob/ob* mice was significantly greater than that of pair fed mice (224). Further, many studies have shown that exogenous administration of leptin in *ob/ob* mice increased VO_2 and reduced RQ (225-227). Like leptin, the EC system alters food intake as well as metabolic rate. For example, rimonabant, a selective CB1 antagonist, increased the energy expenditure in *ob/ob* mice (228). Pair-fed CB1 null mice were leaner and had less body fat compared to wild type mice, suggesting that food intake regulation is not the only mechanism by which the EC system controls energy balance (147). Therefore, pair feeding studies in iMGL mice would be of interest to determine whether intestinal MGL is participating in controlling metabolic rate, independent of appetite regulation.

While it has long been accepted that gut hormones play a role in regulating appetitive behavior, the role of intestinal lipid metabolism in systemic energy metabolism is becoming increasingly appreciated. For example, both DGAT1 null mice and MGAT2 null mice show a resistance to diet induced obesity accompanied by increased metabolic rate (86,201). Here, we show that altered MG levels in the small intestine, by MGL overexpression, significantly changes energy balance via modulation of food intake and energy expenditure. Although currently the precise mechanisms underlying these changes are not clear, the data strongly suggest that alterations in intestinal MG metabolism affect whole body energy homeostasis. The detailed molecular mechanisms need to be explored, and may provide potential targets for obesity therapeutics.

In summary, we demonstrated dynamic changes in intestinal MG metabolizing enzymes, MGAT2 and MGL, during development, suggesting possibilities for diverse regulatory processes to control their expression and activities. Further, a significant induction in intestinal

MGL during high fat feeding was observed, indirectly showing its role in regulating energy balance. Mice overexpressing MGL specifically in small intestine showed increased body fat accumulation via hyperphagia and reduced energy expenditure, indicating a potential function for intestinal MGL in regulating whole body energy homeostasis, presumably via satiety signaling systems.

Literature Cited

1. Radtke, F., and Clevers, H. 2005. Self-renewal and cancer of the gut: two sides of a coin. *Science* 307:1904-1909.
2. Tso, P., and Crissinger, K. 2002. *Overview of digestion and absorption*. Philadelphia: W.B. Saunder Co. 75-90 pp.
3. Shiner, M. 1983. *Ultrastrucrue of the small intestinal mucosa*. New York: Spriner-Verlag Berlin Heidelgerg.
4. Dobbins, W.O., 3rd, and Kawanishi, H. 1981. Bacillary characteristics in Whipple's disease: an electron microscopic study. *Gastroenterology* 80:1468-1475.
5. Madara, J.L., and Trier, J.S. 1987. *Functional morphology of the mucosa of the small intestine.* New York: Raven press. 1209-1249 pp.
6. Barbieri, D., De Brito, T., Hoshino, S., Nascimento, O.B., Martins Campos, J.V., Quarentei, G., and Marcondes, E. 1970. Giardiasis in childhood. Absorption tests and biochemistry, histochemistry, light and electron microscopy of jejunal mucosa. *Arch Dis Child* 45:466-472.
7. Brandborg, L.L., Tankersley, C.B., Gottieb, S., Barancik, M., and Sartor, V.E. 1967. Histological demonstration of mucosal invasion by Giardia lamblia in man. *Gastroenterology* 52:143-150.
8. Ito, S. 1969. Structure and function of the glyco- calyx. *Fed. Proc.* 28:12-25.
9. Gebhard, A., and Gebert, A. 1999. Brush cells of the mouse intestine possess a specialized glycocalyx as revealed by quantitative lectin histochemistry. Further evidence for a sensory function. *J Histochem Cytochem* 47:799-808.
10. Claude, P., and Goodenough, D.A. 1973. Fracture faces of zonulae occludentes from "tight" and "leaky" epithelia. *J Cell Biol* 58:390-400.
11. Schaffer, J.E., and Lodish, H.F. 1994. Expression cloning and characterization of a novel adipocyte long chain fatty acid transport protein. *Cell* 79:427-436.
12. Costa, M., Furness, J.B., and Llewellyn-smith, I.J. 1987. *Histochemistry of the enteric nervous system.* New York: Raven press. 1-40 pp.
13. Gangl, A., and Ockner, R.K. 1975. Intestinal metabolism of plasma free fatty acids. Intracellular compartmentation and mechanisms of control. *J Clin Invest* 55:803-813.
14. Gangl, A., and Renner, F. 1978. In vivo metabolism of plasma free fatty acids by intestinal mucosa of man. *Gastroenterology* 74:847-850.
15. Trotter, P.J., and Storch, J. 1991. Fatty acid uptake and metabolism in a human intestinal cell line (Caco-2): comparison of apical and basolateral incubation. *J Lipid Res* 32:293-304.
16. Ho, S.Y., Delgado, L., and Storch, J. 2002. Monoacylglycerol metabolism in human intestinal Caco-2 cells: evidence for metabolic compartmentation and hydrolysis. *J Biol Chem* 277:1816-1823.
17. Storch, J., Zhou, Y.X., and Lagakos, W.S. 2008. Metabolism of Apical vs. basolateral sn-2-monoacylglycerol and fatty acids in rodent small intestine. *J Lipid Res*.
18. Shiau, Y.F., Boyle, J.T., Umstetter, C., and Koldovsky, O. 1980. Apical distribution of fatty acid esterification capacity along the villus-crypt unit of rat jejunum. *Gastroenterology* 79:47-53.
19. Trotter, P.J., and Storch, J. 1993. Fatty acid esterification during differentiation of the human intestinal cell line Caco-2. *J Biol Chem* 268:10017-10023.
20. O'Doherty, P.J.A. 1978. Phospholipid synthesis in differentiating cells of rat intestine. *Arch. Biochem. and Biophys.* 190:508-513.
21. Badman, M.K., and Flier, J.S. 2005. The gut and energy balance: visceral allies in the obesity wars. *Science* 307:1909-1914.

22. Chen, M., Yang, Y., Braunstein, E., Georgeson, K.E., and Harmon, C.M. 2001. Gut expression and regulation of FAT/CD36: possible role in fatty acid transport in rat enterocytes. *Am J Physiol Endocrinol Metab* 281:E916-923.

23. Storch, J., and Herr, F.M. 2001. *Nutritional regulation of fatty acid transport protein expression.* . Boca Raton: CRC press. 101-130 pp.

24. Cao, J., Hawkins, E., Brozinick, J., Liu, X., Zhang, H., Burn, P., and Shi, Y. 2004. A predominant role of acyl-CoA:monoacylglycerol acyltransferase-2 in dietary fat absorption implicated by tissue distribution, subcellular localization, and up-regulation by high fat diet. *J Biol Chem* 279:18878-18886.

25. Buhman, K.K., Smith, S.J., Stone, S.J., Repa, J.J., Wong, J.S., Knapp, F.F., Jr., Burri, B.J., Hamilton, R.L., Abumrad, N.A., and Farese, R.V., Jr. 2002. DGAT1 is not essential for intestinal triacylglycerol absorption or chylomicron synthesis. *J Biol Chem* 277:25474-25479.

26. Howard, E.R. 1984. Muscle innervation of the gut: structure and pathology. *J R Soc Med* 77:905-909.

27. Patton, J.S. 1981. *Gastrointestinal lipid digestion*. New York: Raven press. 1123-1146 pp.

28. Tso, P., and Crissinger, K. 2002. Digestion and absorption of lipids. In *Biochemical and physiological aspects of human nutrition,*M.H. Stipanuk, editor. Philadelphia,W.B. Saunder Co. 125-141.

29. Hui, D.Y., and Howles, P.N. 2002. Carboxyl ester lipase: structure-function relationship and physiological role in lipoprotein metabolism and atherosclerosis. *J Lipid Res* 43:2017-2030.

30. Carriere, F., Barrowman, J.A., Verger, R., and Laugier, R. 1993. Secretion and contribution to lipolysis of gastric and pancreatic lipases during a test meal in humans. *Gastroenterology* 105:876-888.

31. Carey, M.C., Small, D.M., and Bliss, C.M. 1983. Lipid digestion and absorption. *Annu Rev Physiol* 45:651-677.

32. Verger, R. 1984. *Pancreatic lipase*. Amsterdam: Elsevier. 84-150 pp.

33. Andersson, L., Carriere, F., Lowe, M.E., Nilsson, A., and Verger, R. 1996. Pancreatic lipase-related protein 2 but not classical pancreatic lipase hydrolyzes galactolipids. *Biochim Biophys Acta* 1302:236-240.

34. Lowe, M.E. 2000. Properties and function of pancreatic lipase related protein 2.*Biochemie.* 82:997-1004.

35. Lowe, M.E., Kaplan, M.H., Jackson-Grusby, L., D'Agostino, D., and Grusby, M.J. 1998. Decreased neonatal dietary fat absorption and T cell cytotoxicity in pancreatic lipase-related protein 2-deficient mice. *J Biol Chem* 273:31215-31221.

36. D'Agostino, D., Cordle, R.A., Kullman, J., Erlanson-Albertsson, C., Muglia, L.J., and Lowe, M.E. 2002. Decreased postnatal survival and altered body weight regulation in procolipase-deficient mice. *J Biol Chem* 277:7170-7177.

37. Wang, C.S., and Hartsuck, J.A. 1993. Bile salt-activated lipase. A multiple function lipolytic enzyme. *Biochim Biophys Acta* 1166:1-19.

38. Howles, P.N., Wagner, B., and Davids, L. 1998. Bile salt stimulated lipase is required for proper digestion and absorption of milk triglycerides in neonatal mice. *(Abstract) Faseb J* 12:A851.

39. Howles, P.N., Stemmerman, G.N., Fenoglio-Preiser, C.M., and Hui, D.Y. 1999. Carboxyl ester lipase activity in milk prevents fat-derived intestinal injury in neonatal mice. *Am J Physiol* 277:G653-661.

40. Howles, P.N., Carter, C.P., and Hui, D.Y. 1996. Dietary free and esterified cholesterol absorption in cholesterol esterase (bile salt-stimulated lipase) gene-targeted mice. *J Biol Chem* 271:7196-7202.

41. Huggins, K.W., Camarota, L.M., Howles, P.N., and Hui, D.Y. 2003. Pancreatic triglyceride lipase deficiency minimally affects dietary fat absorption but dramatically decreases dietary cholesterol absorption in mice. *J Biol Chem* 278:42899-42905.

42. Gilham, D., Labonte, E.D., Rojas, J.C., Jandacek, R.J., Howles, P.N., and Hui, D.Y. 2007. Carboxyl ester lipase deficiency exacerbates dietary lipid absorption abnormalities and resistance to diet-induced obesity in pancreatic triglyceride lipase knockout mice. *J Biol Chem* 282:24642-24649.

43. Bruneau, N., Lombardo, D., and Bendayan, M. 1998. Participation of GRP94-related protein in secretion of pancreatic bile salt-dependent lipase and in its internalization by the intestinal epithelium. *J Cell Sci* 111 (Pt 17):2665-2679.

44. Bruneau, N., Nganga, A., Bendayan, M., and Lombardo, D. 2001. Transcytosis of pancreatic bile salt-dependent lipase through human Int407 intestinal cells. *Exp Cell Res* 271:94-108.

45. Bosner, M.S., Gulick, T., Riley, D.J., Spilburg, C.A., and Lange, L.G., 3rd. 1988. Receptor-like function of heparin in the binding and uptake of neutral lipids. *Proc Natl Acad Sci U S A* 85:7438-7442.

46. Wang, C.S., Kuksis, A., Manganaro, F., Myher, J.J., Downs, D., and Bass, H.B. 1983. Studies on the substrate specificity of purified human milk bile salt-activated lipase. *J Biol Chem* 258:9197-9202.

47. Hernell, O., and Blackberg, L. 1982. Digestion of human milk lipids: physiologic significance of sn-2 monoacylglycerol hydrolysis by bile salt-stimulated lipase. *Pediatr Res* 16:882-885.

48. Dinella, R.R., Meng, H.C., and Park, C.R. 1960. Properties of intestinal lipase. *J Biol Chem* 235:3076-3081.

49. Spalinger, J.H., Seidman, E.G., Menard, D., and Levy, E. 1998. Endogenous lipase activity in Caco-2 cells. *Biochim Biophys Acta* 1393:119-127.

50. Tipton, A.D.t., Frase, S., and Mansbach, C.M., 2nd. 1989. Isolation and characterization of a mucosal triacylglycerol pool undergoing hydrolysis. *Am J Physiol* 257:G871-878.

51. Mahan, J.T., Heda, G.D., Rao, R.H., and Mansbach, C.M., 2nd. 2001. The intestine expresses pancreatic triacylglycerol lipase: regulation by dietary lipid. *Am J Physiol Gastrointest Liver Physiol* 280:G1187-1196.

52. Grober, J., Lucas, S., Sorhede-Winzell, M., Zaghini, I., Mairal, A., Contreras, J.A., Besnard, P., Holm, C., and Langin, D. 2003. Hormone-sensitive lipase is a cholesterol esterase of the intestinal mucosa. *J Biol Chem* 278:6510-6515.

53. Tso, P., Nauli, A., and Lo, C.M. 2004. Enterocyte fatty acid uptake and intestinal fatty acid-binding protein. *Biochem Soc Trans* 32:75-78.

54. Strauss, E.W. 1968. *Morphological aspects of triglyceride absorption.* . Washington, D.C.: American Physiological Society. 1377-1406 pp.

55. Stahl, A. 2004. A current review of fatty acid transport proteins (SLC27). *Pflugers Arch* 447:722-727.

56. Stremmel, W., Lotz, G., Strohmeyer, G., and Berk, P.D. 1985. Identification, isolation, and partial characterization of a fatty acid binding protein from rat jejunal microvillous membranes. *J Clin Invest* 75:1068-1076.

57. Abumrad, N.A., and Storch, J. 2006. *Role of membrane and cytosolic fatty acid binding proteins in lipid processin by the small intestine*. New York: Raven press. 1693-1709 pp.

58. Ho, S.Y., and Storch, J. 2001. Common mechanisms of monoacylglycerol and fatty acid uptake by human intestinal Caco-2 cells. *Am J Physiol Cell Physiol* 281:C1106-1117.

59. Stremmel, W. 1988. Uptake of fatty acids by jejunal mucosal cells is mediated by a fatty acid binding membrane protein. *J Clin Invest* 82:2001-2010.

60. Murota, K., and Storch, J. 2005. Uptake of micellar long-chain fatty acid and sn-2-monoacylglycerol into human intestinal Caco-2 cells exhibits characteristics of protein-mediated transport. *J Nutr* 135:1626-1630.

61. Chow, S.L., and Hollander, D. 1979. A dual, concentration-dependent absorption mechanism of linoleic acid by rat jejunum in vitro. *J Lipid Res* 20:349-356.

62. Berk, P.D., and Stump, D.D. 1999. Mechanisms of cellular uptake of long chain free fatty acids. *Mol Cell Biochem* 192:17-31.

63. Schoeller, C., Keelan, M., Mulvey, G., Stremmel, W., and Thomson, A.B. 1995. Role of a brush border membrane fatty acid binding protein in oleic acid uptake into rat and rabbit jejunal brush border membrane. *Clin Invest Med* 18:380-388.

64. Cechetto, J.D., Sadacharan, S.K., Berk, P.D., and Gupta, R.S. 2002. Immunogold localization of mitochondrial aspartate aminotransferase in mitochondria and on the cell surface in normal rat tissues. *Histol Histopathol* 17:353-364.

65. Zhou, S.L., Stump, D., Kiang, C.L., Isola, L.M., and Berk, P.D. 2002. Mitochondrial aspartate aminotransferase expressed on the surface of 3T3-L1 adipocytes mediates saturable fatty acid uptake. *Proc. Soc. Exp. Biol. Med.* 208:263-270.

66. Abumrad, N.A., Sfeir, Z., Connelly, M.A., and Coburn, C. 2000. Lipid transporters: membrane transport systems for cholesterol and fatty acids. *Curr Opin Clin Nutr Metab Care* 3:255-262.

67. Poirier, H., Degrace, P., Niot, I., Bernard, A., and Besnard, P. 1996. Localization and regulation of the putative membrane fatty-acid transporter (FAT) in the small intestine. Comparison with fatty acid-binding proteins (FABP). *Eur J Biochem* 238:368-373.

68. Nassir, F., Wilson, B., Han, X., Gross, R.W., and Abumrad, N.A. 2007. CD36 is important for fatty acid and cholesterol uptake by the proximal but not distal intestine. *J Biol Chem* 282:19493-19501.

69. Drover, V.A., Ajmal, M., Nassir, F., Davidson, N.O., Nauli, A.M., Sahoo, D., Tso, P., and Abumrad, N.A. 2005. CD36 deficiency impairs intestinal lipid secretion and clearance of chylomicrons from the blood. *J Clin Invest* 115:1290-1297.

70. Milger, K., Herrmann, T., Becker, C., Gotthardt, D., Zickwolf, J., Ehehalt, R., Watkins, P.A., Stremmel, W., and Fullekrug, J. 2006. Cellular uptake of fatty acids driven by the ER-localized acyl-CoA synthetase FATP4. *J Cell Sci* 119:4678-4688.

71. Shields, H.M., Bates, M.L., Bass, N.M., Best, C.J., Alpers, D.H., and Ockner, R.K. 1986. Light microscopic immunocytochemical localization of hepatic and intestinal types of fatty acid-binding proteins in rat small intestine. *J Lipid Res* 27:549-557.

72. Lin, M.C., Arbeeny, C., Bergquist, K., Kienzle, B., Gordon, D.A., and Wetterau, J.R. 1994. Cloning and regulation of hamster microsomal triglyceride transfer protein. The regulation is independent from that of other hepatic and intestinal proteins which participate in the transport of fatty acids and triglycerides. *J Biol Chem* 269:29138-29145.

73. Storch, J. 1993. Diversity of fatty acid-binding protein structure and function: studies with fluorescent ligands. *Mol Cell Biochem* 123:45-53.

74. Vassileva, G., Huwyler, L., Poirier, K., Agellon, L.B., and Toth, M.J. 2000. The intestinal fatty acid binding protein is not essential for dietary fat absorption in mice. *Faseb J* 14:2040-2046.

75. Newberry, E.P., Xie, Y., Kennedy, S., Han, X., Buhman, K.K., Luo, J., Gross, R.W., and Davidson, N.O. 2003. Decreased hepatic triglyceride accumulation and altered fatty acid uptake in mice with deletion of the liver fatty acid-binding protein gene. *J Biol Chem* 278:51664-51672.

76. Johnston, J.M., Rao, G.A., and Lowe, P.A. 1967. The separation of the alpha-glycerophosphate and monoglyceride pathways in the intestinal biosynthesis of triglycerides. *Biochim Biophys Acta* 137:578-580.

77. Kayden, H.J., Senior, J.R., and Mattson, F.H. 1967. The monoglyceride pathway of fat absorption in man. *J Clin Invest* 46:1695-1703.
78. Yen, C.L., Stone, S.J., Cases, S., Zhou, P., and Farese, R.V., Jr. 2002. Identification of a gene encoding MGAT1, a monoacylglycerol acyltransferase. *Proc Natl Acad Sci U S A* 99:8512-8517.
79. Yen, C.L., and Farese, R.V., Jr. 2003. MGAT2, a monoacylglycerol acyltransferase expressed in the small intestine. *J Biol Chem* 278:18532-18537.
80. Cao, J., Lockwood, J., Burn, P., and Shi, Y. 2003. Cloning and functional characterization of a mouse intestinal acyl-CoA:monoacylglycerol acyltransferase, MGAT2. *J Biol Chem* 278:13860-13866.
81. Cheng, D., Nelson, T.C., Chen, J., Walker, S.G., Wardwell-Swanson, J., Meegalla, R., Taub, R., Billheimer, J.T., Ramaker, M., and Feder, J.N. 2003. Identification of acyl coenzyme A:monoacylglycerol acyltransferase 3, an intestinal specific enzyme implicated in dietary fat absorption. *J Biol Chem* 278:13611-13614.
82. Cao, J., Cheng, L., and Shi, Y. 2007. Catalytic properties of MGAT3, a putative triacylgycerol synthase. *J Lipid Res* 48:583-591.
83. Cases, S., Smith, S.J., Zheng, Y.W., Myers, H.M., Lear, S.R., Sande, E., Novak, S., Collins, C., Welch, C.B., Lusis, A.J., et al. 1998. Identification of a gene encoding an acyl CoA:diacylglycerol acyltransferase, a key enzyme in triacylglycerol synthesis. *Proc Natl Acad Sci U S A* 95:13018-13023.
84. Cases, S., Stone, S.J., Zhou, P., Yen, E., Tow, B., Lardizabal, K.D., Voelker, T., and Farese, R.V., Jr. 2001. Cloning of DGAT2, a second mammalian diacylglycerol acyltransferase, and related family members. *J Biol Chem* 276:38870-38876.
85. Yen, C.L., Brown, C.H.t., Monetti, M., and Farese, R.V., Jr. 2005. A human skin multifunctional O-acyltransferase that catalyzes the synthesis of acylglycerols, waxes, and retinyl esters. *J Lipid Res* 46:2388-2397.
86. Smith, S.J., Cases, S., Jensen, D.R., Chen, H.C., Sande, E., Tow, B., Sanan, D.A., Raber, J., Eckel, R.H., and Farese, R.V., Jr. 2000. Obesity resistance and multiple mechanisms of triglyceride synthesis in mice lacking Dgat. *Nat Genet* 25:87-90.
87. Stone, S.J., Myers, H.M., Watkins, S.M., Brown, B.E., Feingold, K.R., Elias, P.M., and Farese, R.V., Jr. 2004. Lipopenia and skin barrier abnormalities in DGAT2-deficient mice. *J Biol Chem* 279:11767-11776.
88. Owen, M.R., Corstorphine, C.C., and Zammit, V.A. 1997. Overt and latent activities of diacylglycerol acytransferase in rat liver microsomes: possible roles in very-low-density lipoprotein triacylglycerol secretion. *Biochem J* 323 (Pt 1):17-21.
89. Waterman, I.J., and Zammit, V.A. 2002. Activities of overt and latent diacylglycerol acyltransferases (DGATs I and II) in liver microsomes of ob/ob mice. *Int J Obes Relat Metab Disord* 26:742-743.
90. Stone, S.J., Levin, M.C., and Farese, R.V., Jr. 2006. Membrane topology and identification of key functional amino acid residues of murine acyl-CoA:diacylglycerol acyltransferase-2. *J Biol Chem* 281:40273-40282.
91. Pope, J.L., McPherson, J.C., and Tidwell, H.C. 1966. A study of a monoglyceride-hydrolyzing enzyme of intestinal mucosa. *J Biol Chem* 241:2306-2310.
92. De Jong, B.J., Kalkman, C., and Hulsmann, W.C. 1978. Partial purification and properties of monoacylglycerol lipase and two esterases from isolated rat small intestinal epithelial cells. *Biochim Biophys Acta* 530:56-66.
93. Karlsson, M., Contreras, J.A., Hellman, U., Tornqvist, H., and Holm, C. 1997. cDNA cloning, tissue distribution, and identification of the catalytic triad of monoglyceride lipase. Evolutionary relationship to esterases, lysophospholipases, and haloperoxidases. *J Biol Chem* 272:27218-27223.

94. Karlsson, M., Reue, K., Xia, Y.R., Lusis, A.J., Langin, D., Tornqvist, H., and Holm, C. 2001. Exon-intron organization and chromosomal localization of the mouse monoglyceride lipase gene. *Gene* 272:11-18.

95. Fredrikson, G., Tornqvist, H., and Belfrage, P. 1986. Hormone-sensitive lipase and monoacylglycerol lipase are both required for complete degradation of adipocyte triacylglycerol. *Biochim Biophys Acta* 876:288-293.

96. Jaworski, K., Sarkadi-Nagy, E., Duncan, R.E., Ahmadian, M., and Sul, H.S. 2007. Regulation of triglyceride metabolism. IV. Hormonal regulation of lipolysis in adipose tissue. *Am J Physiol Gastrointest Liver Physiol* 293:G1-4.

97. Ikeda, Y., Okamura, K., and Fujii, S. 1977. Purification and characterization of rat liver microsomal monoacylglycerol lipase in comparison to the other esterases. *Biochim Biophys Acta* 488:128-139.

98. Keough, D.T., de Jersey, J., and Zerner, B. 1985. The relationship between the carboxylesterase and monoacylglycerol lipase activities of chicken liver microsomes. *Biochim Biophys Acta* 829:164-172.

99. Dinh, T.P., Carpenter, D., Leslie, F.M., Freund, T.F., Katona, I., Sensi, S.L., Kathuria, S., and Piomelli, D. 2002. Brain monoglyceride lipase participating in endocannabinoid inactivation. *Proc Natl Acad Sci U S A* 99:10819-10824.

100. Di Marzo, V., Bifulco, M., and De Petrocellis, L. 2004. The endocannabinoid system and its therapeutic exploitation. *Nat Rev Drug Discov* 3:771-784.

101. Di Marzo, V., and Matias, I. 2005. Endocannabinoid control of food intake and energy balance. *Nat Neurosci* 8:585-589.

102. Gibbs, J., Young, R.C., and Smith, G.P. 1973. Cholecystokinin decreases food intake in rats. *J Comp Physiol Psychol* 84:488-495.

103. Kojima, M., Hosoda, H., Date, Y., Nakazato, M., Matsuo, H., and Kangawa, K. 1999. Ghrelin is a growth-hormone-releasing acylated peptide from stomach. *Nature* 402:656-660.

104. Guan, X.M., Yu, H., Palyha, O.C., McKee, K.K., Feighner, S.D., Sirinathsinghji, D.J., Smith, R.G., Van der Ploeg, L.H., and Howard, A.D. 1997. Distribution of mRNA encoding the growth hormone secretagogue receptor in brain and peripheral tissues. *Brain Res Mol Brain Res* 48:23-29.

105. Wu, R., Dong, W., Ji, Y., Zhou, M., Marini, C.P., Ravikumar, T.S., and Wang, P. 2008. Orexigenic hormone ghrelin attenuates local and remote organ injury after intestinal ischemia-reperfusion. *PLoS ONE* 3:e2026.

106. Murphy, K.G., Dhillo, W.S., and Bloom, S.R. 2006. Gut peptides in the regulation of food intake and energy homeostasis. *Endocr Rev* 27:719-727.

107. Feinle-Bisset, C., Patterson, M., Ghatei, M.A., Bloom, S.R., and Horowitz, M. 2005. Fat digestion is required for suppression of ghrelin and stimulation of peptide YY and pancreatic polypeptide secretion by intraduodenal lipid. *Am J Physiol Endocrinol Metab* 289:E948-953.

108. Wren, A.M., Small, C.J., Abbott, C.R., Dhillo, W.S., Seal, L.J., Cohen, M.A., Batterham, R.L., Taheri, S., Stanley, S.A., Ghatei, M.A., et al. 2001. Ghrelin causes hyperphagia and obesity in rats. *Diabetes* 50:2540-2547.

109. English, P.J., Ghatei, M.A., Malik, I.A., Bloom, S.R., and Wilding, J.P. 2002. Food fails to suppress ghrelin levels in obese humans. *J Clin Endocrinol Metab* 87:2984.

110. le Roux, C.W., Patterson, M., Vincent, R.P., Hunt, C., Ghatei, M.A., and Bloom, S.R. 2005. Postprandial plasma ghrelin is suppressed proportional to meal calorie content in normal-weight but not obese subjects. *J Clin Endocrinol Metab* 90:1068-1071.

111. Zorrilla, E.P., Iwasaki, S., Moss, J.A., Chang, J., Otsuji, J., Inoue, K., Meijler, M.M., and Janda, K.D. 2006. Vaccination against weight gain. *Proc Natl Acad Sci U S A* 103:13226-13231.

112. Moran, T.H., and Kinzig, K.P. 2004. Gastrointestinal satiety signals II. Cholecystokinin. *Am J Physiol Gastrointest Liver Physiol* 286:G183-188.

113. Grider, J.R. 1994. Role of cholecystokinin in the regulation of gastrointestinal motility. *J Nutr* 124:1334S-1339S.

114. Muurahainen, N., Kissileff, H.R., Derogatis, A.J., and Pi-Sunyer, F.X. 1988. Effects of cholecystokinin-octapeptide (CCK-8) on food intake and gastric emptying in man. *Physiol Behav* 44:645-649.

115. Beglinger, C., Degen, L., Matzinger, D., D'Amato, M., and Drewe, J. 2001. Loxiglumide, a CCK-A receptor antagonist, stimulates calorie intake and hunger feelings in humans. *Am J Physiol Regul Integr Comp Physiol* 280:R1149-1154.

116. Abbott, C.R., Monteiro, M., Small, C.J., Sajedi, A., Smith, K.L., Parkinson, J.R., Ghatei, M.A., and Bloom, S.R. 2005. The inhibitory effects of peripheral administration of peptide YY(3-36) and glucagon-like peptide-1 on food intake are attenuated by ablation of the vagal-brainstem-hypothalamic pathway. *Brain Res* 1044:127-131.

117. Batterham, R.L., Cowley, M.A., Small, C.J., Herzog, H., Cohen, M.A., Dakin, C.L., Wren, A.M., Brynes, A.E., Low, M.J., Ghatei, M.A., et al. 2002. Gut hormone PYY(3-36) physiologically inhibits food intake. *Nature* 418:650-654.

118. Chelikani, P.K., Haver, A.C., Reeve, J.R., Jr., Keire, D.A., and Reidelberger, R.D. 2006. Daily, intermittent intravenous infusion of peptide YY(3-36) reduces daily food intake and adiposity in rats. *Am J Physiol Regul Integr Comp Physiol* 290:R298-305.

119. Sileno, A.P., Brandt, G.C., Spann, B.M., and Quay, S.C. 2006. Lower mean weight after 14 days intravenous administration peptide YY3-36 (PYY3-36) in rabbits. *Int J Obes (Lond)* 30:68-72.

120. Brynes, A.E., Frost, G.S., Edwards, C.M., Ghatei, M.A., and Bloom, S.R. 1998. Plasma glucagon-like peptide-1 (7-36) amide (GLP-1) response to liquid phase, solid phase, and meals of differing lipid composition. *Nutrition* 14:433-436.

121. Bullock, B.P., Heller, R.S., and Habener, J.F. 1996. Tissue distribution of messenger ribonucleic acid encoding the rat glucagon-like peptide-1 receptor. *Endocrinology* 137:2968-2978.

122. Larsen, P.J., Fledelius, C., Knudsen, L.B., and Tang-Christensen, M. 2001. Systemic administration of the long-acting GLP-1 derivative NN2211 induces lasting and reversible weight loss in both normal and obese rats. *Diabetes* 50:2530-2539.

123. Tourrel, C., Bailbe, D., Meile, M.J., Kergoat, M., and Portha, B. 2001. Glucagon-like peptide-1 and exendin-4 stimulate beta-cell neogenesis in streptozotocin-treated newborn rats resulting in persistently improved glucose homeostasis at adult age. *Diabetes* 50:1562-1570.

124. Buse, J.B., Henry, R.R., Han, J., Kim, D.D., Fineman, M.S., and Baron, A.D. 2004. Effects of exenatide (exendin-4) on glycemic control over 30 weeks in sulfonylurea-treated patients with type 2 diabetes. *Diabetes Care* 27:2628-2635.

125. DeFronzo, R.A., Ratner, R.E., Han, J., Kim, D.D., Fineman, M.S., and Baron, A.D. 2005. Effects of exenatide (exendin-4) on glycemic control and weight over 30 weeks in metformin-treated patients with type 2 diabetes. *Diabetes Care* 28:1092-1100.

126. Dakin, C.L., Small, C.J., Batterham, R.L., Neary, N.M., Cohen, M.A., Patterson, M., Ghatei, M.A., and Bloom, S.R. 2004. Peripheral oxyntomodulin reduces food intake and body weight gain in rats. *Endocrinology* 145:2687-2695.

127. Cohen, M.A., Ellis, S.M., Le Roux, C.W., Batterham, R.L., Park, A., Patterson, M., Frost, G.S., Ghatei, M.A., and Bloom, S.R. 2003. Oxyntomodulin suppresses appetite and reduces food intake in humans. *J Clin Endocrinol Metab* 88:4696-4701.

128. Dakin, C.L., Small, C.J., Park, A.J., Seth, A., Ghatei, M.A., and Bloom, S.R. 2002. Repeated ICV administration of oxyntomodulin causes a greater reduction in body weight gain than in pair-fed rats. *Am J Physiol Endocrinol Metab* 283:E1173-1177.

129. Parlevliet, E.T., Heijboer, A.C., Schroder-van der Elst, J.P., Havekes, L.M., Romijn, J.A., Pijl, H., and Corssmit, E.P. 2008. Oxyntomodulin ameliorates glucose intolerance in mice fed a high-fat diet. *Am J Physiol Endocrinol Metab* 294:E142-147.

130. Gualillo, O., Lago, F., Casanueva, F.F., and Dieguez, C. 2006. One ancestor, several peptides post-translational modifications of preproghrelin generate several peptides with antithetical effects. *Mol Cell Endocrinol* 256:1-8.

131. Zhang, J.V., Ren, P.G., Avsian-Kretchmer, O., Luo, C.W., Rauch, R., Klein, C., and Hsueh, A.J. 2005. Obestatin, a peptide encoded by the ghrelin gene, opposes ghrelin's effects on food intake. *Science* 310:996-999.

132. McKee, K.K., Tan, C.P., Palyha, O.C., Liu, J., Feighner, S.D., Hreniuk, D.L., Smith, R.G., Howard, A.D., and Van der Ploeg, L.H. 1997. Cloning and characterization of two human G protein-coupled receptor genes (GPR38 and GPR39) related to the growth hormone secretagogue and neurotensin receptors. *Genomics* 46:426-434.

133. Fu, J., Gaetani, S., Oveisi, F., Lo Verme, J., Serrano, A., Rodriguez De Fonseca, F., Rosengarth, A., Luecke, H., Di Giacomo, B., Tarzia, G., et al. 2003. Oleylethanolamide regulates feeding and body weight through activation of the nuclear receptor PPAR-alpha. *Nature* 425:90-93.

134. Guzman, M., Lo Verme, J., Fu, J., Oveisi, F., Blazquez, C., and Piomelli, D. 2004. Oleoylethanolamide stimulates lipolysis by activating the nuclear receptor peroxisome proliferator-activated receptor alpha (PPAR-alpha). *J Biol Chem* 279:27849-27854.

135. Yang, Y., Chen, M., Georgeson, K.E., and Harmon, C.M. 2007. Mechanism of oleoylethanolamide on fatty acid uptake in small intestine after food intake and body weight reduction. *Am J Physiol Regul Integr Comp Physiol* 292:R235-241.

136. Matsuda, L.A., Lolait, S.J., Brownstein, M.J., Young, A.C., and Bonner, T.I. 1990. Structure of a cannabinoid receptor and functional expression of the cloned cDNA. *Nature* 346:561-564.

137. Howlett, A.C. 2002. The cannabinoid receptors. *Prostaglandins Other Lipid Mediat* 68-69:619-631.

138. Kulkarni-Narla, A., and Brown, D.R. 2000. Localization of CB1-cannabinoid receptor immunoreactivity in the porcine enteric nervous system. *Cell Tissue Res* 302:73-80.

139. Devane, W.A., Hanus, L., Breuer, A., Pertwee, R.G., Stevenson, L.A., Griffin, G., Gibson, D., Mandelbaum, A., Etinger, A., and Mechoulam, R. 1992. Isolation and structure of a brain constituent that binds to the cannabinoid receptor. *Science* 258:1946-1949.

140. Mechoulam, R., Ben-Shabat, S., Hanus, L., Ligumsky, M., Kaminski, N.E., Schatz, A.R., Gopher, A., Almog, S., Martin, B.R., Compton, D.R., et al. 1995. Identification of an endogenous 2-monoglyceride, present in canine gut, that binds to cannabinoid receptors. *Biochem Pharmacol* 50:83-90.

141. Sugiura, T., Kondo, S., Sukagawa, A., Nakane, S., Shinoda, A., Itoh, K., Yamashita, A., and Waku, K. 1995. 2-Arachidonoylglycerol: a possible endogenous cannabinoid receptor ligand in brain. *Biochem Biophys Res Commun* 215:89-97.

142. Matias, I., Bisogno, T., and Di Marzo, V. 2006. Endogenous cannabinoids in the brain and peripheral tissues: regulation of their levels and control of food intake. *Int J Obes (Lond)* 30 Suppl 1:S7-S12.

143. Kirkham, T.C., and Williams, C.M. 2001. Endogenous cannabinoids and appetite *Nutr. Res. Rev.* 14:65-86.

144. Jamshidi, N., and Taylor, D.A. 2001. Anandamide administration into the ventromedial hypothalamus stimulates appetite in rats. *Br J Pharmacol* 134:1151-1154.

145. Kirkham, T.C., Williams, C.M., Fezza, F., and Di Marzo, V. 2002. Endocannabinoid levels in rat limbic forebrain and hypothalamus in relation to fasting, feeding and satiation: stimulation of eating by 2-arachidonoyl glycerol. *Br J Pharmacol* 136:550-557.

146. Hanus, L., Avraham, Y., Ben-Shushan, D., Zolotarev, O., Berry, E.M., and Mechoulam, R. 2003. Short-term fasting and prolonged semistarvation have opposite effects on 2-AG levels in mouse brain. *Brain Res* 983:144-151.

147. Cota, D., Marsicano, G., Tschop, M., Grubler, Y., Flachskamm, C., Schubert, M., Auer, D., Yassouridis, A., Thone-Reineke, C., Ortmann, S., et al. 2003. The endogenous cannabinoid system affects energy balance via central orexigenic drive and peripheral lipogenesis. *J Clin Invest* 112:423-431.

148. Horvath, T.L. 2003. Endocannabinoids and the regulation of body fat: the smoke is clearing. *J Clin Invest* 112:323-326.

149. Dinh, T.P., Kathuria, S., and Piomelli, D. 2004. RNA interference suggests a primary role for monoacylglycerol lipase in the degradation of the endocannabinoid 2-arachidonoylglycerol. *Mol Pharmacol* 66:1260-1264.

150. Cravatt, B.F., Giang, D.K., Mayfield, S.P., Boger, D.L., Lerner, R.A., and Gilula, N.B. 1996. Molecular characterization of an enzyme that degrades neuromodulatory fatty-acid amides. *Nature* 384:83-87.

151. Matias, I., Gonthier, M.P., Orlando, P., Martiadis, V., De Petrocellis, L., Cervino, C., Petrosino, S., Hoareau, L., Festy, F., Pasquali, R., et al. 2006. Regulation, function, and dysregulation of endocannabinoids in models of adipose and beta-pancreatic cells and in obesity and hyperglycemia. *J Clin Endocrinol Metab* 91:3171-3180.

152. Gomez, R., Navarro, M., Ferrer, B., Trigo, J.M., Bilbao, A., Del Arco, I., Cippitelli, A., Nava, F., Piomelli, D., and Rodriguez de Fonseca, F. 2002. A peripheral mechanism for CB1 cannabinoid receptor-dependent modulation of feeding. *J Neurosci* 22:9612-9617.

153. Bensaid, M., Gary-Bobo, M., Esclangon, A., Maffrand, J.P., Le Fur, G., Oury-Donat, F., and Soubrie, P. 2003. The cannabinoid CB1 receptor antagonist SR141716 increases Acrp30 mRNA expression in adipose tissue of obese fa/fa rats and in cultured adipocyte cells. *Mol Pharmacol* 63:908-914.

154. Osei-Hyiaman, D., DePetrillo, M., Pacher, P., Liu, J., Radaeva, S., Batkai, S., Harvey-White, J., Mackie, K., Offertaler, L., Wang, L., et al. 2005. Endocannabinoid activation at hepatic CB1 receptors stimulates fatty acid synthesis and contributes to diet-induced obesity. *J Clin Invest* 115:1298-1305.

155. Pinto, L., Capasso, R., Di Carlo, G., and Izzo, A.A. 2002. Endocannabinoids and the gut. *Prostaglandins Leukot Essent Fatty Acids* 66:333-341.

156. Di Carlo, G., and Izzo, A.A. 2003. Cannabinoids for gastrointestinal diseases: potential therapeutic applications. *Expert Opin Investig Drugs* 12:39-49.

157. Storr, M.A., and Sharkey, K.A. 2007. The endocannabinoid system and gut-brain signalling. *Curr Opin Pharmacol* 7:575-582.

158. Izzo, A.A., Fezza, F., Capasso, R., Bisogno, T., Pinto, L., Iuvone, T., Esposito, G., Mascolo, N., Di Marzo, V., and Capasso, F. 2001. Cannabinoid CB1-receptor mediated regulation of gastrointestinal motility in mice in a model of intestinal inflammation. *Br J Pharmacol* 134:563-570.

159. Massa, F., Marsicano, G., Hermann, H., Cannich, A., Monory, K., Cravatt, B.F., Ferri, G.L., Sibaev, A., Storr, M., and Lutz, B. 2004. The endogenous cannabinoid system protects against colonic inflammation. *J Clin Invest* 113:1202-1209.

160. Burdyga, G., Lal, S., Varro, A., Dimaline, R., Thompson, D.G., and Dockray, G.J. 2004. Expression of cannabinoid CB1 receptors by vagal afferent neurons is inhibited by cholecystokinin. *J Neurosci* 24:2708-2715.

161. Coleman, R.A., and Haynes, E.B. 1984. Hepatic monoacylglycerol acyltransferase. Characterization of an activity associated with the suckling period in rats. *J Biol Chem* 259:8934-8938.

162. Poirier, H., Niot, I., Degrace, P., Monnot, M.C., Bernard, A., and Besnard, P. 1997. Fatty acid regulation of fatty acid-binding protein expression in the small intestine. *Am J Physiol* 273:G289-295.

163. Sul, H.S., and Wang, D. 1998. Nutritional and hormonal regulation of enzymes in fat synthesis: studies of fatty acid synthase and mitochondrial glycerol-3-phosphate acyltransferase gene transcription. *Annu Rev Nutr* 18:331-351.

164. Coleman, R.A., Lewin, T.M., and Muoio, D.M. 2000. Physiological and nutritional regulation of enzymes of triacylglycerol synthesis. *Annu Rev Nutr* 20:77-103.

165. Lewin, T.M., Granger, D.A., Kim, J.H., and Coleman, R.A. 2001. Regulation of mitochondrial sn-glycerol-3-phosphate acyltransferase activity: response to feeding status is unique in various rat tissues and is discordant with protein expression. *Arch Biochem Biophys* 396:119-127.

166. Kim, T.S., and Freake, H.C. 1996. High carbohydrate diet and starvation regulate lipogenic mRNA in rats in a tissue-specific manner. *J Nutr* 126:611-617.

167. Bradford, M.M. 1976. A rapid and sensitive method for the quantitation of microgram quantities of protein utilizing the principle of protein-dye binding. *Anal Biochem* 72:248-254.

168. Waterman, I.J., Price, N.T., and Zammit, V.A. 2002. Distinct ontogenic patterns of overt and latent DGAT activities of rat liver microsomes. *J Lipid Res* 43:1555-1562.

169. Jamdar, S.C., Moon, M., Bow, S., and Fallon, H.J. 1978. Hepatic lipid metabolism. Age-related changes in triglyceride metabolism. *J Lipid Res* 19:763-770.

170. Muoio, D.M., Seefeld, K., Witters, L.A., and Coleman, R.A. 1999. AMP-activated kinase reciprocally regulates triacylglycerol synthesis and fatty acid oxidation in liver and muscle: evidence that sn-glycerol-3-phosphate acyltransferase is a novel target. *Biochem J* 338 (Pt 3):783-791.

171. Park, H., Kaushik, V.K., Constant, S., Prentki, M., Przybytkowski, E., Ruderman, N.B., and Saha, A.K. 2002. Coordinate regulation of malonyl-CoA decarboxylase, sn-glycerol-3-phosphate acyltransferase, and acetyl-CoA carboxylase by AMP-activated protein kinase in rat tissues in response to exercise. *J Biol Chem* 277:32571-32577.

172. Onorato, T.M., Chakraborty, S., and Haldar, D. 2005. Phosphorylation of rat liver mitochondrial glycerol-3-phosphate acyltransferase by casein kinase 2. *J Biol Chem* 280:19527-19534.

173. Hulo, N., Bairoch, A., Bulliard, V., Cerutti, L., De Castro, E., Langendijk-Genevaux, P.S., Pagni, M., and Sigrist, C.J. 2006. The PROSITE database. *Nucleic Acids Res* 34:D227-230.

174. Lidmer, A.S., Kannius, M., Lundberg, L., Bjursell, G., and Nilsson, J. 1995. Molecular cloning and characterization of the mouse carboxyl ester lipase gene and evidence for expression in the lactating mammary gland. *Genomics* 29:115-122.

175. Gallo, L.L., Chiang, Y., Vahouny, G.V., and Treadwell, C.R. 1980. Localization and origin at rat intestinal cholesterol esterase determined by immunocytochemistry. *J Lipid Res* 21:537-545.

176. Douglas, D.N., Dolinsky, V.W., Lehner, R., and Vance, D.E. 2001. A role for Sp1 in the transcriptional regulation of hepatic triacylglycerol hydrolase in the mouse. *J Biol Chem* 276:25621-25630.

177. Lehner, R., and Vance, D.E. 1999. Cloning and expression of a cDNA encoding a hepatic microsomal lipase that mobilizes stored triacylglycerol. *Biochem J* 343 Pt 1:1-10.

178. Coleman, R.A., and Haynes, E.B. 1983. Selective changes in microsomal enzymes of triacylglycerol and phosphatidylcholine synthesis in fetal and postnatal rat liver. Induction of microsomal sn-glycerol 3-phosphate and dihydroxyacetonephosphate acyltransferase activities. *J Biol Chem* 258:450-456.

179. Manowitz, N.R., Tso, P., Drake, D.S., Frase, S., and Sabesin, S.M. 1986. Dietary supplementation with Pluronic L-81 modifies hepatic secretion of very low density lipoproteins in the rat. *J Lipid Res* 27:196-207.

180. Xia, T., Mostafa, N., Bhat, B.G., Florant, G.L., and Coleman, R.A. 1993. Selective retention of essential fatty acids: the role of hepatic monoacylglycerol acyltransferase. *Am J Physiol* 265:R414-419.

181. Sztalryd, C., and Kraemer, F.B. 1994. Regulation of hormone-sensitive lipase during fasting. *Am J Physiol* 266:E179-185.

182. Villena, J.A., Roy, S., Sarkadi-Nagy, E., Kim, K.H., and Sul, H.S. 2004. Desnutrin, an adipocyte gene encoding a novel patatin domain-containing protein, is induced by fasting and glucocorticoids: ectopic expression of desnutrin increases triglyceride hydrolysis. *J Biol Chem* 279:47066-47075.

183. Zimmermann, R., Strauss, J.G., Haemmerle, G., Schoiswohl, G., Birner-Gruenberger, R., Riederer, M., Lass, A., Neuberger, G., Eisenhaber, F., Hermetter, A., et al. 2004. Fat mobilization in adipose tissue is promoted by adipose triglyceride lipase. *Science* 306:1383-1386.

184. Jenkins, C.M., Mancuso, D.J., Yan, W., Sims, H.F., Gibson, B., and Gross, R.W. 2004. Identification, cloning, expression, and purification of three novel human calcium-independent phospholipase A2 family members possessing triacylglycerol lipase and acylglycerol transacylase activities. *J Biol Chem* 279:48968-48975.

185. Murase, T., Mizuno, T., Omachi, T., Onizawa, K., Komine, Y., Kondo, H., Hase, T., and Tokimitsu, I. 2001. Dietary diacylglycerol suppresses high fat and high sucrose diet-induced body fat accumulation in C57BL/6J mice. *J Lipid Res* 42:372-378.

186. Nagao, T., Watanabe, H., Goto, N., Onizawa, K., Taguchi, H., Matsuo, N., Yasukawa, T., Tsushima, R., Shimasaki, H., and Itakura, H. 2000. Dietary diacylglycerol suppresses accumulation of body fat compared to triacylglycerol in men in a double-blind controlled trial. *J Nutr* 130:792-797.

187. Kamphuis, M.M., Mela, D.J., and Westerterp-Plantenga, M.S. 2003. Diacylglycerols affect substrate oxidation and appetite in humans. *Am J Clin Nutr* 77:1133-1139.

188. Murase, T., Aoki, M., Wakisaka, T., Hase, T., and Tokimitsu, I. 2002. Anti-obesity effect of dietary diacylglycerol in C57BL/6J mice: dietary diacylglycerol stimulates intestinal lipid metabolism. *J Lipid Res* 43:1312-1319.

189. Fride, E., Bregman, T., and Kirkham, T.C. 2005. Endocannabinoids and food intake: newborn suckling and appetite regulation in adulthood. *Exp Biol Med (Maywood)* 230:225-234.

190. Chon, S.H., Zhou, Y.X., Dixon, J.L., and Storch, J. 2007. Intestinal monoacylglycerol metabolism: developmental and nutritional regulation of monoacylglycerol lipase and monoacylglycerol acyltransferase. *J Biol Chem* 282:33346-33357.

191. Cohn, S.M., Simon, T.C., Roth, K.A., Birkenmeier, E.H., and Gordon, J.I. 1992. Use of transgenic mice to map cis-acting elements in the intestinal fatty acid binding protein gene (Fabpi) that control its cell lineage-specific and regional patterns of expression along the duodenal-colonic and crypt-villus axes of the gut epithelium. *J Cell Biol* 119:27-44.

192. Angelichio, M.L., Beck, J.A., Johansen, H., and Ivey-Hoyle, M. 1991. Comparison of several promoters and polyadenylation signals for use in heterologous gene expression in cultured Drosophila cells. *Nucleic Acids Res* 19:5037-5043.

193. Folch, J., Lees, M., and Sloane Stanley, G.H. 1957. A simple method for the isolation and purification of total lipides from animal tissues. *J Biol Chem* 226:497-509.

194. Newberry, E.P., Xie, Y., Kennedy, S.M., Luo, J., and Davidson, N.O. 2006. Protection against Western diet-induced obesity and hepatic steatosis in liver fatty acid-binding protein knockout mice. *Hepatology* 44:1191-1205.

195. Homan, R., and Anderson, M.K. 1998. Rapid separation and quantitation of combined neutral and polar lipid classes by high-performance liquid chromatography and evaporative light-scattering mass detection. *J Chromatogr B Biomed Sci Appl* 708:21-26.

196. Weir, J.B. 1949. New methods for calculating metabolic rate with special reference to protein metabolism. *J Physiol* 109:1-9.

197. Tornqvist, H., and Belfrage, P. 1976. Purification and some properties of a monoacylglycerol-hydrolyzing enzyme of rat adipose tissue. *J Biol Chem* 251:813-819.

198. Tornqvist, H., Krabisch, L., and Belfrage, P. 1974. Simple assay for monoacylglycerol hydrolase activity of rat adipose tissue. *J Lipid Res* 15:291-294.

199. Saario, S.M., and Laitinen, J.T. 2007. Monoglyceride lipase as an enzyme hydrolyzing 2-arachidonoylglycerol. *Chem Biodivers* 4:1903-1913.

200. Gotto, A.M., Levy, R.I., John, K., and Fredrickson, D.S. 1971. On the protein defect in abetalipoproteinemia. *N Engl J Med* 284:813-818.

201. Yen, C.L., Cheong, M.L., Moriwaki, J., Zhou, P., Marmor, S., Hubbard, B., Wong, J., and Farese, R.V., Jr. 2007. In *FESEB summer conference Abstract #55*

202. Okazaki, T., Sagawa, N., Okita, J.R., Bleasdale, J.E., MacDonald, P.C., and Johnston, J.M. 1981. Diacylglycerol metabolism and arachidonic acid release in human fetal membranes and decidua vera. *J Biol Chem* 256:7316-7321.

203. Rindlisbacher, B., Reist, M., and Zahler, P. 1987. Diacylglycerol breakdown in plasma membranes of bovine chromaffin cells is a two-step mechanism mediated by a diacylglycerol lipase and a monoacylglycerol lipase. *Biochim Biophys Acta* 905:349-357.

204. Prescott, S.M., and Majerus, P.W. 1983. Characterization of 1,2-diacylglycerol hydrolysis in human platelets. Demonstration of an arachidonoyl-monoacylglycerol intermediate. *J Biol Chem* 258:764-769.

205. Bisogno, T., Berrendero, F., Ambrosino, G., Cebeira, M., Ramos, J.A., Fernandez-Ruiz, J.J., and Di Marzo, V. 1999. Brain regional distribution of endocannabinoids: implications for their biosynthesis and biological function. *Biochem Biophys Res Commun* 256:377-380.

206. Ben-Shabat, S., Fride, E., Sheskin, T., Tamiri, T., Rhee, M.H., Vogel, Z., Bisogno, T., De Petrocellis, L., Di Marzo, V., and Mechoulam, R. 1998. An entourage effect: inactive endogenous fatty acid glycerol esters enhance 2-arachidonoyl-glycerol cannabinoid activity. *Eur J Pharmacol* 353:23-31.

207. Liu, Y.L., Connoley, I.P., Wilson, C.A., and Stock, M.J. 2005. Effects of the cannabinoid CB1 receptor antagonist SR141716 on oxygen consumption and soleus muscle glucose uptake in Lep(ob)/Lep(ob) mice. *Int J Obes (Lond)* 29:183-187.

208. Jbilo, O., Ravinet-Trillou, C., Arnone, M., Buisson, I., Bribes, E., Peleraux, A., Penarier, G., Soubrie, P., Le Fur, G., Galiegue, S., et al. 2005. The CB1 receptor antagonist rimonabant reverses the diet-induced obesity phenotype through the regulation of lipolysis and energy balance. *Faseb J* 19:1567-1569.

209. Petersen, G., Sorensen, C., Schmid, P.C., Artmann, A., Tang-Christensen, M., Hansen, S.H., Larsen, P.J., Schmid, H.H., and Hansen, H.S. 2006. Intestinal levels of anandamide and oleoylethanolamide in food-deprived rats are regulated through their precursors. *Biochim Biophys Acta* 1761:143-150; discussion 141-142.

210. Rodriguez de Fonseca, F., Navarro, M., Gomez, R., Escuredo, L., Nava, F., Fu, J., Murillo-Rodriguez, E., Giuffrida, A., LoVerme, J., Gaetani, S., et al. 2001. An anorexic lipid mediator regulated by feeding. *Nature* 414:209-212.

211. Burdyga, G., Varro, A., Dimaline, R., Thompson, D.G., and Dockray, G.J. 2006. Ghrelin receptors in rat and human nodose ganglia: putative role in regulating CB-1 and MCH receptor abundance. *Am J Physiol Gastrointest Liver Physiol* 290:G1289-1297.

212. Lowe, M.E. 2002. The triglyceride lipases of the pancreas. *J Lipid Res* 43:2007-2016.

213. K. Hofmann, W.S. 1993. TMBASE - A database of membrane spanning protein segments. *Biol. Chem.* 374:166.

214. Tusnady, G.E., and Simon, I. 1998. Principles governing amino acid composition of integral membrane proteins: application to topology prediction. *J Mol Biol* 283:489-506.

215. Mazumder, B., Seshadri, V., and Fox, P.L. 2003. Translational control by the 3'-UTR: the ends specify the means. *Trends Biochem Sci* 28:91-98.

216. Barreau, C., Paillard, L., and Osborne, H.B. 2005. AU-rich elements and associated factors: are there unifying principles? *Nucleic Acids Res* 33:7138-7150.

217. Hirokawa, T., Boon-Chieng, S., and Mitaku, S. 1998. SOSUI: classification and secondary structure prediction system for membrane proteins. *Bioinformatics* 14:378-379.

218. Krogh, A., Larsson, B., von Heijne, G., and Sonnhammer, E.L. 2001. Predicting transmembrane protein topology with a hidden Markov model: application to complete genomes. *J Mol Biol* 305:567-580.

219. Piomelli, D. 2003. The molecular logic of endocannabinoid signalling. *Nat Rev Neurosci* 4:873-884.

220. Sanchez, M.G., Ruiz-Llorente, L., Sanchez, A.M., and Diaz-Laviada, I. 2003. Activation of phosphoinositide 3-kinase/PKB pathway by CB(1) and CB(2) cannabinoid receptors expressed in prostate PC-3 cells. Involvement in Raf-1 stimulation and NGF induction. *Cell Signal* 15:851-859.

221. Galve-Roperh, I., Rueda, D., Gomez del Pulgar, T., Velasco, G., and Guzman, M. 2002. Mechanism of extracellular signal-regulated kinase activation by the CB(1) cannabinoid receptor. *Mol Pharmacol* 62:1385-1392.

222. Graham, E.S., Ball, N., Scotter, E.L., Narayan, P., Dragunow, M., and Glass, M. 2006. Induction of Krox-24 by endogenous cannabinoid type 1 receptors in Neuro2A cells is mediated by the MEK-ERK MAPK pathway and is suppressed by the phosphatidylinositol 3-kinase pathway. *J Biol Chem* 281:29085-29095.

223. Berger, A., Crozier, G., Bisogno, T., Cavaliere, P., Innis, S., and Di Marzo, V. 2001. Anandamide and diet: inclusion of dietary arachidonate and docosahexaenoate leads to increased brain levels of the corresponding N-acylethanolamines in piglets. *Proc Natl Acad Sci U S A* 98:6402-6406.

224. Levin, N., Nelson, C., Gurney, A., Vandlen, R., and de Sauvage, F. 1996. Decreased food intake does not completely account for adiposity reduction after ob protein infusion. *Proc Natl Acad Sci U S A* 93:1726-1730.

225. Breslow, M.J., Min-Lee, K., Brown, D.R., Chacko, V.P., Palmer, D., and Berkowitz, D.E. 1999. Effect of leptin deficiency on metabolic rate in ob/ob mice. *Am J Physiol* 276:E443-449.

226. Pelleymounter, M.A., Cullen, M.J., Baker, M.B., Hecht, R., Winters, D., Boone, T., and Collins, F. 1995. Effects of the obese gene product on body weight regulation in ob/ob mice. *Science* 269:540-543.

227. Hwa, J.J., Fawzi, A.B., Graziano, M.P., Ghibaudi, L., Williams, P., Van Heek, M., Davis, H., Rudinski, M., Sybertz, E., and Strader, C.D. 1997. Leptin increases energy expenditure and selectively promotes fat metabolism in ob/ob mice. *Am J Physiol* 272:R1204-1209.

228. Liu, Y.L., Connoley, I.P., Wilson, C.A., and Stock, M.J. 2005. Effects of the cannabinoid CB1 receptor antagonist SR141716 on oxygen consumption and soleus muscle glucose uptake in Lep(ob)/Lep(ob) mice. *Int J Obes (Lond)* 29:183-187.

Appendix

Levels of enterocyte fatty acid-binding proteins (FABPs) in wild type and

CD36 null mice small intestine and liver

1. Introduction

CD36/ fatty acid translocase (FAT) is an 88kDa, integral membrane protein facilitating LCFA uptake in various tissues. It is abundantly expressed in skeletal muscle, adipose tissue, heart, and small intestine (1). Impaired FA uptake and metabolism in these tissues have been well demonstrated in the CD36 deficient rodent model (2-5), indicating its important role for LCFA transport. Focusing on its intestinal function, CD36 is highly expressed in rodent small intestine apical plasma membrane with proximal to distal and villus to crypt gradients, and its expression is up-regulated by high fat feeding (6), indirectly suggesting its function in lipid absorption. Furthermore, Dover et.al. showed a defect in intestinal lipid secretion (4) and, more recently, Nassir et. al. (5) reported reduced LCFA uptake in the proximal intestine in CD36 null mice.

Two FABPs present in the small intestine (IFABP and LFABP) are believed to function in the intracellular trafficking of LCFA and other hydrophobic ligands (7). Their expression shows a similar pattern as for CD36, suggesting a potential functional interaction between these proteins. In fact, a direct interaction between CD36 and heart FABP (HFABP) was demonstrated in milk-fat globule membranes by coimmunoprecipitation (8). However, it is unknown whether a similar interaction is also present in enterocytes. Therefore, we examined the effect of CD36/FAT deficiency on the intracellular FABP expression levels in various tissues. As a part of study, the expressions of intestinal FABPs (IFABP and LFABP) as well as hepatic LFABP levels in CD36 KO mice were compared to those of wild type mice.

2. Experimental procedures

CD36 null and wild type mice small intestine and liver were generously provided by Dr. Nada Abumrad (Washington University, St. Louis, MO). Intestinal mucosal samples were divided into four equal length segments from proximal to distal regions (#1- #4 segments). Tissues were homogenized in 10 volumes of homogenization buffer on ice for 30 sec. using a Wheaton tissue

homogenizer (Wheaton Science, Millville, NJ). Homogenization buffer contained 100 mM Tris with 1 mM EDTA, 1 mM dithiothreitol (DTT), 1 mM phenyl methyl sulphonyl fluoride (PMSF), aprotinin (5mg per 1ml buffer), and leupeptin (10mg per 1ml buffer). The crude tissue homogenates were centrifuged at 600×g for 10 min at 4 ℃ to remove unbroken cell debris, and supernatant were analyzed for protein concentration using the Bradford assay (9). The quantification of IFABP and LFABP levels were performed by Western Analysis as described in chapter 2. Briefly, 30 μg of samples from the proximal intestine (#1-3 segments) and liver, and 150 μg of samples from distal intestine (#4 segment) were loaded onto 15% acrylamide gels. Along with tissue samples, 0.15- 4 μg of purified IFABP or LFABP protein were loaded onto the gel as a standard to calculate the absolute amount of the protein in each sample. Dilutions of antibodies were as follows: anti-rat IFABP (1: 10,000, custom prepared from Affinity Biosystems); anti-human LFABP (1: 60,000, generously provided by Dr. Jacques Veerkamp), and anti-rabbit IgG (1:10,000, GE Healthcare, Piscataway, NJ). Quantification of protein bands was performed using UN-SCAN IT (Silk Scientific, Inc, Orem, UT).

3. Results

There was no statistically significant difference in either IFABP or LFABP levels in CD36 null mice small intestine, compared to those of wild type animals, in any of the proximal to distal regions of the small intestine (Fig.1and 2). The different expression patterns of IFABP and LFABP distribution along the longitudinal axis of the small intestine were in agreement with previous reports; IFABP was more widely expressed along the axis, with highest levels in the distal jejunum, whereas LFABP showed a relatively more narrow distribution, with highest levels in the proximal jejunum, and rapidly declining thereafter (10). Levels of both proteins were quite abundant, estimated at 4% (two FABP levels together) of total cellular protein, which is consistent with the report of Gordon et.al., showing that mRNA of both FABPs are approximately 5% of total cellular RNA pool (11).

Figure. 1

**Comparison of IFABP levels in wild type and CD36 KO mice
In the small intestine**
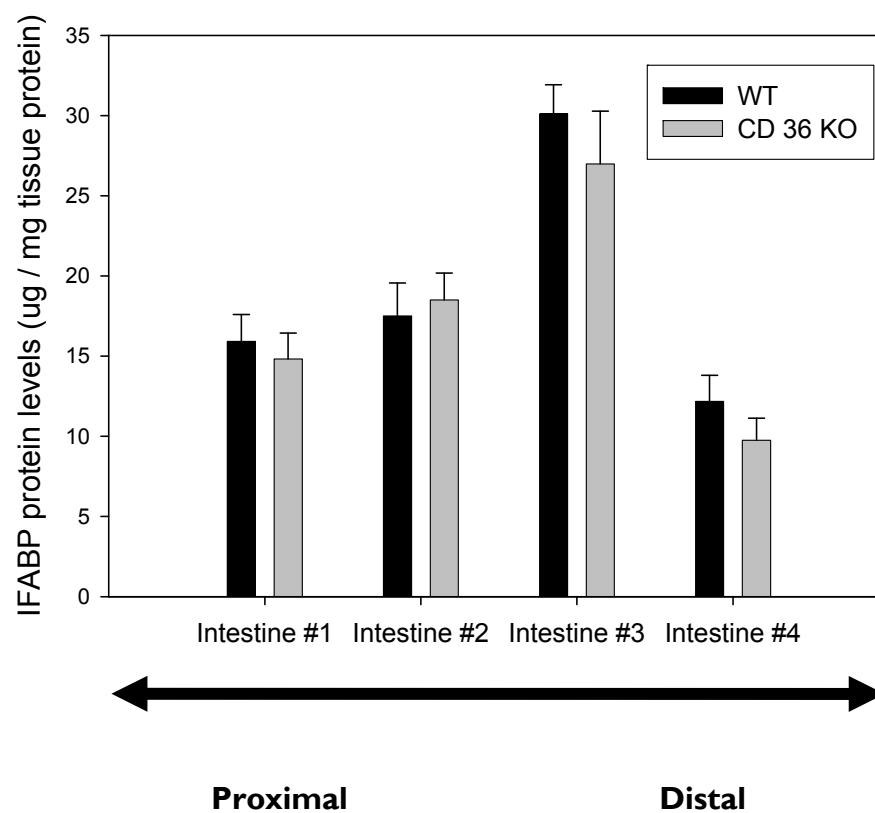
**Figure. 1 Comparison of IFABP levels in wild type and CD36 null mice
in the small intestine.**
Data represent mean ± S.E., n= 5-6

Figure. 2

Comparison of LFABP levels in wild type and CD36 KO mice in the small intestine
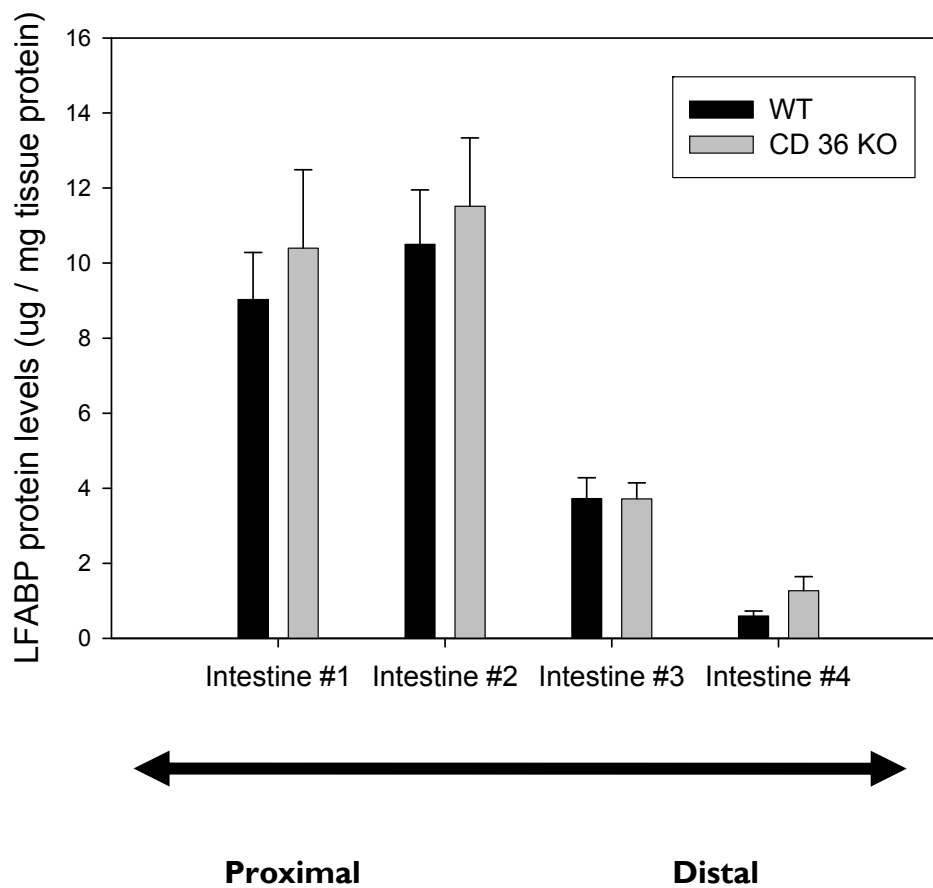
Figure. 2 Comparison of LFABP levels in wild type and CD36 null mice in the small intestine.
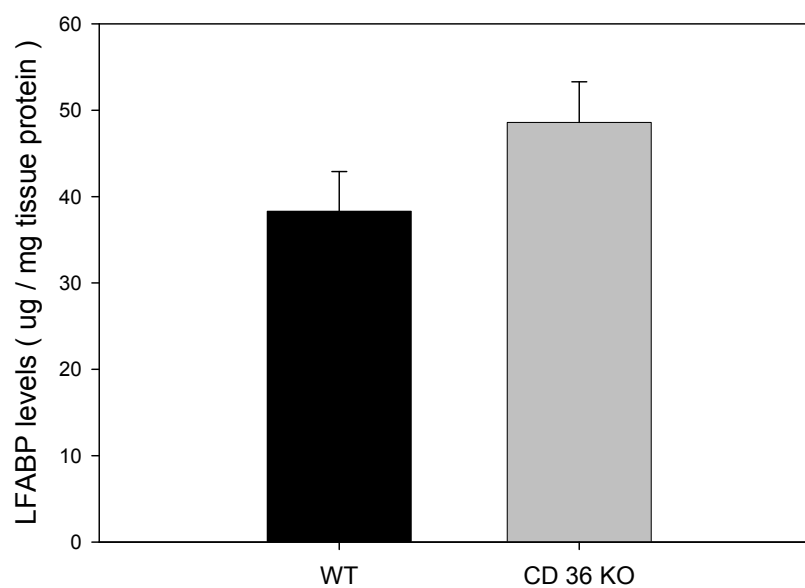Data represent mean ± S.E., n= 5-6

Hepatic LFABP levels in CD36 null mice were compared to those in wild type mice. No substantial change was found, though a trend toward a slight increase in the CD36 null mice was observed (Fig. 3).

4. Discussion

The effect of genetic deletion of the transmembrane LCFA transporter, CD36 on intracellular FABPs levels was examined in mouse small intestine and liver. There was no significant alteration in cellular FABP expression in either small intestine or liver. The CD36 null mice were generated by Febbraio et.al in 1999 (3). Defective LCFA uptake and metabolism in their mice was much more pronounced in adipose tissue and muscle (2), whereas the influence of its deletion in intestinal lipid absorption was uncertain, despite abundant CD36 expression in the small intestine. As mentioned earlier, only very recently (2005), Dover et.al. were able to show some degree of impaired chylomicron secretion (4), but were still unable to show any change in initial rates of LCFA uptake in enterocytes isolated from CD 36 null mice, casting a doubt on its uptake function in the intestine. A more comprehensive approach by Nassir et. al., examining effects of CD36 deletion in each intestinal segment from the proximal to the distal region, was able to show a significant reduction (50%) in LCFA uptake but only in the proximal-section of the small intestine (5).

We found that CD36 deficiency did not affect LFABP or IFABP protein levels in the proximal region of intestine. Nassir et.al. also reported no change in IFABP message levels in CD36 null mice intestine, consistent with the current observation for IFABP protein (5). In contrast, they found a significant down regulation of LFABP and DGAT1 mRNA in CD36 KO intestine, implicating a potential association of these proteins, perhaps in the process of TG esterification. The lack of parallel changes in IFABP suggests a lack of functional interaction with

Figure. 3

Comparison of LFABP levels in wild type and CD36 KO mice in liver

Figure. 3 Comparison of LFABP levels in wild type and CD36 null mice in liver.
Data represent mean ± S.E., n= 4-6, *p*= 0.16

CD36. Differential partitioning of LCFA by IFABP compared to LFABP was speculated; IFABP might direct FA toward phospholipid synthesis whereas LFABP is rather involved in TG synthesis for subsequent chylomicron secretion (12). Supporting this proposal, the expression pattern of CD36 in the small intestine is more similar to that of LFABP, rather than IFABP (5, 10). Nevertheless, we did not find any changes in LFABP protein expression following CD36 deletion. The discordance between LFABP mRNA and protein levels is surprising since most studies have found that LFABP is transcriptionally regulated (13).

Hepatic LFABP levels in CD36 null mice were not altered as well, possibly due to the lack of hepatic expression of CD36 in wild type animals (1). We also examined effects of CD36 null on FABP levels in other tissues, and found a substantial down-regulation of AFABP and HFABP in CD36 null adipose tissue and muscle, respectively. In contrast, the HFABP level in heart was significantly increased, suggesting a functional interaction between CD36 and FABPs in these tissues. Although there was no change in the two FABP levels in the small intestine by CD36 deficiency, more direct approaches such as coimmunoprecipitation of the FABPs with CD36 would provide a valuable insight in order to understand LCFA uptake and trafficking in the small intestine.

Literature Cited

1. Abumrad, N.A., el-Maghrabi, M.R., Amri, E.Z., Lopez, E., and Grimaldi, P.A. 1993. Cloning of a rat adipocyte membrane protein implicated in binding or transport of long-chain fatty acids that is induced during preadipocyte differentiation. Homology with human CD36. *J Biol Chem* 268:17665-17668.

2. Coburn, C.T., Knapp, F.F., Jr., Febbraio, M., Beets, A.L., Silverstein, R.L., and Abumrad, N.A. 2000. Defective uptake and utilization of long chain fatty acids in muscle and adipose tissues of CD36 knockout mice. *J Biol Chem* 275:32523-32529.

3. Febbraio, M., Abumrad, N.A., Hajjar, D.P., Sharma, K., Cheng, W., Pearce, S.F., and Silverstein, R.L. 1999. A null mutation in murine CD36 reveals an important role in fatty acid and lipoprotein metabolism. *J Biol Chem* 274:19055-19062.

4. Drover, V.A., Ajmal, M., Nassir, F., Davidson, N.O., Nauli, A.M., Sahoo, D., Tso, P., and Abumrad, N.A. 2005. CD36 deficiency impairs intestinal lipid secretion and clearance of chylomicrons from the blood. *J Clin Invest* 115:1290-1297.

5. Nassir, F., Wilson, B., Han, X., Gross, R.W., and Abumrad, N.A. 2007. CD36 is important for fatty acid and cholesterol uptake by the proximal but not distal intestine. *J Biol Chem* 282:19493-19501.

6. Poirier, H., Degrace, P., Niot, I., Bernard, A., and Besnard, P. 1996. Localization and regulation of the putative membrane fatty-acid transporter (FAT) in the small intestine. Comparison with fatty acid-binding proteins (FABP). *Eur J Biochem* 238:368-373.

7. Storch, J., and Corsico, B. 2008. The Emerging Functions and Mechanisms of Mammalian Fatty Acid-Binding Proteins. *Annu Rev Nutr*.

8. Spitsberg, V.L., Matitashvili, E., and Gorewit, R.C. 1995. Association and coexpression of fatty-acid-binding protein and glycoprotein CD36 in the bovine mammary gland. *Eur J Biochem* 230:872-878.

9. Bradford, M.M. 1976. A rapid and sensitive method for the quantitation of microgram quantities of protein utilizing the principle of protein-dye binding. *Anal Biochem* 72:248-254.

10. Sacchettini, J.C., Hauft, S.M., Van Camp, S.L., Cistola, D.P., and Gordon, J.I. 1990. Developmental and structural studies of an intracellular lipid binding protein expressed in the ileal epithelium. *J Biol Chem* 265:19199-19207.

11. Gordon, J.I., Smith, D.P., Alpers, D.H., and Strauss, A.W. 1982. Cloning of a complementary deoxyribonucleic acid encoding a portion of rat intestinal preapolipoprotein AIV messenger ribonucleic acid. *Biochemistry* 21:5424-5431.

12. Abumrad, N.A., and Storch, J. 2006. *Role of membrane and cytosolic fatty acid binding proteins in lipid processin by the small intestine*. New York: Raven press. 1693-1709 pp.

13. Storch, J., and Herr, F.M. 2001. *Nutritional regulation of fatty acid transport protein expression.* . Boca Raton: CRC press. 101-130 pp.

Curriculum Vita

Su-Hyoun Chon

October 2008	**Doctor of Philosophy in Nutritional Sciences** Rutgers, The State University of New Jersey, NJ
February 1998	**Bachelor of Science in Food and Nutrition** Duk-Sung Women's University, Seoul, Korea
September 2001 to July 2002	**Teaching Assistant** Department of Nutritional Sciences Rutgers, The State University of New Jersey, NJ
September 2002 to present	**Graduate Research Assistant** Department of Nutritional Sciences Rutgers, The State University of New Jersey, NJ

Publication:

Chon, S-H, Zhou, Y-X, Dixon, J.L., Brinker, A., Quadro, L., and Storch, J. 2008. Over-expression of monoacylglycerol lipase (MGL) in mouse small intestine results in an obese phenotype. *FASEB J.* 807.12

Chon, S.H., Zhou, Y.X., Dixon, J.L., and Storch, J. 2007. Intestinal monoacylglycerol metabolism: developmental and nutritional regulation of monoacylglycerol lipase and monoacylglycerol acyltransferase. *J Biol Chem* 282:33346-33357.